

**A Sensor Toolkit to Facilitate Context-Awareness
for Just-In-Time Questioning**

by

Louis F. Lopez

Submitted to the Department of Electrical Engineering and Computer Science
in Partial Fulfillment of the Requirements for the Degree of
Master of Engineering in Electrical Engineering and Computer Science
at the Massachusetts Institute of Technology

May 19, 2005 [June 2005]

Copyright 2005 Louis F. Lopez. All rights reserved.

The author hereby grants to M.I.T. permission to reproduce and
distribute publicly paper and electronic copies of this thesis
and to grant others the right to do so.

Author _____

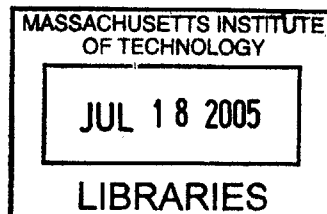
Department of Electrical Engineering and Computer Science
May 19, 2005

Certified by _____

Stephen Intille, Ph.D.
Research Scientist
Thesis Supervisor

Accepted by _____

Arthur C. Smith
Chairman, Department Committee on Graduate Theses



BARKER

A Sensor Toolkit to Facilitate Context-Awareness
for Just-In-Time Questioning

by
Louis F Lopez

Submitted to the
Department of Electrical Engineering and Computer Science

May 19, 2005

In Partial Fulfillment of the Requirements for the Degree of
Master of Engineering in Electrical Engineering and Computer Science

ABSTRACT

Studying human behavior is a task that researchers in many diverse fields from medicine to ubiquitous computing perform to identify potential health risks or to better understand how computers can assist people. One effective means of acquiring data on human behavior is through just-in-time (JIT) questioning whereby researchers ask a person context-sensitive questions concerning their current activities or well being at appropriate times. *Automatic* JIT questioning is now possible, and it involves mobile or in-home computing devices that use sensors to determine when to ask real-time contextually-specific questions about a person's state. Unfortunately, there is a lack of dedicated, inexpensive, and easy-to-use sensors that are tailored to operate in a JIT questioning framework. This work describes the construction of a toolkit of sensors dedicated to providing the necessary, real-time contextual data that is needed to facilitate JIT questioning. Among the sensors in the toolkit are a heart rate monitor, an electrical current sensor, a UV radiation exposure sensor, a proximity and location sensor, and a multiple switch input sensor. The data returned by the sensors of the JITQ toolkit can be used to create context-sensitive computing devices that can determine appropriate times to ask JIT questions. The sensor toolkit can provide researchers with an affordable and robust option for carrying out behavioral studies using the JIT questioning paradigm.

Thesis Supervisor: Stephen Intille, Ph.D.
Title: Research Scientist, House_n

Acknowledgements

This thesis has been a long and trying journey and I would not have made to the end without the support and brilliance of the following people:

Special thanks to Dr. Stephen Intille for supervising this thesis and providing his guidance and advice when I needed it.

Emmanuel Munguia Tapia, whose brilliant design of the MITes served as a base platform for all the sensors described in this thesis.

Randy Rockinson who helped me with the software side of things, helped me with some data collection, and provided an ear for my bad jokes.

Kent Larson, Ron McNeil, Jennifer Beaudin, Jason Nawyn, Pallavi Kaushik, Christine Liu, Deenie Pacik, and Robert Marlatt who all assisted me in one way or another from comments and suggestions to administrative support.

My past and new friends who encouraged me along the way and helped me to see the brighter side of life.

Last but not least, **my parents**, whose love and support I will forever be thankful for. I owe them everything I have today and I dedicate this thesis to them.

Contents

Acknowledgements	5
Contents	7
List of Figures	11
List of Tables	15
Chapter 1 Introduction	17
1.1 Design Criteria	18
1.2 The Sensors of the JITQ Toolkit.....	20
1.3 MIT Environmental Sensors (MITes).....	21
Chapter 2 Heart Rate Monitor (HRM) Sensor	23
2.1 Related work	23
2.2 Design	24
2.3 Performance Testing and Results.....	27
2.4 Deployment.....	28
2.5 Limitations	29
2.6 Summary	32
Chapter 3 Wireless Electrical Current Sensor	33
3.1 Related work	33
3.2 Design	35
3.3 Performance Testing and Results.....	39
3.4 Limitations	41
3.5 Summary	43
Chapter 4 Ultraviolet Radiation (UVR) Sensor	45
4.1 Related work	45
4.2 Design	46
4.3 Performance Testing and Results.....	48
4.4 Deployment.....	51
4.5 Limitations	51

4.6	Summary	53
Chapter 5	Proximity and Location Sensor	55
5.1	Related Work	55
5.2	Design	56
5.3	Performance Testing and Results.....	59
5.4	Deployment.....	67
5.5	Limitations	67
5.6	Summary	69
Chapter 6	Multi-Switch Input Sensor	71
6.1	Design	71
6.2	Deployment.....	77
6.3	Limitations	77
6.4	Summary	79
Chapter 7	Conclusion.....	81
Appendix A	MITes Standard Extension Modifications.....	83
A.1	Increasing Access to I/O Pins	83
A.2	Utilizing the Analog-to-Digital Converter	88
Appendix B	Building the Heart Rate MITes Sensor	91
B.1	Materials.....	91
B.2	Schematic Diagrams.....	91
B.3	Assembly Procedure.....	93
Appendix C	Building the Ultraviolet MITes sensor	107
C.1	Materials.....	107
C.2	Schematic	107
C.3	Assembly Procedure.....	108
Appendix D	Building the Beacon	113
D.1	Materials.....	113
D.2	Schematic Diagram.....	113
D.3	Assembly Procedure	114
Appendix E	Building the Electrical Current Sensor	127

E.1 Materials	127
E.2 Pinout and Schematic Diagrams.....	128
E.3 Assembly Procedure.....	129
Appendix F Additional Current Sensor Tests.....	141
F.1 Adjustable Setting Lamp	141
F.2 Multiple-Speed Blender.....	142
F.3 Rice Cooker	143
F.4 Bread Toaster.....	143
F.5 LCD Television	144
F.6 VCR.....	145
F.7 CRT Monitor	146
Appendix G Information for Obtaining the MITes Devices.....	149
Bibliography	151

List of Figures

Figure 1.1: MITes receiver and transmitter devices	22
Figure 2.1: High level connectivity diagram of HRM system.....	25
Figure 2.2: Inside view of completed HRM sensor	27
Figure 2.3: HRM sensor with battery	27
Figure 3.1: Current sensor firmware program flowchart	38
Figure 3.2: Bread-maker machine with current sensor.....	39
Figure 3.3: Close-up view of current sensor wrapped around split power cable.....	39
Figure 3.4: Current sensing results on bread making machine	40
Figure 4.1: UVR sensor with wrist strap	47
Figure 4.2: Sensor data calibration with UV sensor 1	49
Figure 4.3: Sensor data calibration with UV sensor 2	50
Figure 5.1: Proximity and Location sensor beacon	59
Figure 5.2: Interior view of beacon.....	59
Figure 5.3: Open space beacon results.....	61
Figure 5.4: User wearing beacon	62
Figure 5.5: Beacon position on chest.....	62
Figure 5.6: Zone demarcation with user facing toward TV	63
Figure 5.7: Zone demarcation with user facing away from TV.....	64
Figure 6.1: Pull-up and pull-down switch configurations	72
Figure 6.2: Simple matrix layout	73
Figure 6.3: Matrix scanning example	73
Figure 6.4: Example matrix data format	75
Figure 6.5: Wearable chording keyboard by Alex Mekelburg	77
Figure A.1: Solder points to access microcontroller I/O pins.....	84
Figure A.2: Multi-switch example pinout diagram.....	85
Figure A.3: Header attachment underside view.....	86
Figure A.4: Header attachment topside view.....	86

Figure A.5: Close-up of wire connection to DIO4	87
Figure A.6: Connection of DIO3 and DIO4 to the header pins	88
Figure A.7: Attachment of 2-pin header	89
Figure A.8: Finished ADC enabled MITes device	90
Figure B.1: POLAR receiver connection pad labels.....	92
Figure B.2: Schematic of the Heart Rate MITes sensor	92
Figure B.3: Power plug	93
Figure B.4: Different views of power jack hole	94
Figure B.5: Tape barrier on the rear of the power jack.....	94
Figure B.6: Power jack with	95
Figure B.7: Finished installation of the.....	95
Figure B.8: Voltage shifter IC and protoboard adapter	96
Figure B.9: Black header to remove	97
Figure B.10: Flush bottom surface.....	97
Figure B.11: Voltage shifter IC in position	98
Figure B.12: 5+ Volt wire attachment	99
Figure B.13: Voltage regulator board with capacitors.....	100
Figure B.14: Positive terminal bridge.....	101
Figure B.15: Attaching power to POLAR receiver	102
Figure B.16: Installation and connection of voltage regulator	103
Figure B.17: MITes transmitter with header receptacles.....	104
Figure B.18: Completed views of Heart Rate MITes sensor	105
Figure B.19: Heart rate monitor with battery.....	105
Figure C.1: Schematic diagram of UV Sensor.....	107
Figure C.2: Protoboard and component arrangement.....	109
Figure C.3: Protoboard underside	109
Figure C.4: Test fitting protoboard	109
Figure C.5: Zener diode placement.....	109
Figure C.6: Soldering wires	110
Figure C.7: Positioning MITes device.....	110

Figure C.8: Finished UV Sensor.....	111
Figure D.1: Schematic diagram indicating connections to attenuator IC	113
Figure D.2: MITes transmitter preparation	114
Figure D.3: Preparation of the protoboard adapter board	115
Figure D.4: Detailed view of individual pins.....	115
Figure D.5: Finished view of soldered attenuator IC.....	116
Figure D.6: Attenuator board positioning.....	116
Figure D.7: Connecting ground and 220pF capacitor.....	117
Figure D.8: Attaching the 5k resistor.....	117
Figure D.9: Connecting +3V signal to pad3	117
Figure D.10: Attaching 220 pF Cap and Antenna	118
Figure D.11: Box before tab removal	119
Figure D.12: Box with tab removed	119
Figure D.13: Notch sizing.....	119
Figure D.14: Finished view of notches	119
Figure D.15: Box after eight layer aluminum wrapping.....	120
Figure D.16: Plastic strip cut to length and creased.....	120
Figure D.17: Side view with strip attached.....	121
Figure D.18: Front-side view of strip	121
Figure D.19: Location of hot glue for thumb pressure point	122
Figure D.20: Finished view of pressure point.....	122
Figure D.21: Positioning battery connector	123
Figure D.22: Completed view of MITes connection	124
Figure D.23: Finished beacon	125
Figure E.1: MITes header pinout	128
Figure E.2: Schematic of Current Sensor	128
Figure E.3: PC board section of interest	130
Figure E.4: Description of traces to remove or bridge.....	130
Figure E.5: Mounting the preliminary electronic components	131
Figure E.6: Mounting MAX4544 IC and attaching wires	132

Figure E.7: Cutting 2mm trace gap.....	133
Figure E.8: Finished view	133
Figure E.9: Mounting MAX5160 IC and protoboard	133
Figure E.10: Attaching digital pot wires.....	134
Figure E.11: Connecting wires to protoboard.....	134
Figure E.12: Positioning MITes device with header receptacle	135
Figure E.13: Header positioning and gluing as see from above	135
Figure E.14: Header positioning and gluing as seen from the PC board edge	135
Figure E.15: Completed wiring of MAX5160 IC to header receptacle.....	136
Figure E.16: Mounting Zener diode.....	137
Figure E.17: Notch and holes on casing	138
Figure E.18: Battery connector in position with wires	138
Figure E.19: Attaching battery wires to header	138
Figure E.20: Connecting the switch.....	139
Figure E.21: Notches for the switch	140
Figure E.22: Closed box view of switch.....	140
Figure E.23: PC board installed with transformer	140
Figure E.24: Finished Current Sensor.....	140
Figure F.1: Current sensor results for adjustable lamp.....	141
Figure F.2: Current sensor results for blender	142
Figure F.3: Current sensor data for rice cooker	143
Figure F.4: Current sensor data for toaster	144
Figure F.5: Current sensor data for Television	145
Figure F.6: Current sensor data for VCR.....	146
Figure F.7: Current sensor data for CRT Monitor	146

List of Tables

Table 2.1: Estimated Costs of HRM sensor.....	27
Table 2.2: MITes versus reference BPM measurements	28
Table 2.3: HRM sensor interference observations.....	29
Table 2.4: HRM sensor battery life estimate	32
Table 3.1: Estimated Costs of the current sensor.....	39
Table 3.2: Current sensor battery life estimates.....	43
Table 4.1: Estimated Costs of the UVR sensor.....	48
Table 4.2: UVR sensor angle test results	52
Table 4.3: UV Sensor battery life estimate	53
Table 5.1: Estimated Costs of the UVR sensor.....	59
Table 5.2: Average ranges for each output power setting in open space.....	62
Table 5.3: Average ranges for each output power setting in home environment	65
Table 5.4: Beacon battery life estimates	69
Table 6.1: Multi-switch sensor battery life estimates	79
Table A.1: I/O Pin Restrictions.....	83
Table E.2: Pin connections for MAX5160 to header receptacle	136

Chapter 1

Introduction

Researchers of various fields from medicine to ubiquitous computing are in need of robust tools, which are easy to use, to aid in the study of human behavior. These tools can consist of sensors that provide behavioral data by reporting information on a person's state and interaction with the environment. Such sensors could allow medical researchers to detect behavioral anomalies and identify potential health problems. From a ubiquitous computing perspective, behavioral information can provide computers with added ability to better assist people in the home or office.

Using sensor data alone to infer what a user is doing is limiting because the data may not be rich enough to provide accurate results. Rather, the data should be used to provide hints to help a computing device become context-aware and ask a user questions at appropriate times. In other words, instead of inferring what a person is doing at a given moment, a computing device can just ask the user. The idea of context-aware questioning originates from the experience sampling method (ESM) where a person's state is "sampled" periodically through questioning [1]. Unfortunately, continuous questioning can interrupt user activities and become quite irritating [1]. A context-sensitive device (aided by sensors) can be less intrusive on a person's natural state by asking questions only at appropriate times. Therefore, the ideal paradigm is not a continuous sampling method associated with ESM but rather a "just-in-time" querying method that strives to minimize user interruption.

"Just-In-time" querying or JITQ for short is a concept already in use. For example, House_n (a research group part of the MIT Department of Architecture) used JITQ to aid in preventative health care [2]. Ambulatory as well as positional sensors provided the contextual hints that allowed a PDA to choose appropriate times to ask how a person was feeling. In a different application, House_n researchers slightly modified

the JITQ paradigm such that context-sensitive motivations rather than questions were provided to help change behavior [3]. With context-sensitive motivations, sensors are used to provide contextual hints with the intent of modifying behavior. JITQ is potentially useful for studying human behavior, but it depends on a set of sensors that can provide the appropriate contextual hints.

1.1 Design Criteria

The development of a collection of sensors is the primary goal of this work. The sensors can best be described as a toolkit designed to help study human behavior within a JITQ framework. The JITQ sensor toolkit, as it shall henceforth be called, must meet some basic criteria to set it apart from other sensor devices that currently exist. These criteria are robustness, ease-of-use, portability, and affordability. Meeting these criteria in the sensor toolkit is the paramount design challenge of this work.

1.1.1 Robustness

A limitation of many electronic devices being developed is that they are usually built in research laboratories and are designed to work only in such environments.

Unfortunately, there is less control in environments outside the laboratory, which may cause problems when operating electronic devices. For example, outside the laboratory devices can be bumped or jostled (especially those that are worn on the body) and there could be electromagnetic interference that can adversely affect a device's operation.

Designing sensors for data collection outside the laboratory requires attention to a device's packaging as well as its susceptibility to external forms of noise, both electrical and physical. Robust packaging that restricts the movement of components can help prevent a sensor from breaking. Minimal length wires and properly shielded casings can help to minimize noise susceptibility.

1.1.2 Ease of Use

Keeping devices simple and easy to use increases their usefulness because they can be deployed with less training overhead than more complex devices. Easy-to-use sensors can also be used by researchers who are not familiar with computational technology. Simplicity must be extended to both installation and use/maintenance of the sensors. For installation, the idea behind the JITQ sensor toolkit is a “set and forget” paradigm. Once a sensor is placed on a person or installed in room, it should be able to transmit data continuously without further intervention. Ease of use means sensors should provide a simple unified data format and be able to self-configure, if applicable, with little or no user intervention. The sensors should require infrequent or easy battery replacement, and they should require little or no post configuration.

1.1.3 Portability

The key to moving sensors outside the laboratory is to remove any tethers that limit the portability of the device. In general, there are two significant limitations with any electrical data collection device: a power source and means of data transmission. To address both limitations, the sensors of the JITQ toolkit are built on an existing wireless sensor platform designed by Emmanuel Munguia Tapia called MITes (M.I.T. Environmental Sensors) [4]. MITes require infrequent battery due to efficient power saving techniques and have integrated 2.4GHz wireless transmission capability. Additional sensor components can be augmented to MITes devices and powered by the MITes power supply—a coin-sized lithium battery. Additional portability is achieved by interfacing receiver MITes to Compaq iPAQ PDAs or laptop computers, which can be carried by users. Utilizing a PDA for data collection and data processing is ideal for implementing JITQ because a user can be questioned at almost any time and location.

1.1.4 Affordability

Although there exist sensors that could be used instead of the JITQ sensor toolkit, their use is prohibitive due to costs from manufacturing, marketing, support, etc. The JITQ

sensor toolkit is made low cost by employing the inexpensive MITes platform which is significantly less expensive than the Intel Mote, another common wireless sensor option. [4]. MITes achieve their low cost by employing a relatively simple single board design that integrates power, sensors, and processing in one package. An advantage of low cost devices is that more can be purchased and deployed for a given dollar amount than their more expensive counterparts. Decreasing the commitment of funds on device hardware can allow researchers with small budgets to engage in experiments that may otherwise be too cost prohibitive.

1.2 The Sensors of the JITQ Toolkit

In this work, the five different types of sensors were developed that can be applied to different fields of study from medicine to computing. The design, construction, and testing of the JITQ sensor toolkit differs for each sensor type, but the steps follow a general pattern. First, the specific hardware needed for a particular type of sensor is identified. Second, the hardware is interfaced with the wireless MITes platform including all firmware required for operation. Last, the devices are tested in lab and then in a real world environment to verify their operation and robustness. Chapters 2 through 6 detail the design and results of the proposed sensors that comprise the toolkit. The following is a list of the sensors of toolkit:

- Heart Rate Monitor
- Wireless Electrical Current Sensor
- Ultraviolet Radiation Exposure Sensor
- Proximity and Location Sensor
- Multi-Switch Input Sensor

The toolkit also includes the original, unmodified MITes devices which have onboard accelerometers. In their original form, the MITes sensors are used for measuring bodily movements as well as movement and use of household objects. The next subsection provides details about the MITes platform.

1.3 MIT Environmental Sensors (MITes)

The JITQ sensor toolkit depends on the MITes as an infrastructure for power and wireless connectivity. MITes are a versatile, low power, and low cost platform for wireless sensing applications developed by Emmanuel Munguia Tapia at House_n. They serve as ubiquitous sensors for collecting data on human activities in natural settings [4]. MITes are equipped with onboard accelerometers which provide movement data that is wirelessly transmitted. These devices are deployed in the homes of volunteers and installed in the PlaceLab, a facility House_n developed for studying the behavior of people in a realistic home-like setting.

MITes, from a hardware standpoint, actually can refer to two distinct components: the MITes transmitter and MITes receiver. The transmitter is a small device measuring 1.2×1.0×0.25 inches. The transmitters are small enough to fit in medicine pill boxes of similar dimensions, which make them discrete and easy to wear or mount. The receiver unit is about twice the size of the transmitter (shown in Figure 1.1) and is capable of receiving data from multiple transmitters. Data is relayed to a PC or PDA through a RS232 compatible serial port. MITes receivers and transmitters utilize a Nordic RF24E1 MCU+transceiver chip, which is field programmable, as the central processing unit. Both devices also have onboard 2-axis accelerometers with expandable ports for a third axis accelerometer. In general, the term “MITes” refers to the MITes transmitter units while the MITes receivers are simply referred to as “receivers.”

MITes (i.e. the transmitters) can be subdivided into two categories or types: on-body and static. On-body MITes are worn on different parts of the body (such as the wrist or ankle) and are used to monitor physical movement. These MITes sample and transmit the accelerometer signals 200 times per second. Static MITes are designed to detect movement and broadcast a unique ID when such an event occurs. These MITes are also known as object-movement MITes and tend to be used for detecting environmental interactions such as cabinet doors opening. Unlike the on-body MITes, static MITes sample accelerometer signals about 5 times a second and transmit an ID only when movement occurs.

Two existing wireless sensor technologies known as Berkeley Motes and Smart Its sensors are comparable in functionality to the MITes [4]. The MITes have a distinct cost advantage due to their use of the Nordic IC and on-board accelerometers. Also, the MITes, unlike the Motes and Smart Its, do not communicate using a network infrastructure but rather communicate with the receiver directly, which reduces some communication overhead. Thus, benefits of a sensor network infrastructure such as inter-sensor communication and interaction are absent in the MITes. The MITes are similarly sized to that of the Intel Motes, but Motes require snap-on boards for sensors and batteries. MITes are a single board design with built-in power and sensors. Ultimately, the single board design makes MITes smaller than a similarly equipped Mote [4]. The use of a 3 cm microstrip antenna also helps to maintain the small stature of the MITes.

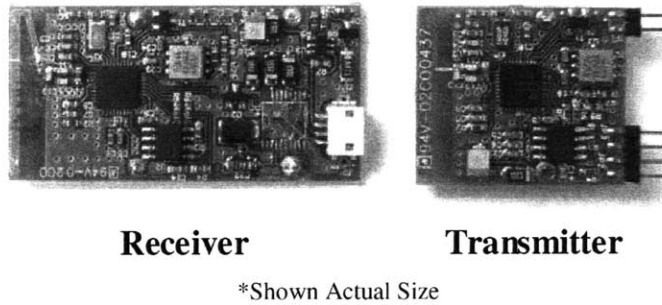


Figure 1.1: MITes receiver and transmitter devices

Chapter 2

Heart Rate Monitor (HRM) Sensor

Ambulatory monitoring is used in the medical community to gather data on such bodily information as heart rate, blood pressure, body temperature, etc. This information, especially heart rate, can be of use to human behavioral researchers because it gives real-time clues to the mood or activity level of a person. Some behavioral researchers rely on self-report recall surveys, time diaries or retrospective questioning, which are often plagued by biases or are burdensome for the user to maintain [1]. JITQ has an advantage over surveys because questions are asked at the time activities occur. Heart rate is an important source of bodily state because it changes based on the psychological state or physical activity of a person. When heart rate data is analyzed in conjunction with movement data, more can be concluded about a person's state. For example, an exercising person will have both high heart rate and bodily movement. A mentally stressed person may have a high heart rate and a normal amount of bodily movement. Concluding that a person is exercising or feels stressed is more difficult with movement or heart rate data alone.

2.1 Related work

Researchers have used sensor networks to gather ambulatory data in order to understand the state of a person's body. A Body Area Network (BAN) or Personal Area Network (PAN) consisting of a networked conglomerate of bodily sensors [5] serve as inspiration for the HRM sensor. Researchers have used data collected from people to gauge their individual stress levels through various correlations of the raw data. The HRM sensor provides personal biometric data that can be correlated with other biological data to achieve more complex conclusions about a person's bodily or mental state.

From a strictly hardware standpoint, other technologies exist which can collect several types of biological data including heart rate. Vivometrics' LifeShirt™ and Sensatex's Smart Shirt are perhaps the ideal technologies for ambulatory monitoring but their costs range from \$500 to over \$7,000 for each unit. Unfortunately these devices tend to be difficult if not impossible to adapt to a JITQ framework because data is not real-time accessible. Sensor data from such shirts usually has to be interpreted by a proprietary data logger that may not be able to stream real-time data to an external device such as a microcontroller. Another difficulty with sensor based shirts is that the individual sensors tend to be immobile since most are woven into the fabric of the shirts. The sensors of the JITQ toolkit are not restricted to occupying any specific locations and are therefore more versatile.

Polar, the leader in consumer-based wireless heart rate transmitter bands and receivers makes portable heart rate monitors in the form of a wearable strap transmitter known as the WearLink and a wrist watch style receiver. The wrist watch provides such features as a heart rate display and adjustable heart rate limits. Unfortunately the wrist watch receiver cannot be used within a JITQ framework because there is no way to access the heart rate data. Fortunately, Polar does make a receiver unit that can provide real-time heart rate information and the unit serves as the core component of the HRM sensor.

2.2 Design

Polar's leadership in consumer-based wireless heart rate transmitter bands and receivers makes it a popular choice for researchers. Polar manufactures both wearable wireless transmitters and receiver units that are found in commercial exercise equipment such as treadmills. The transmitter and receiver units share a proprietary form of wireless communication to send heartbeat data from one device to another. Upon reception of heartbeat signal data, the Polar receiver decodes and outputs heartbeat information in two ways: serially or beat-to-beat. A microcontroller can interpret the data from either of the two forms of output and provide some meaningful information in the form of a digital beats-per-minute (BPM) value.

A MITes transmitter contains an onboard microcontroller that is capable of receiving decoded heartbeat information from the Polar receiver. Assuming the Polar transmitter and receiver link is functional and heartbeats are being transmitted, the MITes transmitter serves as a liaison between the Polar components and the MITes receiver. The primary job of the MITes receiver is to continuously listen for incoming heartbeat data from the Polar receiver, compute a BPM value, and transmit that value to the MITes receiver which is interfaced to a computer or PDA. Figure 2.1 shows a high level view of the HRM system and how each major component interconnects.

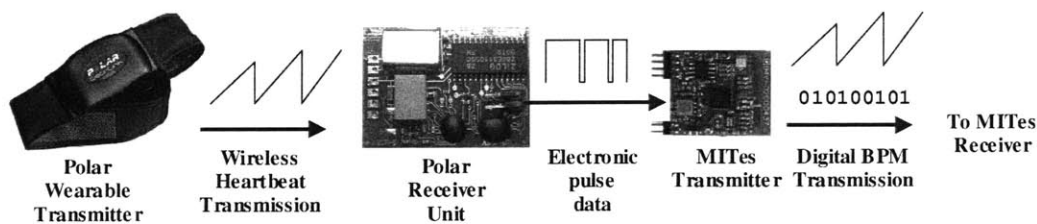


Figure 2.1: High level connectivity diagram of HRM system

2.2.1 Implementation

The design challenge lies in the interface between the Polar receiver unit and the MITes transmitter. Several problems must be overcome. The first is the voltage difference between the two devices. The MITes device operates and accepts only three volt signals whereas the Polar receiver operates at five volts. The second problem concerns the selection of a power source and is related to the first problem. The MITes device and Polar receiver are wired as one unit and must have a single power source. The last problem is more of a design choice. The Polar receiver outputs two types of data: a standard RS232 serial data and an active low, beat-to-beat pulse signal. Using the serial data would be straightforward since the BPM is represented digitally in the data stream. The beat-to-beat pulse signal is representative of the actual heartbeat being transmitted. Extracting the BPM from a pulse signal requires significant calculation effort by the MITes.

The voltage difference between the Polar receiver unit and MITes device presents an interfacing problem. The solution is to use a voltage shifter IC to convert the five volt signals from the Polar receiver down to three volts which the MITes can accept. It may be possible to interface the two devices directly, but a voltage shifter IC can help to extend the life of the MITes device by reducing stress on its I/O ports.

The MITes device is normally powered by a 3V lithium coin cell (CR2032), but the Polar receiver requires a power source greater than five volts for operation. A separate 9V battery can be used to power only the Polar receiver, but this battery would be in addition to the coin cell used by the MITes transmitter. The final solution was to use a 9V battery as the power source for both devices. As a consequence of eliminating the 3V coin cell, a separate 3V voltage regulator was needed to power the MITes device. The voltage regulator takes power not from the battery but from the 5 volt power source provided by the voltage regulators on the Polar receiver itself.

The last problem concerns the use of either the serial or pulse signals from the Polar transmitter. Using the serial information requires the use of a hardware serial port on the MITes device's microcontroller. Unfortunately, the MITes transmitters do not have easy access to the serial port I/O pins, which makes it very difficult to connect the serial output to the MITes device. The other option is to use the pulse signal output, which can be connected to any available I/O pin on the MITes device. The caveat of using the pulse signal is that the BPM must be calculated by the microcontroller. The use of the pulse signal was chosen because it required minimal hardware modifications to the MITes device (one resistor was removed). The BPM is calculated in firmware by measuring the period of time between pulses, inverting that value, and doing a units conversion to beats-per-minute. This value is represented as an integer and transmitted to the MITes receiver.

The MITes transmitter and Polar receiver are compactly packaged to fit in a pill box. The MITes' 3V voltage regulator is also small enough to fit in the pillbox. A small 1.3 millimeter power jack, placed inside the box, provides a robust terminal for supplying power to the sensor. A 9V battery with a custom-made power plug connects to the power jack to provide power for the HRM system.

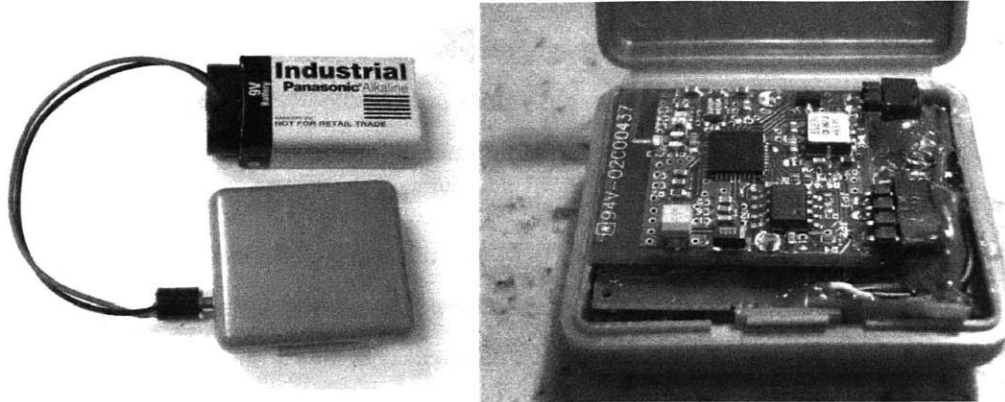


Figure 2.3: HRM sensor with battery

Figure 2.2: Inside view of completed HRM sensor

2.2.2 Estimated Cost Per Device

The HRM sensor consists of two main components: the MITes transmitter and Polar receiver. The MITes can be made at a cost of about \$41 and \$26 in quantities below and above 80 units respectively [4]. The Polar receiver costs \$36 in per device. For costs associated with the other components varies with quantity, thus the highest price is used. Using the highest price provides an upper-bound for the estimate of the cost per device.

Table 2.1: Estimated Costs of HRM sensor

Quantity	Estimated Price
Less than 80	\$92
More than 80	\$76

2.3 Performance Testing and Results

The performance of the HRM sensor is judged by its BPM calculation accuracy. Limitations are discussed in section 2.5. Accuracy is tested using reference tool made by Polar. The reference tool is a heartbeat simulator that mimics the wireless signal of a wearable Polar transmitter. Heartbeat rate is adjusted with an analog dial. The simulator

takes the place of the wearable strap and acts as a consistent reference for comparison with the MITes' value. The experimental procedure consisted of dialing the simulator to different heartbeat rates and reporting the values of both the MITes transmitter and a manual measurement of the simulator's actual rate. A manual measurement is necessary since the simulator does not have a digital readout. Table 2.2 provides the results from the BPM accuracy test. In general, the HRM sensor closely follows the reference. The differences in the values are the result of the imprecision of the simulator's analog adjustment dial. A small error in the dial adjustment is difficult to correct and thus, the actual reference BPM value is sometimes slightly higher than the value calculated by the MITes device.

Table 2.2: MITes versus reference BPM measurements

MITes Transmitter Calculated BPM	Reference BPM
50	50
60	60.5
70	71.25
80	80.75
90	91
100	100.5

2.4 Deployment

The HRM sensor is currently employed in a behavior study conducted by researchers at Boston University. BU researchers attach on-body accelerometer MITes, Polar transmitters, and the HRM sensor to members of cleaning staff at a local Marriot hotel to gather and annotate activity data as they perform their cleaning duties. The HRM sensor in conjunction with the on-body MITes provides a richer data set from which to analyze behavioral patterns.

Similar data collection using the HRM sensor as well as on-body and static MITes (used to detect interaction with objects) is done at the PlaceLab. Video streams from

cameras positioned throughout the PlaceLab are also stored. The sensor and video data is analyzed collectively with sophisticated algorithms to extract behavioral patterns and other such information.

2.5 Limitations

The HRM sensor has some limitations that affect its operation and use. The wireless link between the Polar transmitter and receiver as well as the MITes transmission link are susceptible to interference from certain types of everyday appliances. A few qualitative tests were performed to observe and the effect of appliances which emit electromagnetic interference on the HRM sensor. The Polar transmitter strap was used in conjunction with the HRM sensor rather than the Polar simulator to provide more realistic results. Two microwave ovens (one old and one new) as well as a vacuum cleaner were the appliances used in the test.

Table 2.3: HRM sensor interference observations

Appliance	Observations
Old microwave oven	The HRM sensor transmits sporadic data and occasionally stops transmitting BPM values when in very close proximity to the microwave oven (within two feet). Moving to a position about a yard away restores normal operation.
New microwave oven	The HRM sensor seems experience no adverse effects. No sporadic data or any transmission cutouts were observed.
Vacuum cleaner	The HRM sensor stops transmitting when the vacuum's motor is in close proximity to the HRM sensor (within one foot). Sporadic data was observed as the HRM sensor was moved away from the vacuum's motor. Normal operation resumed when the sensor was placed about a yard away from the appliance.

The observations described in Table 2.3 generally show that appliances which generate electromagnetic interference have a negative effect on the operation of the HRM sensor. With the microwave ovens, there was a distinct difference between the new and old ovens. It may be that the older oven has developed leaks that are allowing small amounts of the microwave energy to escape into the surrounding area. The microwaves may be causing interference between the Polar transmitter and receiver units which leads to sporadic values and sometimes loss of the signal. The newer oven is probably not

leaking any microwave energy and therefore does not noticeably interfere with the HRM sensor's operation. The vacuum cleaner produces electromagnetic interference through its motor. Putting the HRM sensor in close proximity seems to have a similar effect on the sensor as the old microwave oven. Fortunately, normal operation resumes once the sensor is moved at least a yard from the vacuum cleaner's motor.

Another test was performed to determine which wireless link (Polar or MITes) is being most affected by the electromagnetic interference. An on-body MITes transmitter was placed in the vicinity of the old microwave and tested to see if its transmitted packets were being lost. The results showed that about 17-20% of the transmission packets were lost when the microwave was turned on. Since most of the transmitted packets were still being received, the complete signal loss that occurs with the HRM sensors must be due to the Polar wireless link, not the MITes. If the Polar wireless link was not affected by the microwave's interference, the BPM values would still be received—just less frequently (i.e. some packets would be lost).

In most cases, interference from appliances will not affect the HRM sensor as significantly as general noise in the raw heartbeat signal. Heartbeat signals measured by the wearable Polar transmitter are quite noisy and can often cause the HRM sensor to report sporadic values. Sporadic values tend to deviate significantly from the average BPM values (sometimes by as much as a factor of two). There are also smaller deviations in the heartbeat that tend to cause the BPM values to change by about plus or minus ten beats per second. These smaller deviations are partially due to noise but probably also due to momentary increases or decreases in heartbeat rate due to breathing or bodily movement.

Filtering the BPM values returned by the HRM sensor is a way to overcome noisy data. A median filter can be used to filter out outliers. Averaging can help smooth out the smaller deviations in the data to obtain a more stable BPM value. Unfortunately, the side-effect of using window-based filters is time lagged data. In many cases, heartbeat rate tends to be a slow changing signal and therefore time lags are an acceptable tradeoff for a smoother signal.

Beyond the noise-induced limitations, there are some temporal and physical limitations that govern the HRM sensor's behavior. The HRM sensor relies heavily on the characteristics of the wireless link between the Polar transmitter and receiver. The Polar receiver continuously searches the air for coded or non-coded signals from the wearable Polar transmitter. Each search attempt times out after about five seconds if no signal is found. After each timeout, the receiver resets and tries the search again. Once a signal is acquired the heartbeat information is passed along to the MITes transmitter. In practice, acquisition of the Polar transmitter's signal occurs under 10 seconds but could take as long as 20 seconds. In most cases a fresh battery in the Polar transmitter provides very fast acquisition (under 5 seconds) whereas a transmitter with an aged battery has a weaker signal and takes longer to acquire (between 10 and 20 seconds). The strength of the Polar transmission signals seems to be dependent on the strength of the power source for the Polar transmitters.

The HRM sensor is also limited by a maximum distance of separation between the sensor and the Polar transmitter. In practice the distance tends to be two to three feet depending on the Polar transmitter's battery strength. Separating the sensor and Polar transmitter beyond three feet stops the transmission of BPM values. Normally a user wears the Polar strap transmitter and places the HRM sensor in a pocket or attaches it to a belt, which is usually within operating range.

2.5.1 Battery Life Estimation

Estimating the battery life of a fresh nine volt battery connected to a HRM sensor requires knowledge of the current consumed by both the Polar receiver and MITes transmitter. The current consumed by the Polar receiver was measured to be a constant six milliamps. The microcontroller on the MITes device, in the worst case, consumes a constant three milliamps with occasional 500 microsecond bursts of 16 milliamps for heart rate data transmission. These transmission bursts consume negligible current with respect to the constant nine milliamps drawn by the microcontroller and Polar receiver unit. The battery life can be estimated by simply assuming the HRM sensor draws a

constant nine milliamps at all times. This value applies to heartbeat rates from 1 to 255 BPM because the constant nine milliamps is dominant over all other factors.

Table 2.4: HRM sensor battery life estimate

HRM sensor current consumption	Estimated battery life*
9 mA (constant)	60 hours (2.5 days)

*Based on a 9V, 570 mAh Panasonic alkaline battery

2.6 Summary

The heart rate monitor sensor is designed to interface with existing Polar transmitters and receivers to provide a real-time heart rate value for use in a JIT questioning application. The Polar transmitter is a wearable device that a person places around his or her chest. Once a heartbeat signal is being transmitted, the HRM sensor receives the signal, computes the BPM value, and transmits that value to a MITes receiver that is connected to a computer or PDA. Heart rate data when analyzed in conjunction with physical motion data can provide a much richer data set from which context can be derived and used to study human behavior.

Chapter 3

Wireless Electrical Current Sensor

Ubiquitous sensing devices can be placed in homes to provide information on the state of lights, appliances, and other electrical devices [6]. MITes were once used with reed switches and small magnets to determine if a light switch is physically in the on or off position. A more direct way to determine if a light or any other electrical device is being used is to measure its current consumption. A current sensor can detect if an appliance is on or off or going through intermediate stages of operation by observing current consumption over time. People's interactions with household appliances and other objects in an environment can provide useful behavioral information to researchers. From the context of JITQ, a person can be queried on their current activity based on what appliances are in use. For example, cooking requires the use of toasters, can openers, microwave ovens, and other appliances. Therefore, sensing the operation of such appliances could allow a researcher to ask questions only during relevant cooking activities. As part of the toolkit, an electrical current sensor was developed to passively sense the current consumed by an appliance and transmit that data to a MITes receiver for further processing. This sensors can be placed on almost any electrical device and provide reliable information as to when an appliance is in use.

3.1 Related work

Electronic Educational Devices, Inc. (www.doubleed.com) has developed a commercially available power analyzer device that is, in essence, a highly sophisticated current sensor. The Watt's Up, as the device is called, is designed to monitor the power consumption of household appliances in order to identify wasteful, inefficient appliances. The Watt's Up Pro provides some additional features such data logging and a software "savings" calculator to help determine cost savings of a newly installed, more efficient appliance.

In addition to providing readings of power consumption in watts, the Watt's Up provides fifteen other measurement readings such as RMS current, voltage, power factor, and energy costs. The Watt's Up and Watt's Up Pro sell for \$95.95 and \$130.95 respectively.

The current sensor of the JITQ toolkit and the Watt's Up are similar in the sense that they are both current monitoring devices. The difference lies in the ability to adapt the devices into a JIT questioning framework. The toolkit's current sensor uses the MITes platform which is designed for real-time access to data through wireless transmissions. The Watt's Up is also capable of real-time data access but this feature is available only through third-party software. Data logging is the only means of data collection implemented in the software that is bundled with the Watt's Up. There is also a different usage model between the two devices. The Watt's Up is designed for precise, focused monitoring and not necessarily meant to be widely distributed on all household appliances. The toolkit's current sensor is compact (fits in a pillbox with a wired extension for the current transformer) and can be placed, discretely, on many different appliances throughout a household.

Another related work is the Web Ready Appliances Protocol (WRAP) developed by WRAP SpA, which is a spin-off company from Italian home appliance manufacturer Merloni Elettrodomestici. The concept behind WRAP is the ability to control appliances via the Internet using computers and cell phones. WRAP provides the means of obtaining meaningful state information of an appliance which could include both real-time and logged data. WRAP is still in development and has not made its way into mainstream appliances, but the knowledge of WRAP and its potential usefulness is becoming more widespread.

Web access to an appliance provides a means of accessing appliance state data but adds dependencies on Internet connectivity and additional software needed to query appliances. The current sensor is meant to be modular and since it only needs to monitor wall current, it only requires that an appliance connects to an electrical outlet via a power cable (around which it can wrap its current transformer). Thus, the current sensor can on almost any appliance, old or new and can be easily retrofit into existing homes.

3.2 Design

The ideal current sensor is a device that can measure the current consumption of an appliance without interrupting its current flow and without regard to amount of current it consumes. A naïve sensor design would place a resistor in the current path and measure the resulting RMS voltage that is dropped across it (i.e. Ohm's law). Unfortunately, appliances that use several amps of current can overload such a resistor if it is not rated for such current. Another consequence of using a resistor directly is the heat that is produced due to power dissipation. The direct resistor approach is not ideal because it interrupts the flow of current through a wire.

A better approach is to use the alternating magnetic field produced by the current through an appliance's power cord. A current transformer can convert the magnetic fields into a voltage proportional to the current running through the power cord. The voltage can then be conditioned through the use of Op-Amps to be input to a microcontroller. A problem still exists because a microcontroller's analog input can usually just take a small range of voltages (e.g. MITes devices can only accept signals in the range of 0 to 1.5 volts). Representing a high current appliance with the same voltage range as a low current device is not possible without losing information from either the high or low current range.

Additional complexity is required in the analog conditioning circuitry to address the issue with sensing high and low current appliances using the same voltage range. The sensor requires a means of switching between high and low current "modes" of operation. This high and low current mode can be achieved partly by using two different types of resistors with the current transformer. The current transformer provides an output voltage range that depends on the resistor that is placed across its outputs. A resistor with a value on the order of kilo-ohms can be used for low current appliances (below 1 amp) while a value on the order of a hundred ohms can be used for high current appliances (above 1 amp). Unfortunately, even with high and low current resistors more sublevels are needed to represent appliances within the low and high current ranges.

In addition to the high and low current resistors, an adjustable gain stage is needed. The gain stage amplifies the voltage from the current transformer to rescale the

output voltage range to take up the entire input voltage range of microcontroller. Internally, the microcontroller represents an analog input by first converting it to a digital value via an onboard analog-to-digital converter (ADC). Scaling the output voltage from the current transformer to take up the entire input voltage range means that full range of current usage by an appliance will be represented with the full digital range of the ADC. Ultimately, the gain stage in conjunction with the selectable resistors allows appliances that use different amounts of current to be adequately represented with the limited voltage range of the MITes' ADC.

The resistors and gain stage represent the variables or parameters of the analog conditioning circuitry. It is the microcontroller's responsibility to select the correct parameters based on the appliance being monitored. Allowing the microcontroller to select the parameters simplifies the use of the sensor from the user's standpoint. The selection of the resistor and gain stage value is automatic and does not require the manual setting of the parameters for each appliance.

Automatic selection of the resistor and gain values requires that the microcontroller know some information about appliance being monitored. This information can be acquired through a learning state called "training" mode. In training mode the sensor must learn what maximum amount of current is used by an appliance and use this value to configure the resistor and gain. By finding the maximum current consumption of an appliance, the microcontroller can represent that value using the highest digital value possible. Any smaller current usage amounts will be fractional amounts with respect to that maximum value.

Training mode simplifies the sensor's use because it automates the process of selecting the resistor and gain value. All a user must do is connect the sensor to an appliance's power cord, set it to training mode, let it run for some amount of time, and then set it back to normal (non-training) mode. In normal mode, the sensor will remember the best configuration from the training session and will start measuring and reporting current consumption of the appliance.

3.2.1 Implementation

The main components of the sensor are the current transformer, the high and low current resistors, the controllable gain stage, and the MITes transmitter with onboard microcontroller. The current transformer chosen for the sensor is made by CR Magnetics, Inc. and has a split-core design. The split-core allows the transformer to be wrapped around the power cord of an appliance without interrupting current flow. Magnetic fields from an appliance's power cable induce a current in the transformer's coils that generate a voltage drop across the output resistor.

The resistors chosen for the high and low current modes depend on the range of currents that the sensor should measure. A value of $4.7\text{ k}\Omega$ and $147\ \Omega$ was chosen for the low and high current resistors respectively. Using these resistors gives a theoretical effective RMS current range of about 30 milliamps to 28 amps which covers most household appliances.

The controllable gain stage consists of a micro-power Op-Amp and a digital potentiometer. The Op-Amp is configured to be a non-inverting gain amplifier with the digital potentiometer as the feedback resistor. The microcontroller on the MITes device sets the gain by moving the wiper in the digital potentiometer, which changes its resistance and, ultimately, the gain of the stage.

The major subcomponents are combined together along with a full-wave rectification stage (an AC to DC converter) and a controllable analog switch IC to select between the high and low current resistors. A low-pass filter is placed between the rectification and gain stage to remove the 60 Hz frequency component associated with wall current. Also a SPDT slide switch is connected to the MITes device to allow a user to toggle between training and normal mode. The full schematic and assembly directions can be found in Appendix E.

With the hardware in place, firmware must be written to implement the automatic training and normal sensing modes. The program is sufficiently complicated to warrant a flowchart diagram to explain its behavior. The basic flow of the firmware program follows the flowchart laid out in Figure 3.1. Starting from the top of the chart, when the sensor is powered on, it loads the last configuration (or default if none was previously

saved) and enters normal mode. In normal mode, the sensor periodically samples the current on the appliance's power cord and transmits the digital value representing that current. The sensor is placed in training mode by toggling a switch. Once in training mode, the sensor probes the current line and keeps a record of the maximum current it encounters. Current consumption, in training mode, is represented as a resistor selection and gain value. To stop training mode a user can do one of two things: toggle the switch or let the 18 hour timeout expire. Both actions return the current sensor to normal operation which uses the last saved resistor value and gain setting.

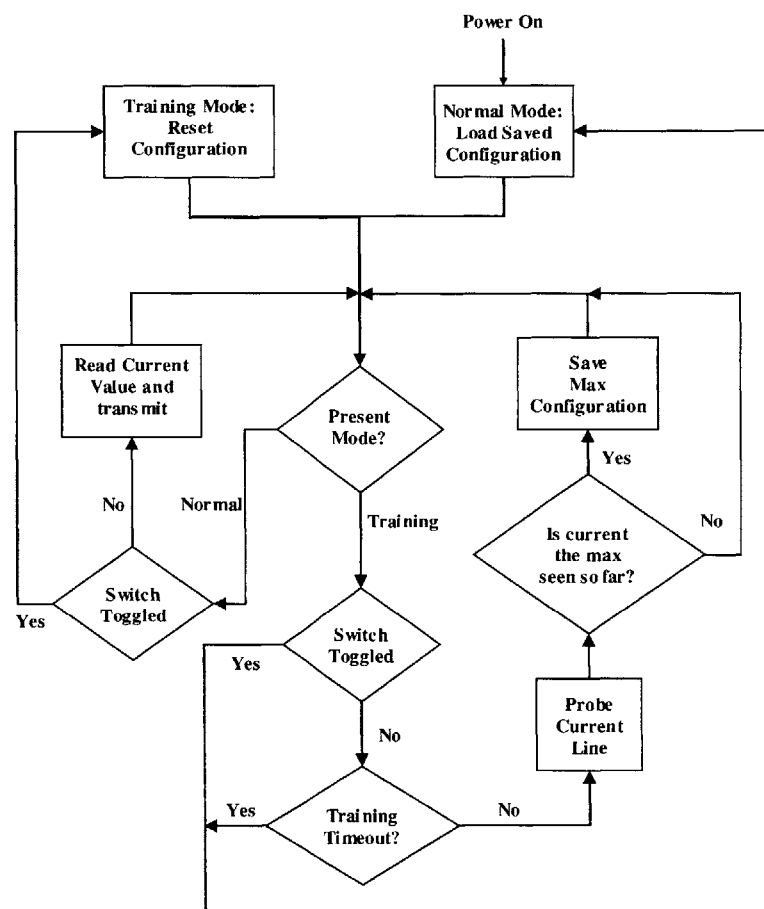


Figure 3.1: Current sensor firmware program flowchart

3.2.2 Estimated Cost Per Device

The most expensive component (other than the MITes transmitter) is the current transformer at \$12 each. Again, the MITes' cost is based on quantity. As was done with the HRM sensor, the maximum price of all other components is used to get an upper bound on cost.

Table 3.1: Estimated Costs of the current sensor

Quantity	Estimated Price
Less than 80	\$72
More than 80	\$57

3.3 Performance Testing and Results

Adequately testing the current sensor's training and normal sampling ability requires the use of an appliance with multiple states and varying current consumption. One such device is a bread-making machine. This machine goes through various states using a combination of heat and mechanical motion to mix, knead, and bake bread. The potentially different amounts of current used in different states tests the effectiveness of the current sensor's learning ability in training mode and also the sampling ability in

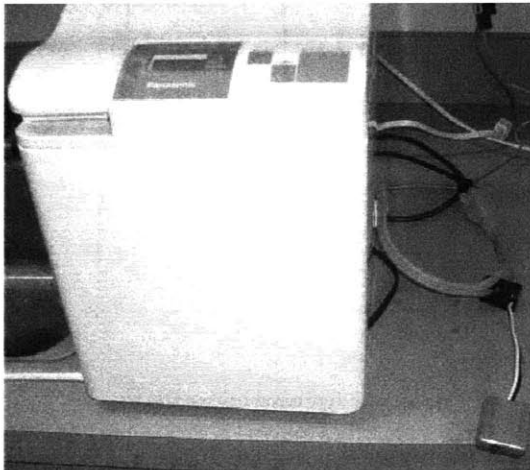


Figure 3.2: Bread-maker machine with current sensor

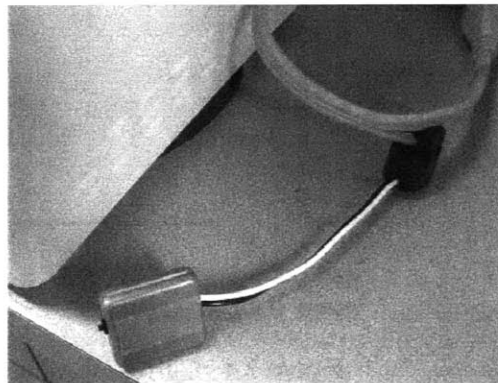


Figure 3.3: Close-up view of current sensor wrapped around split power cable

normal mode. Eight other appliances were also tested and their plots are available in Appendix F.

A total of two bread making cycles were needed to complete the current sensor test. During the first cycle the current sensor was placed in training mode and allowed to train for the entire bread making cycle. Once training was complete, a second bread making cycle was initiated and the current sensor was set to run in normal mode. Each bread-making cycle took three hours to complete. The current sensor completed training mode with a maximum current configuration consisting of the 147 Ω (high current) resistor selection and a gain of 7. Figure 3.4 shows the plot of the current sensing over the three hour bread making cycle.

From Figure 3.4, it can be seen that the training was successful. The current sensor was able to rescale the largest current value it detected to the maximum digital value the ADC can represent (the 10-bit ADC can represent inputs with a maximum

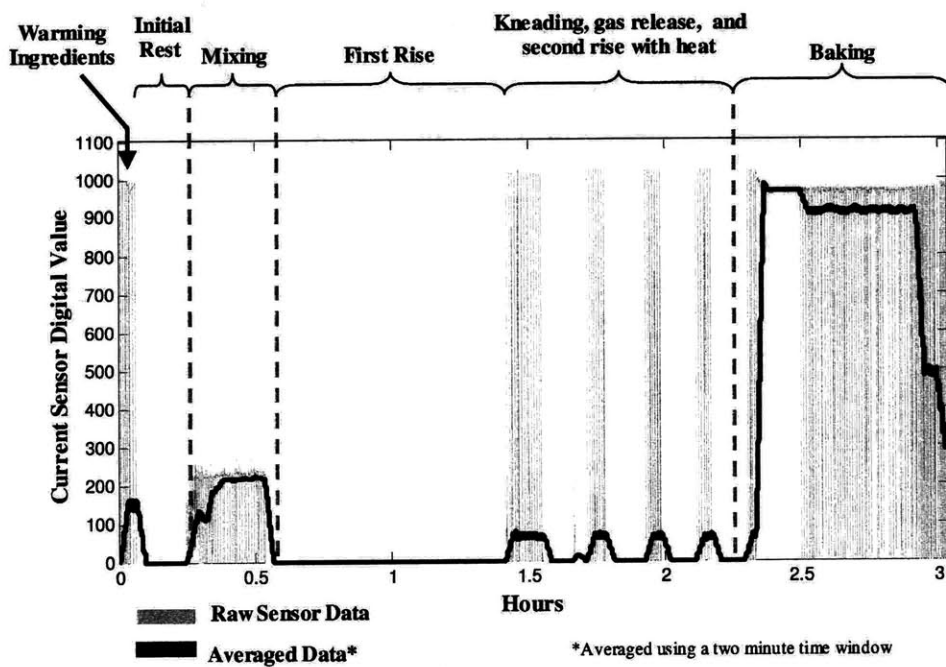


Figure 3.4: Current sensing results on bread making machine

digital value of 0 to 1023). From the plot, it is obvious that the heating element in the

bread making machine is responsible for the maximum current consumption. Current consumption from running the mixing motor is about a quarter of the maximum value.

The different regions of the plot can be segmented with some a priori knowledge about the steps involved in bread making (and some information from the machine's manual). The first step is a temperature equalization stage whereby all the raw ingredients are allowed to reach a consistent temperature (the machine actually warms up the ingredients above room temperature). The mixing stage shows current usage due to the mixing motor, which spins a mixing blade to blend the ingredients into dough. For the next hour, the machine essentially consumes no current which leads one to believe that the dough is being allowed to rise without perturbation. Following the first rise is a series of kneading/gas release and rise sequences which involve some mixing and heating. Based on the average current consumption, there is relatively little heat and mixing going on. The final stage is the actual baking which is easily identified by the relatively high average current consumption of the machine.

The bread making machine represents a complex appliance that exemplifies the training and current sampling abilities of the current sensor. Other appliances such as a lamp, blender, rice cooker, and toaster would provide similar plots that reflect their unique operational characteristics. From a JITQ perspective, the current sensor can be used on these types of appliances and others such as televisions or microwave ovens to provide some information on human behavior. For example scenario may involve a person using various kitchen appliances during the preparation of a meal. The current sensor could be used to monitor such appliances and provide some context as to when the preparation of a meal is occurring and what appliances are involved. TV watching could also be monitored in a similar way.

3.4 Limitations

The limitations in the current sensor's design are due to the discrete components that are used to build it. The high and low current resistors (147 Ω and 4.7 k Ω) limit the current sensing range to be from 30 milliamps up to 28 amps RMS. Appliances that consume current amounts beyond these ranges can not be represented by the full digital range of

the sensor. If an appliance uses more than 28 amps, the sensor's reading saturates. Appliances using less than 30 milliamps cannot be fully represented by the 0 to 1023 digital range of the sensor. For most household appliances, the sensor's range of sensitivity is adequate but very high current appliances such as large electric ranges can exceed the range of the current sensor. The current sensor can be modified to accommodate a larger current range but doing so requires the replacement of the high current resistor. The drawback of increasing the high current range is decreased resolution because the digital range gets stretched over a larger current range.

Another limitation is the current sensor's response time to changes in an appliances' current consumption. The resistor-capacitor (RC) low-pass filter used to attenuate the 60 Hz power line frequency has a time constant of 100 milliseconds. The step response, based on the time constant, reaches 98% of the final value in $4 \times RC$ or about half a second. Response time affects both the normal and training modes of operation. In normal mode, the sensor will not be able to detect current changes that occur faster than 100 milliseconds. The response time, therefore, limits the sampling rate to about 10 times a second. The sensor is, by default, set to sample every second to preserve battery life.

Training mode is also affected by the response time because the sensor must wait for at least half a second after switching resistors before it can take a current reading. If the sensor does not wait, it may read a current value that is lower than the true value because the capacitor did not have enough time to reach the correct voltage. The sensor can theoretically probe the current line up to twice a second but it is, by default, set to sample every four seconds—again to preserve the battery.

The current transformer has a physical limitation that requires it to wrap around one wire in power cord, not the entire cord. The current sensor does not work if the transformer is wrapped around the whole cord because the net current through it is zero. For correct operation the transformer must wrap around either the hot or neutral lines of the power cord. In some cases, the two lines in a power cord can be safely split using a sharp knife. Some power cords, unfortunately, cannot be safely split because they may not be adequately insulated. The universal solution is to use a three-prong extension cord

that can be split to accommodate the current sensor. The extension cord can then be used on any appliance without modifying its power cord.

3.4.1 Battery Life Estimation

The current sensor exploits the power-down state of the microcontroller to help prolong battery life. The two main components that consume power are the microcontroller and the Op-Amp in the gain stage. The Op-Amp in the rectification stage uses a negligible amount of current compared to the other two components. The microcontroller has a power-down state and an active state that use two microamps and three milliamps respectively. Transmission of packets occurs every second in normal mode and every four seconds in training mode. For each transmission the microcontroller is awoken from power down state for a period of about 35 milliseconds during which it samples (or probes), transmits, and powers down. The transmission packet is sent six times for redundancy and each packet consumes 16 milliamps for 500 microseconds. The Op-Amp constantly draws about 500 microamps in the worst case. The battery life estimates were computed for two cases: continuous normal and training mode. The continuous training mode scenario assumes that the current sensor does not have the 18 hour timeout to return it back to normal mode.

Table 3.2: Current sensor battery life estimates

Scenario	Estimated battery life*
Continuous normal mode operation (one second per transmission)	14 days**
Continuous training mode operation (four seconds per transmission and no 18 hour timeout)	17 days**

*Based on 220 mAh CR2032 Lithium coin cell

**Worst case estimate

3.5 Summary

The current sensor is an adaptable device that can provide a measurement of current consumption by an appliance over a large range (30 milliamps to 28 amps). The sensor utilizes a current transformer that wraps around an appliance's power cord and serves as a

passive means of monitoring electric current. The sensor has a “training” mode that allows it “learn” the maximum current consumed by an appliance and adapt to appliances that use different amounts of current. The sensor uses this maximum value to subsequently rescale its internal digital representation which allows for full-range representation of the measured current. From a JITQ context, the current sensor can provide information on the use of appliances around a household to provide contextual clues for human behavior and activities.

Chapter 4

Ultraviolet Radiation (UVR) Sensor

Skin cancer researchers require an understanding of the amounts of daily sunlight exposure people get. Researchers have used UV-sensitive spore-film based sensors to record total daily ultraviolet radiation exposure [7] but these sensors do not provide UV dosage information at a given time of the day—only a cumulative result for the whole day. A real-time sensor for UVR exposure that is inexpensive, yet portable would allow skin cancer researchers to better understand the sun exposure habits of people by providing real-time exposure readings and allowing for JIT questioning. For example, at times of peak sun exposure, questions could be asked to understand what a person may be doing during times of high UVR exposure. Being able to ask questions at the appropriate times may help researchers develop new ideas for context-sensitive interventions to reduce people's exposure to harmful UV radiation.

4.1 Related work

The one-time use film-based sensors used by researchers in [7] cost about \$50-70 each (including analysis services). Film prices are comparatively inexpensive to more sophisticated electronic sensors that can cost hundreds to thousands of dollars. Professional ultraviolet radiometers or dosimeters can measure UVR intensity and exposure in real time with great accuracy but tend to be large, bulky, and not easily portable. Dosimeters the size of wrist watches with their own data loggers exist and have been used in research studies [8]. The drawback to many existing dosimeter devices is either, (a) they are quite expensive, or (b) they are not easy to use in the context of JITQ because the logged data is not accessible in real-time. As part of the JITQ toolkit, a UVR sensor will provide cancer researchers as well human behavioral researchers with the

ability to obtain real-time UVR exposure information in an easy-to-use and relatively inexpensive package.

4.2 Design

The critical component of the UVR sensor is an ultraviolet-sensitive device that can convert irradiance to a measurable voltage or current. A microcontroller can measure the voltage or current and provide a real-time digital value that is proportional to the UVR irradiance at a certain time and place. Typical UVR sensitive components include photodiodes or phototransistors. The spectral response of the component must be carefully considered because not all wavelengths of radiation in the UV spectrum contribute evenly to erythema (tissue damage resulting in sunburn and cancer). The International Commission on Illumination (CIE) devised a reference action spectrum that describes the relative weighting of UV wavelengths with respect to their effect on erythema [9]. Using a photo-sensitive device with a spectral response that is similar to the reference action spectrum allows for more realistic readings of UVR exposure with respect to the effect on erythema.

Photodiodes are not difficult to use and are available with spectral responses close to the reference action spectrum defined by CIE. One design challenge to using photodiodes is the need to amplify the voltage or current that it outputs when illuminated with UVR. The current from a photodiode tends to be on the order of microamps, which is too small for most microcontrollers to read. An Op-Amp with a large (400 killo-ohms to 1 mega-ohm) feedback resistor is sufficient to amplify the signal from a photodiode for use with a microcontroller.

The photo-sensitive device can be packaged compactly with the MITes transmitter and worn on the body. The MITes transmitter reads the signals from the photodiode and transmits the corresponding digital value to the MITes receiver. A computer or PDA attached to the receiver can use the data to compute a real-time exposure value or simply report the current UV Index.

4.2.1 Implementation

The photodiode used to build the UV sensor is the UVI EryF Photodiode Sensor made by Sglux and distributed by Boston Electronics (at a price of \$45 each). The photodiode has a special optical filter that shapes its spectral response to conform closely to CIE's reference action spectrum. The output of the photodiode is proportional to the UV Index metric which can be converted to other standard units such as the standard erythema dose (SED).

Interfacing the photodiode to a microcontroller first requires a current-to-voltage conversion/amplification stage. The photodiode is designed for use in photovoltaic mode which means that no voltage is applied to the photodiode. Rather, the small current that is generated by the photodiode is used to create a voltage drop across a large resistor. For the amplification stage, a micro-power Op-Amp is used with an 800 k Ω resistor in its feedback path. The schematics and assembly instructions are provided in Appendix C.

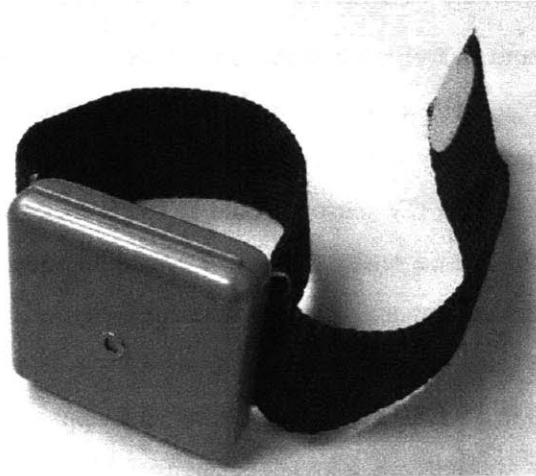


Figure 4.1: UVR sensor with wrist strap

This voltage from the Op-Amp's output is then provided to the MITes' analog-to-digital converter (ADC) to convert it into a digital value. The MITes transmitter can then transmit that digital value to a receiver. There exists a problem with the raw digital value, though. The digital value is proportional to the UV Index of the UVR irradiating the photodiode but the constant of proportionality is unknown and could change from

device to device. To convert the digital value to UV Index units, the UV sensor must first be calibrated against a known reference to obtain the calibration constants. This process is discussed in the performance testing and results section.

4.2.2 Estimated Cost Per Device

The UV-sensitive photodiode is the most expensive component of the UVR sensor. The following table summaries the estimated costs.

Table 4.1: Estimated Costs of the UVR sensor

Quantity	Estimated Price
Less than 80	\$90
More than 80	\$75

4.3 Performance Testing and Results

To test the operation and performance of the UV sensors, a reference UVR measurement source is needed for comparison. This reference will also be used to determine the calibration constants necessary to convert the digital reading into UV Index units. The ideal means of calibrating the UV sensors would be to have a controllable UVR lamp that can be set to specific irradiance settings. The UV sensor and a reference UV dosimeter would be placed under the lamp and readings taken as the lamp's irradiance is changed. Unfortunately, such a setup may be difficult to find and very expensive (a reference UV dosimeter can cost up to \$5000). Unfortunately, no such apparatus could be located in the Boston area. As a contingency, a less expensive (and less accurate) way of performing the calibration was developed that uses the information off a weather station website. The website provides periodic updates of the UV index throughout the day. Calibration of the sensor would involve collecting data throughout the day and comparing it to the weather station's reference data.

AccuWeather.com's weather service was used in the calibration of the UV sensor. A Java program was created to gather UV Index readings from the website every minute and store it a file. Gathering UV sensor data was done by manually placing the sensor in

direct view of the sun and logging the maximum digital value every 30 minutes. At the end of the day, the two data sets were compared and calibration constants were determined by running a best-fit algorithm on the data. The algorithm searches a range of calibration values and finds the set that minimizes the absolute difference (error) between the measured and reference data.

The results shown in Figure 4.3 and Figure 4.2 show the raw sensor data collected from two different sensors on a cloudless day and the reference data collected by the script from the AccuWeather website. The reference data is scaled by 1/40 just to bring it into view within the plots. Applying the best-fit algorithm, two calibrations constants are obtained. The first is a negative offset that is subtracted from all the sensor data values. The second is a scaling factor that adjusts the digital value range of the ADC (0 to 1023) down to the UV Index scale (0 to 16). The order in which the configuration constants are applied is offset first then the scaling factor. Both figures show the non-calibrated and calibrated data on the same plot.

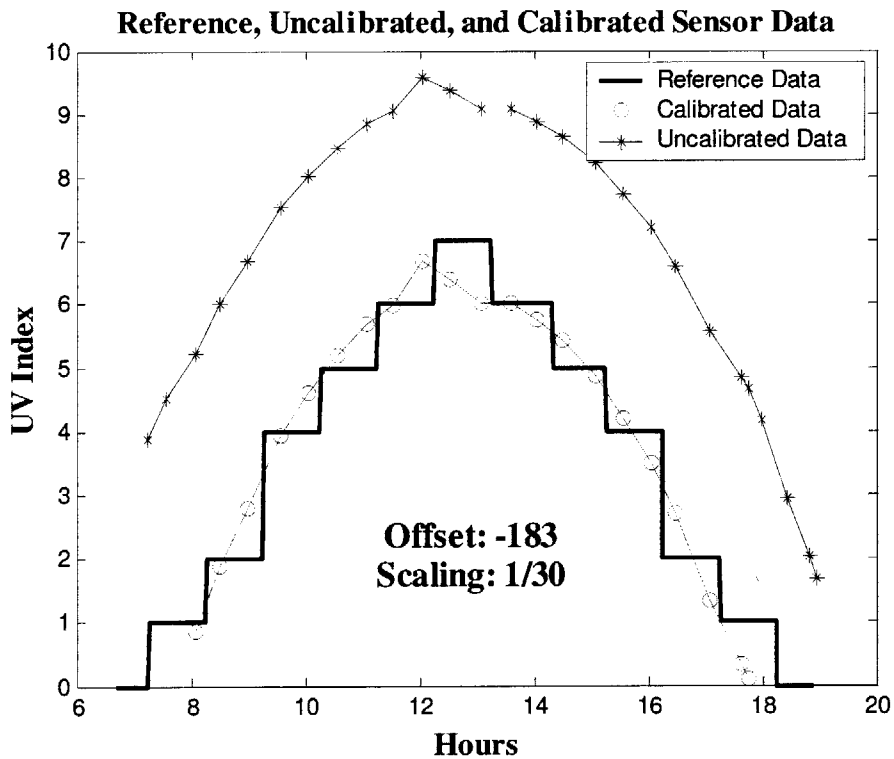


Figure 4.2: Sensor data calibration with UV sensor 1

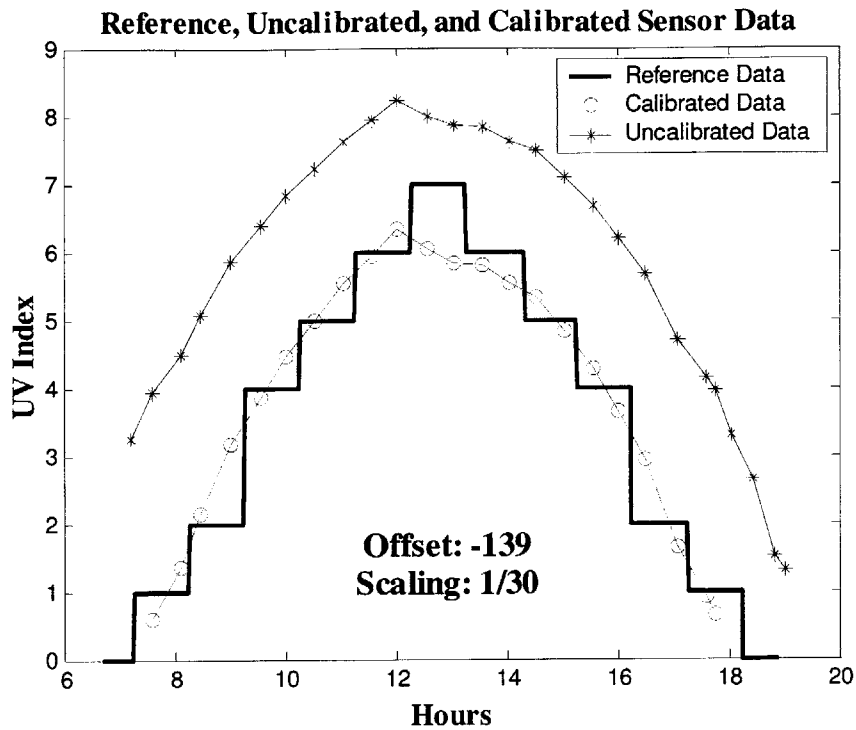


Figure 4.3: Sensor data calibration with UV sensor 2

The calibration constants calculated for each sensor show a difference in the offset but the scaling value remains the same. The offset difference can be attributed to minor differences in voltage sensitivity between the two MITes in the UVR sensors. More specifically, the MITes' have slightly different voltage sensitivities due to small variances in the values of its electronic components. Higher precision and smaller tolerance components could be used to build the MITes but such components would add additional cost to the devices. Ultimately, different UVR sensors will likely output different values for a given UV irradiance. Before any analysis, the calibration constants must be applied to the UVR sensor data. Doing so helps to normalize the readings across different sensors. The conclusion from the calibration test is that different sensors show small variances in their reading and must be calibrated individually to obtain their unique offset and scaling parameters.

The maximum UV Index that can be represented by the UV sensors can be derived using the calibration constants. The MITes device in each sensor has a maximum

digital range of 0 to 1023, which is due to the 10-bit ADC. For a maximum ADC value of 1023, the corresponding UV Index is 28 and 29 for UV sensors 1 and 2 respectively. These values lead to a UV Index resolution of about 0.027 per digital value.

4.4 Deployment

Plans are developing to make use of the UV sensor in a pilot study headed by Dr. David O'Riordan of the Cancer Research Center of Hawaii and Dr. Karen Glanz of Emory University. The study aims to determine the advantages (or disadvantages) of using electronic sensors versus the more common film-based sensors. The prospect of real-time data from electronic sensors is a strong motivation and advantage over the use of film-based sensors. Ultimately, the electronic UV sensors would serve as a basis for studying people's sun exposure habits and perhaps provide PDA-assisted intervention to help prevent overexposure and reduce the risk of skin cancer.

4.5 Limitations

The UV sensor has some limitations that affect its operation. The main limitation is the requirement for the UVR sensor to face the irradiance source (e.g. the sun) directly to obtain an accurate reading. This limitation is due to the physical construction of the UV photodiode. The photodiode's UVR sensitive area is recessed within its protective metal casing. Light that approaches at an angle larger than about 45 degrees is blocked from reaching the UV sensitive area by the walls of the metal casing. Unfortunately, the amount by which the sensitive area is recessed seems to vary slightly among photodiodes of the same type. A test involving the positioning of the UV sensor at different angles was performed to determine how different angles affect the amount of UV light received. Two different sensors were used to for comparison against one another. Table 4.2 displays the results of the test

Table 4.2: UVR sensor angle test results

Angle with respect to the sun	UV Sensor 1 reading	UV Sensor 2 reading
0 degrees	340	293
45 degrees	24	64
90 degrees	6	1

From the data in Table 4.2, a deviation of 45 degrees from the zero results in about 7% and 20% of the zero degree UVR intensity for sensor 1 and 2 respectively. From the data it is also evident that the sensitive area in sensor 1 is further recessed in the metal protective shell than in sensor 2. These results show give an idea of the limited angle range of the UVR sensor.

Reducing the angle limitation may be possible by using either a curved lens or more photodiodes. A curved lens placed atop the photodiode's opening can help reflect UV radiation toward the sensitive area at wider angles due to the domed shape. Unfortunately, acquiring such a lens may be difficult for a specific photodiode. Boston Electronics, the photodiode's distributor, does not carry or know of any such lens for the EryF photodiode.

An alternative, yet expensive, option would be to use more photodiodes and arrange them to face different angles. A microcontroller can read each photodiode and transmit the maximum reading. Unfortunately, at \$45 dollars per photodiode, this solution could be too cost prohibitive.

4.5.1 Battery Life Estimation

The UVR sensor is a fairly low power device that exploits the power-down mode of the microcontroller to prolong battery life. Only two components draw power: the microcontroller and the Op-Amp. The microcontroller is kept in power down mode most of the time but becomes active every second for about 35 milliseconds to sample and transmit a UV reading. The microcontroller draws only two microamps in power down mode and three milliamps when it is active. Each data packet transmission is done six times for redundancy to ensure the receiver receives the data. Each transmission draws

16 milliamps for 500 microseconds. The Op-Amp draws some operating power but it is ignored since it is negligible with respect to the microcontroller's power consumption.

The following table provides the estimated battery life result.

Table 4.3: UV Sensor battery life estimate

UV Sensor transmission rate	Estimated Battery Life*
One sample per second	62 days

*Based on 220 mAh CR2032 Lithium coin cell

4.6 Summary

The UV sensor is designed to be a wearable device that can provide real-time UVR exposure data. The UV sensitive photodiode is the principle component of the sensor and its spectral response is in close agreement with the erythema reference action spectrum determined by the International Commission on Illumination (CIE). The UVR sensor converts readings from the photodiode into a digital value which is then transmitted to a MITes receiver for further processing by a computer or PDA. The digital value can be converted to the UV Index scale by applying the calibration constants determined for each UVR sensor. The calibration constants are derived through a comparison of sensor readings with a reference (e.g. from a UV radiometer/dosimeter or weather station website). A best-fit analysis is performed on the sensor and reference data to calculate the actual calibration constants that minimize the error between the two.

Chapter 5

Proximity and Location Sensor

Knowledge of a person's location in a space or proximity to an object may allow researchers to determine better times to interrupt a person with Just-In-Time questioning. For example, a person who has positioned him or herself in front of a television for an extended period of time is possibly watching it. A computer can infer that the person is likely to be watching TV and decide that it is an appropriate time to ask TV related questions. Other types of sensors, such as on-body MITes, used in conjunction with the proximity and location sensor can also help algorithms that perform JIT querying to determine appropriate times to ask questions.

5.1 Related Work

There has been much prior work in sensor networks to determine the distance between people and objects. For example, the Cricket project developed at MIT consists of a collection of stationary RF/ultrasonic transmission beacons and wearable passive listener tags. The system uses a combination of radio frequency and ultrasonic waves for communication and positional measurements respectively. The beacons transmit ultrasonic waves that are detected by listener tags, and the relative distance of beacons to listeners is based on time-of-flight propagation of the sound waves [10]. The experimental accuracy of Cricket is defined in terms of a location granularity equal to 4×4 feet [10]. The location granularity value basically means that the minimum spacing of beacons is in a 4×4 feet grid which can locate listener tags within a square area of 4×4 feet. The use of two forms of communications helps to overcome the limitations of using RF or ultrasound individually. Although the MITes only communicate via RF and cannot make time-of-flight measurements, the idea of using beacons and listener devices is the basis of the proximity and location sensor. Cricket is fairly robust and low cost (<

\$10 per device [10]) but the system was not necessarily designed in the context of JIT questioning and thus may not lend itself easily to such an application. The beacon-receiver paradigm can be carried over to the MITes which would allow for an easier integration into a JITQ framework.

Position tracking within a JITQ context was implemented at House_n using infrared beacons and a wearable receiver [6]. By positioning the infrared beacons on a ceiling, a person wearing the receiver could be tracked as he or she moved around a room. The problem with using light as a tracking mechanism is the requirement for the receiver to be within line-of-sight of the transmitter. It could also be the case that infrared reflections can cause a receiver to inadvertently pick up light transmissions from beacons in different parts of a room. Thus, the infrared tracking system provides crude positional information [6]. Replacing infrared with MITes' RF signals provides a unidirectional means of implementing position tracking and proximity detection because RF can permeate a space more effectively than radiated light. Also, RF signals can travel through opaque objects more easily than light-based signals.

5.2 Design

MITes, unlike Cricket, are not designed for distance measuring, but the onboard microcontroller has a feature that can be exploited to provide such functionality. This special feature is a software controlled RF transmission output power adjustment mechanism. For normal operation, the MITes are run at the maximum output power which provides their maximum transmission range. There are a total of four output power settings which adjust output power and therefore the effective transmission range. A MITes transmitter can be set to cycle through the four antenna output power settings, sending data packets with each setting. These packets will be transmitted and received at different maximum distances or ranges because the propagation through the air varies. A receiver MITes device that happens to be out of range of the first two power settings but within range of the last two will, theoretically, only receive packets sent with the last two power settings.

The proximity and location sensor consists of a MITes transmitter (the beacon) which cycles through its output power settings as it sends RF packets to a receiver. Each RF packet contains a value from zero to three which indicates the output power setting used to send the packet (zero is the minimum power setting). The packets also contain the unique ID of the beacon to distinguish it from other beacons. A receiver MITes device is placed in a known location and continuously listens for transmissions from beacons. Placing the beacon right next to the receiver will allow packets sent with all four settings to be received. As the beacon is moved away from the receiver, the packets sent with the lowest power setting are lost in succession as the distance becomes greater than their respective transmission ranges.

In theory, the result of using varying output power settings is a rough determination of distance depending on the types of packets received by the receiver. The receiver can keep a running tab on the types of packets it is receiving. When the packets corresponding to setting zero are present, it can be assumed that the beacon is within that transmission range. The same idea applies to the other output power settings.

5.2.1 Implementation

Ideally, the MITes transmitter device should not require physical modifications to implement the idea of cycling through output power settings. Changes in firmware to instruct the microcontroller to change the output power settings were initially the only changes deemed necessary. Unfortunately, preliminary tests proved that there were two major problems with the beacons. The first problem was found by simply moving the beacon to different locations within an office space. The zero setting had an effective range that spanned across rooms and proved to be too large to useful room-level distance measuring. To facilitate room level distance measuring, setting zero must have an effective range of around two to three feet. The solution was to find some means of attenuating the output power by a significant amount to scale the range of setting 0 to the desired two to three feet. The ranges for the other power settings would also be scaled.

Attenuating the RF transmission signal beyond the capability of the microcontroller requires an external RF attenuation IC chip. The IC takes as input the RF

signal and outputs a signal of diminished strength. The HMC274QS16 digital RF attenuator made and distributed by Hittite Microwave Corp. was employed for this application. The attenuator IC attenuates the output signal by a fixed amount to scale down the transmission ranges. The procedure required to integrate the attenuator IC onto the MITes is described in Appendix D.

The second problem followed the first one and is an unfortunate consequence of the prototypical nature of the beacons. Integrating the attenuator IC initially appeared to be ineffective in reducing the RF transmission range for setting zero. The new range was noticeably diminished but still extended beyond room level distances. The problem was due to RF leakage caused by the imperfect hand-soldered connections and lack of a ground plane beneath the attenuator IC. Since the MITes board was not redesigned to incorporate an attenuator IC, imperfections introduced by attaching the attenuator IC to the MITes device's RF output were manifested in the form of RF leaks. The RF leakage originates from metal traces before the attenuation stage and overshadows the desired attenuated signal transmitted after the attenuation stage.

Fixing the problem required a means of blocking the RF leakage and only allowing the attenuated signal to be transmitted. The solution was to create a shielded box to encapsulate the MITes device and make an opening for the antenna to stick out. A pill box wrapped in eight to nine layers of aluminum ducting tape adequately blocked the leakage RF signals. The attenuated signal was allowed to propagate through a small opening on the side of the box.

The final form of the beacon is comprised of a MITes transmitter device modified to connect an RF attenuator IC (and chip antenna). The MITes transmitter is housed in an aluminum shielded pillbox case that can be opened for battery replacement service. The modifications needed to provide adequate behavior from the beacon was more than initially expected and unfortunately still suffers from some non-idealities. Still, the general behavior is as expected with setting 0 having a range of about 3 feet and the higher settings with successively larger ranges. The range results are shown and discussed in the performance testing and results section.



Figure 5.1: Proximity and Location sensor beacon

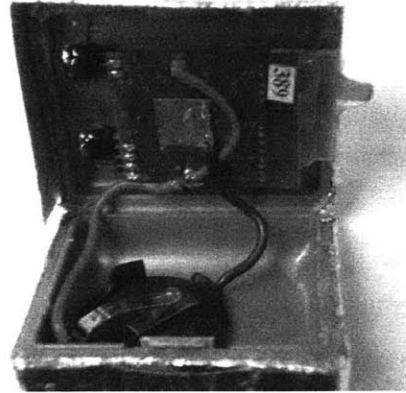


Figure 5.2: Interior view of beacon

5.2.2 Estimated Cost Per Device

The beacon has only a few components that do not contribute much to the total cost. The following table summarizes the estimated costs.

Table 5.1: Estimated Costs of the UVR sensor

Quantity	Estimated Price
Less than 80	\$48
More than 80	\$33

5.3 Performance Testing and Results

Two types of performance testing were performed to determine the effective range of each RF output power setting. The first test was designed to give a sense of the ideal or maximum performance. Thus, an open space with clear line-of-sight paths between the beacon and the receiver was used to simulate an ideal environment. The second test simulated a more realistic setting for room level distance measuring. The PlaceLab was used for the second test because of its home-like environment.

5.3.1 Open Space Environment

The first test was performed in a gymnasium with a large open area that allowed for clear line-of-sight paths between the beacon and receiver. To systematically map the transmission ranges to distances, a grid was constructed of 5.25 by 4.5 feet squares. The receiver was placed at the origin and the beacon was moved to each position on the grid directly facing the receiver. Over time, the receiver collects the packets corresponding to different output power settings sent by the beacon. A program written in Java was used to tabulate the received packets and provide a percentage probability for receiving each type of packet. The percentage received was calculated by dividing the total number of received packets of each type divided by the number transmitted by the beacon (a configurable option in the firmware program).

The transmission rate used in the first test was set such that the beacon cycled through all four output power settings three times per second. Thus, a total of twelve transmissions are sent by the beacon each second (actually, each transmission is sent 6 times for redundancy which gives a total of 72 transmitted packets but the Java program filters out redundant packets). The Java program tabulates data over eight second windows and provides a percentage for each output power setting. To obtain the percentages for each grid point, the average over four percentage values was calculated.

Figure 5.3 provides a plot of the grid points, the average percentages received for each point, and rough shapes corresponding to the range areas or *zones* for each output power setting. Each zone is labeled by a number corresponding to the minimum output power setting that packets can be sent and received. All packets sent with output power settings greater than the minimum setting for each zone can be assumed to be received as well.

As can be seen from Figure 5.3, the areas for each zone are not very uniform and in some cases actually contain points where no packets of any type were received. Zero reception points are an unfortunate and uncontrollable artifact of the non-uniform antenna radiation patterns associated with the beacon's antenna. The beacon's antenna radiation pattern is distorted due to lack of proper PCB layout for the attenuator IC and chip antenna. The metal shielded casing may also be causing some distortion through

reflections off its surface. An improved version of the beacon would require a redesign of the underlying MITes transmitter device to incorporate an attenuator IC with chip antenna.

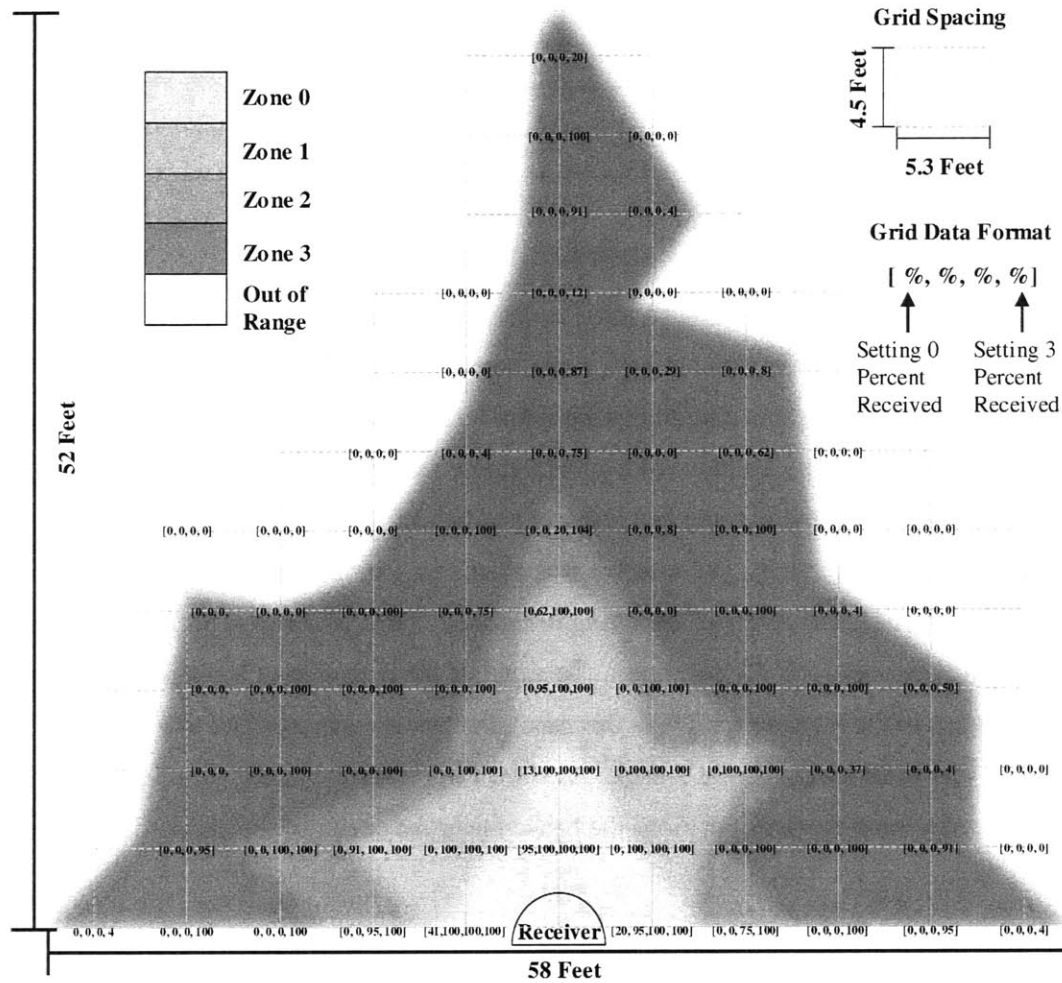


Figure 5.3: Open space beacon results.

The effective ranges for each output power setting are determined by averaging the distances of the boundaries of each zone with respect to the antenna position. Table 5.2 summarizes the approximate ranges for each output power setting.

Table 5.2: Average ranges for each output power setting in open space

Output Power Setting	Average range
0	8 ft
1	12.5 ft
2	16 ft
3	31 ft

5.3.2 Simulated Home Environment

The PlaceLab was used to provide a more realistic performance assessment of the beacon due to its home-like environment. Like a real home, the PlaceLab has living room furniture, tables, appliances and other such items. Thus, the beacon's performance at the PlaceLab would be representative of a general home setting.

In the home environment, the receiver and beacon were positioned differently than in the open space test. The receiver was placed on top of a TV, which is located against a wall near the corner of the living room area. Thus, all beacon position data was taken with respect to the TV's position. To simulate the detection of a person's position with respect to the receiver (or TV in this case), the beacon was attached to a wearable harness and worn around a user's neck. As shown in Figure 5.4 and Figure 5.5, wearing the beacon around the neck positions the beacon near the center of the chest. Such

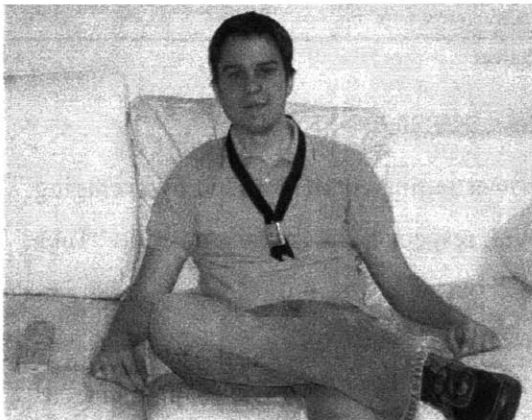


Figure 5.4: User wearing beacon



Figure 5.5: Beacon position on chest

positioning provides the least bodily obstruction when the person is facing the receiver.

Similar to the open space experiment, a grid of 3x3 feet squares was created to map different points throughout the living room and kitchen area. The person wearing the beacon was instructed to visit each grid point located on the floor or furniture. For points where the person could stand, measurements were taken for positions facing toward and 180 degrees away from the TV. On the sofa, the person could sit in a relaxed position facing the TV or lay down as if to take a nap. The percentages for each of the grid points were tabulated and labeled on two plots. The first plot (shown in Figure 5.6) shows percentages for each grid point corresponding to the person facing the TV (i.e. the beacon facing the receiver). The zones are colored with the same convention used in the open space plot. The second plot (shown in Figure 5.7) reports the reception percentages when the person is facing away from the TV. Zones zero and one do not exist because packets sent with output power settings zero and one are completely blocked by the body.

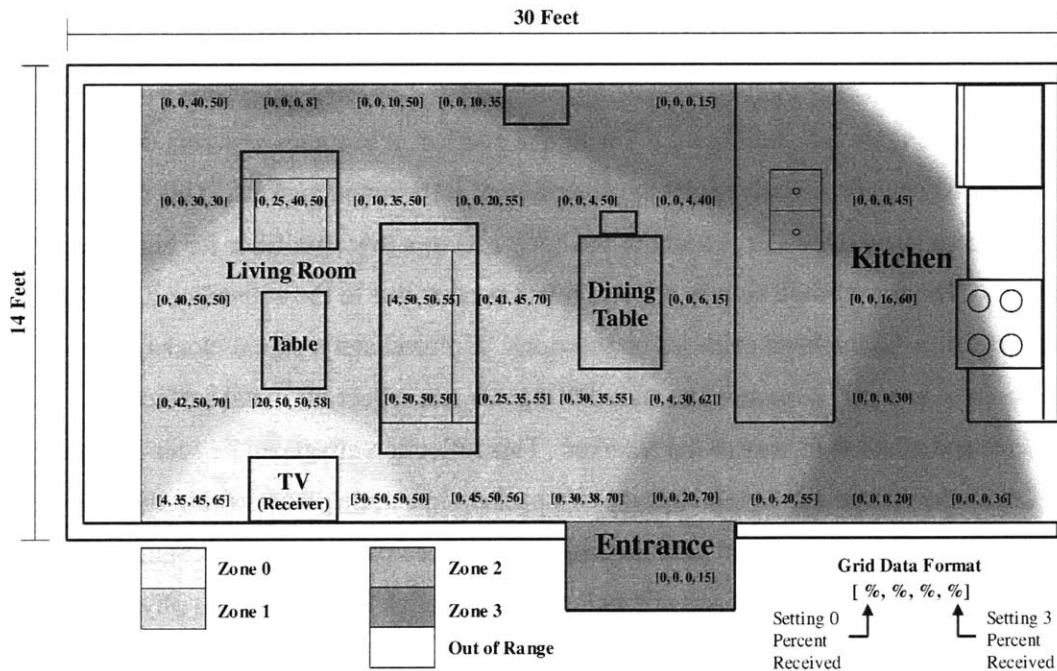
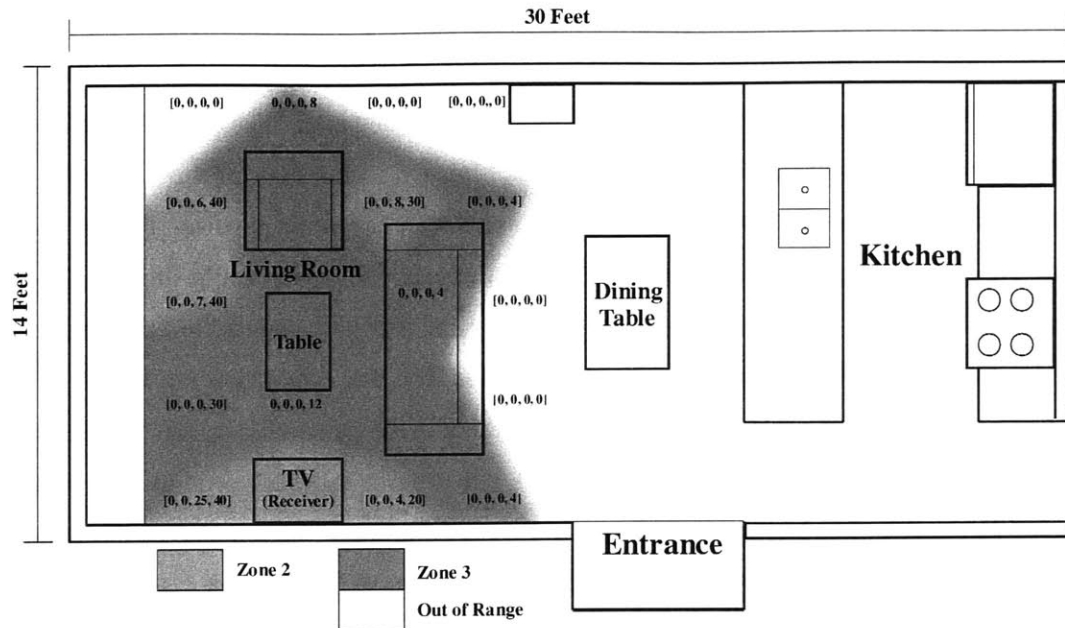


Figure 5.6: Zone demarcation with user facing toward TV



*Data on sofa indicates a laying down/napping position

Figure 5.7: Zone demarcation with user facing away from TV

Comparing Figure 5.6 and Figure 5.7 with one another, it becomes apparent that the human body can drastically affect the reception of transmitted packets. This is not unexpected since the water content of the body acts as a low pass filter for high frequency signals. The transmitted signals are also much weaker due to the attenuator IC and the imperfections in the hand soldered connections. Unfortunately, signal blockage due to the body is not very consistent because RF signals can reflect off metal surfaces or objects and make their way to the receiver. This reflection effect can be seen in Figure 5.7 from the sporadic reception of type two packets in certain places within the zone three. Ultimately, the system that tabulates the received packets must account for the possibility of losses due to bodily blocking—even though if the beacon is physically close to the receiver. With the receiver on the TV, it is usually the case that people will face the TV when watching it and therefore most packets will not be obstructed by the body. When a person is not watching TV, his or her body may be facing away which would lead to less received packets because most will be blocked.

The average ranges corresponding to the four output power settings for the case where a person is facing the TV (Figure 5.6) are shown in Table 5.3. For output power settings one and two, the average ranges are approximately the same as in Table 5.2. For setting zero, the range is about a third of the range in the open space case. This can probably be attributed to bodily interference since the beacon is worn close against the chest. The average range for setting three is not a true measure of the maximum range for zone three since it is clipped by the wall to the north of the TV.

Table 5.3: Average ranges for each output power setting in home environment

Output Power Setting	Average range
0	2.5 ft
1	10 ft
2	15 ft
3	20 ft

5.3.3 Choosing Operating Parameters

Effective operation of the beacon requires knowledge of certain configuration parameters. These parameters include the packet transmission rate, battery life of the beacon, and the number of different beacons in use simultaneously. Each parameter has an associated set of tradeoffs that should be considered when choosing parameter values.

High transmission rate is critical to obtaining the most accurate and updated beacon location information. In the open space and home environment tests, a rate of 12 transmissions per second (72 transmissions when including redundant packets) was used. High transmission rate is useful because it helps to overcome packet loss due to imperfections in the beacon's construction and obstacles that may block transmission. Lowering the transmission rate places more importance on the successful reception of each packet. Another benefit of high transmission rate is quicker updates on the current positional information of the beacon. In the tests, the Java program used a four second window to tabulate the incoming packets and present results. Thus, there is a four second

delay between position updates. Decreasing the transmission rate would require widening the listening window in order to receive the same number of total packets. A significant decrease in transmission rate could require a time window on the order of minutes. In such a window, a person may have enough time to move around in a space without an update in positional information during such movement.

High transmission rate is inversely related to the battery life of the beacon. Each packet transmission consumes battery power in addition to the power needed to run the microcontroller. A lower bound estimate of the number of days the beacon can last transmitting 12 unique packets a second is approximately five days. Such a transmission rate may be suitable for week long experiments but insufficient for anything longer without battery replacement. Lowering the transmission is an option but it might require a larger listening window which leads to slower positional updates.

The final parameter is related to the issue of using multiple beacons simultaneously. In the test performed in the home environment, only one physical beacon was used but the receiver was configured to listen to five other RF channels. This receiver configuration gives the illusion that five other beacons (or other MITes sensors) are used. The receiver time multiplexes the different sensors by listening to each one for five milliseconds one after the other. Unfortunately, the more channels there are, the lower the effective sampling rate for each channel. The beacons make up for the lowered sampling rate by sending each packet six times for redundancy. There are different MITes sensors such as on-body accelerometer MITes devices that rely on a high receiver sampling rate. Since it is common for a MITes receiver to listen to many different types of sensors on different channels, it is important to use as few channels as necessary to maintain the highest receiver sampling rate for each channel. Each beacon should be placed on their own unique channel so as not to interfere with the signals of other beacons. As a result there is a tradeoff with number of beacons and other sensors versus the maximum sampling rate the receiver can physically achieve.

It may be possible to place multiple beacons on the same channel without a chance of collision. Doing so would require reducing the transmission rate to a point where the beacon transmission intervals can be interleaved without overlap. Two

beacons can be placed on the same channel and guaranteed never to collide if they are synchronized to transmit once on alternating seconds. To achieve this behavior, the beacons must first be set to transmit one packet (actually six redundant packets) every two seconds. Next the beacons are synchronized by powering up the first followed by the other beacon one second later. Since they are synchronized to be one second apart in transmission, it is guaranteed that their RF packets will not collide. The same procedure can be generalized for more than two beacons at the expense of decreasing their transmission rates. In practice, such slow transmission rates take longer to tabulate and most packets may be lost due to the body or other obstacles. Such slow transmission rates are better suited for tracking objects that occasionally get relocated to different positions within a room.

5.4 Deployment

Currently the proximity and location sensor are planned for use in a University of North Carolina study related to people and their TV watching habits. The beacon and on-body accelerometer MITes will be worn by family members in their home. A receiver is placed on or near the TV in order to obtain beacon positions with respect to the TV. The proximity of a person wearing the beacon to a TV can be derived from the types of packets received (or not received). The on-body MITes devices provide extra context based on movement. Combining the data from the beacon(s) and accelerometers provides a richer set of data that can be used to determine the likelihood that a person is or is not watching TV.

5.5 Limitations

The proximity and location sensor are limited in many ways mainly due to the weakness of the transmission signals and the imperfections in the solder connections of the attenuator IC and chip antenna. The weakness of the signal is advantageous because it limits the range of the beacon's transmissions and gives rise to room level distance measuring. Unfortunately, such weak RF signals can be easily blocked by the body (as

seen in Figure 5.7). Other people standing in the line of sight path between the beacon and the receiver can also block the signal. A computing device which interprets the data must allow for some error due to signal blocking and perhaps filter out fast changing data.

Irregularities in the radiation pattern of the antenna on the beacons can be attributed to the imperfections in the soldering. Hand soldering the attenuator IC and chip antenna without the proper ground plane layout and PCB trace sizes distorts the radiation pattern. As a result, the zone demarcations are not very smooth and continuous. Another consequence of the distorted radiation pattern is the presence of spots within the different zones where there is zero reception of all packet types. These areas of zero reception tend to be small (one to two feet square). To improve the radiation pattern, the MITes device must be redesigned to incorporate an attenuator IC with either a chip or microstrip antenna (the latter being the less expensive option). Proper ground plane layout with correct trace sizes should improve the continuity of the radiation pattern.

5.5.1 Battery Life Estimation

The beacon's battery life is directly related to its transmission rate. Operating the beacon at the relatively high transmission rate of 12 transmissions per second (72 total transmissions) is offset by an operation time of about five days. A slow rate such as one transmission a second can provide much longer operation time at the expense of longer tabulation time and slower position updates.

Calculating the battery life is based on the current consumption of the MITes' microcontroller when it is powered down and actively transmitting. Powered down state only consumes two microamps. When actively transmitting, the microcontroller uses three milliamps plus a maximum of 16 milliamps per transmission. Each transmission takes 500 microseconds with a total of 6 transmissions for every packet (for redundancy). The microcontroller remains active for about 35 milliseconds for each distinct packet transmission. Table 5.4 provides battery life estimates for three different transmission rates. The first rate was used for the performance testing. The second is half the first

rate. The last rate estimates the beacon's battery life with a relatively slow transmission rate of one transmission per second.

Table 5.4: Beacon battery life estimates

Transmission Rate (redundant rate)	Estimated Battery Life*
12 (72) transmissions per second	5 days**
6 (36) transmissions per second	10 days***
1 (6) transmissions per second	62 days

*Based on 220 mAh CR2032 Lithium coin cell

**In practice actual time is about 4 ½ days

***In practice actual time is about 8 days

5.6 Summary

The proximity and location sensor consists of one or more beacons and a standard MITes receiver. The beacon utilizes a feature that allows it to send RF packets of varying transmission range by varying the output power used to send each packet. The beacon cycles through output power settings as it transmits packets. Depending on the distance of the beacon with respect to the receiver, certain packets sent with weakest output power settings may be lost. The loss of such packets provides an indirect measure of the distance of the beacon from the MITes receiver because each output power setting has a finite range of transmission. Thus, by keeping track of the packets sent with the weakest output power setting, a beacon's distance can be roughly determined within a radius of the receiver's location.

Chapter 6

Multi-Switch Input Sensor

As more of a convenience than a novel feature, a multi-switch input sensor is made part of the JITQ sensor toolkit. This sensor basically allows for up to 10 direct switch inputs or up to 25 inputs in a matrix configuration. From a JITQ standpoint, switch sensors provide real-time information that can be used to ask questions based on patterns of pressed and released switches. Many possible applications exist from keyboard-like devices to sensing events such as opening/closing cabinets.

6.1 Design

The microcontroller on the MITes transmitter has a total of eleven input/output (I/O) pins that can potentially be used as switch inputs. Of the eleven, one pin cannot be used because it is used to control the EEPROM memory chip which contains the firmware program. Thus, there are ten potential inputs that can be connected to switches. Some devices, such as a keyboard, may require more than ten switch inputs. A total of 25 switches can be sensed using a matrix configuration. The microcontroller can quickly scan all the switches by rows and columns to see if any have been pressed. Another feature of the multi-switch sensor is its ability to detect if multiple switches are pressed. The main benefit of multiple switch press recognition is the multitude of switch combinations that are realizable.

Direct switch connections are the simplest to implement for the multi-switch sensor. Each switch is independent of one another and can be pressed individually or simultaneously with other switches. The microcontroller simply polls the I/O ports individually and reports the switch states. For direct connection the switches connect directly to the I/O ports with either pull-up or pull-down resistors. In pull-up configuration, a logic low value is sent to the I/O pin when the switch is pressed and a

high value otherwise. The pull-down configuration is the opposite whereby a pressed switch signals logic high and a logic low otherwise. The pull-up and pull-down switch schematics are seen in Figure 6.1. Both configurations work equally well but the pull-up configuration was arbitrarily chosen for the multi-switch sensor.

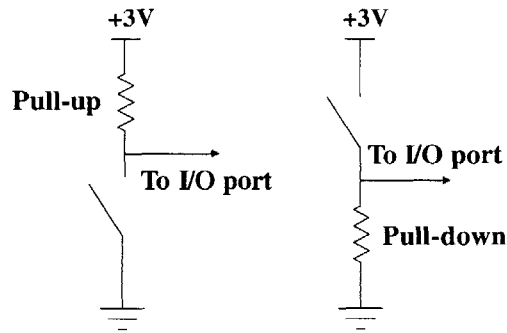


Figure 6.1: Pull-up and pull-down switch configurations

To get more switch inputs than the amount possible through direct connection, a matrix configuration can be used. The cost of using a matrix configuration is complexity in the firmware and restrictions on certain switch press combinations. Using a matrix to arrange switches is not a novel idea and is in fact used in computer keyboards and other grid-like input interfaces. The design and functionality of the matrix configuration shown here is based on a wireless keyboard design described in a white paper by Nordic Semiconductor [11]. The basic idea behind the matrix consists of switches arranged in a grid as shown in Figure 6.2. The grid is simplified to have only four switches for this example but can be generalized to N by N switches (five by five is the absolute max for a MITes transmitter). Each switch connects to a row and column and is uniquely identified by their row and column numbers.

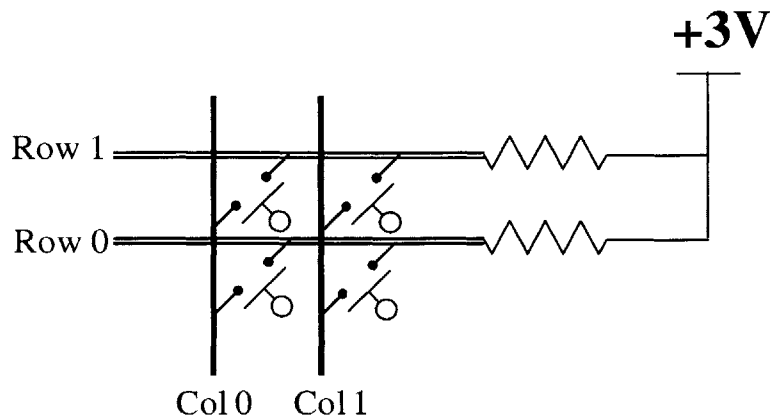


Figure 6.2: Simple matrix layout

The microcontroller scans the matrix by placing a bit pattern on the column lines and reading the resultant outputs on the row lines. The bit patterns place a logic zero on a single column while setting the other column lines to logic one. If a button is pressed on a column line that is driven with a logic zero, the corresponding row will output logic zero instead of the usual logic one. The presence of a logic zero on a row line is a clear indication that a switch is pressed. Pressing multiple switches results in multiple zeros reported through the row lines.

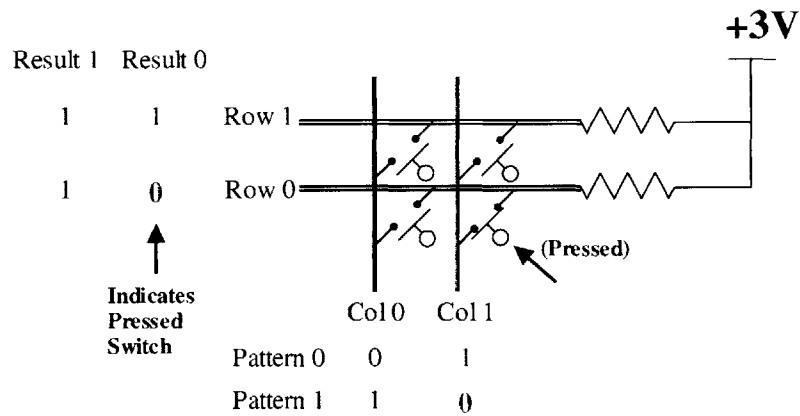


Figure 6.3: Matrix scanning example

Detecting multiple switch presses is a difficult task if the wrong paradigm is used. For example, one approach is to transmit the switch states as soon as a user presses them. The problem is that from the microcontroller's perspective, a multiple switch press may look like several individual switch presses done very quickly in succession (on the order of tens milliseconds). The user may believe that all the switches were pressed at once, but the microcontroller is fast enough to see each individual switch press. The microcontroller, therefore, interprets the switches pressed individually, not as a group. This problem is a type of race condition.

To eliminate the problem, a different switch pressing paradigm is used. Switches pressed as a group must first all be pressed down and then released to commit the switch presses. The microcontroller takes note of which keys are pressed and when one or more switches are released, it transmits the original pressed switch state. This new paradigm eliminates the possibility that the microcontroller will misinterpret a multiple switch press because the race-condition is eliminated. A user can take an indefinite amount of time pressing all the switches that form a group and then simply release one or all the switches to transmit the pressed value. The press-then-release paradigm of switch pressing is used for both direct and matrix configurations in the multi-switch sensor.

6.1.1 Implementation

The multi-switch sensor's design consists of some hardware (wiring the switches) but is mostly firmware. The multi-switch sensor's firmware program is where most of the sensor's design takes place. The firmware contains the algorithm that scans the I/O ports in both direct and matrix configurations. A user must specify in the firmware code the I/O pins and configuration (direct or matrix) used by the multi-switch sensor. This specification is done through C-style #DEFINE constants and is documented in the firmware source code file.

The output format of the multi-switch sensors is in the form of a bit field where each bit represents a switch. The bit is set to one if a switch is pressed and zero otherwise. The multi-switch sensor scans the I/O ports in ascending numeric order and creates the output binary representation to reflect that order. For example, if I/O pins

DIO2 to DIO5 are used in direct configuration the algorithm would scan DIO2 first then DIO3 and so on to DIO5. The output binary representation for the switch states would be four bits long where the first bit (bit zero) would correspond to the state of the switch on DIO2 and the last bit (bit three) would correspond to DIO5. A program that interprets these binary outputs would simply check to see if a bit is set to one to determine if one or more switches is pressed.

The output format changes when using the matrix configuration because the firmware program uses a more complex scanning routine. As shown in Figure 6.3, the microcontroller drives the column lines sequentially with logic zero and the outputs on the rows indicate if any switches are pressed. As the columns are driven with logic zero in ascending order, the output from the row lines are read and concatenated to a binary string by the firmware program. The final binary string becomes the multi-switch output and contains state information from all the switches in the matrix. The number of bits in the output will be equal to the number of rows times the number of columns in the matrix. For the example matrix given in Figure 6.2, the output binary representation will look like the binary string of Figure 6.4. In general, the rows for each column are concatenated in ascending order with ascending column order. Bit zero corresponds to the switch located at row and column zero. The last switch in the matrix (at the opposite corner of the first) corresponds to the last bit in the binary string.

1	0	0	0
Row 1	Row 0	Row 1	Row 0
Col 1	Col 1	Col 0	Col 0

Figure 6.4: Example matrix data format

A final feature of the firmware program is an idle state which consumes less power and preserves battery life. The firmware keeps track of switch press activity and after 10 seconds of inactivity, the multi-switch enters idle mode. In idle mode, the microcontroller is put into a power down state which consumes only two microamps of

current. The microcontroller checks the switches every 30 milliseconds in idle mode and switches back to normal mode if it detects any switch presses.

The firmware program takes care of the scanning of the I/O ports but it is the hardware switches that provide the actual inputs. The switches must be wired in pull-up configuration. For direct switch configuration, it is sufficient to simply follow the diagram of Figure 6.1 for each switch. In matrix configuration, some planning is required prior to wiring the switches. First, the switches must be assigned to unique positions within a matrix. Assignment means that each switch will be a member of a row and column and the [row, column] coordinate will be unique for each switch. Each switch consists of two terminals one of which connects to a column line and the other to a row line (the decision is arbitrary but must be consistent). The wiring is done by connecting all the switches to their respective row lines and then to their respective columns. The row lines at one end must terminate with 10 kilo-ohm pull-up resistors connected to the +3V power supply (as shown in Figure 6.2). The other end of the row lines are inputs to the microcontroller. The column lines only connect as drivable output lines to the microcontroller.

One important difference between setting up the firmware for direct and matrix configurations is the direction of the I/O pins that are used. Microcontrollers can set the direction of their I/O pins as either inputs or outputs but not both. For direct switch configuration, all I/O pins are set as inputs since the switches drive the pins directly. In matrix configuration, the row lines connect to input I/O pins and the columns connect to output I/O pins. In the firmware source code, there is an option to specify which pins are inputs or outputs. Output pins do not apply to direct switch configuration and therefore the firmware ignores any output pin settings.

6.1.2 Estimated Cost Per Device

The multi-switch sensor does not make use of any components that add significantly to the cost of the MITes transmitter. The cost of each device is simply to cost of the MITes transmitter which is \$41 in quantities less than 80 and \$26 each for more than 80.

6.2 Deployment

The multi-switch sensor was used in a chording keyboard designed by Alex Mekelburg, an MIT mechanical engineer. Mekelburg created a QWERTY-style hand-wearable typing device that utilized 15 separate switch buttons in matrix configuration. The buttons could be pressed individually or in combinations (chords) to achieve the different characters available on a traditional QWERTY keyboard. A multi-switch sensor was used to interpret the button presses and transmit them wirelessly to a Java program. The program interprets the key presses and displays them on the screen. Ideally, the device could provide a more efficient, alternative keyboarding interface to a PDA or laptop computer.

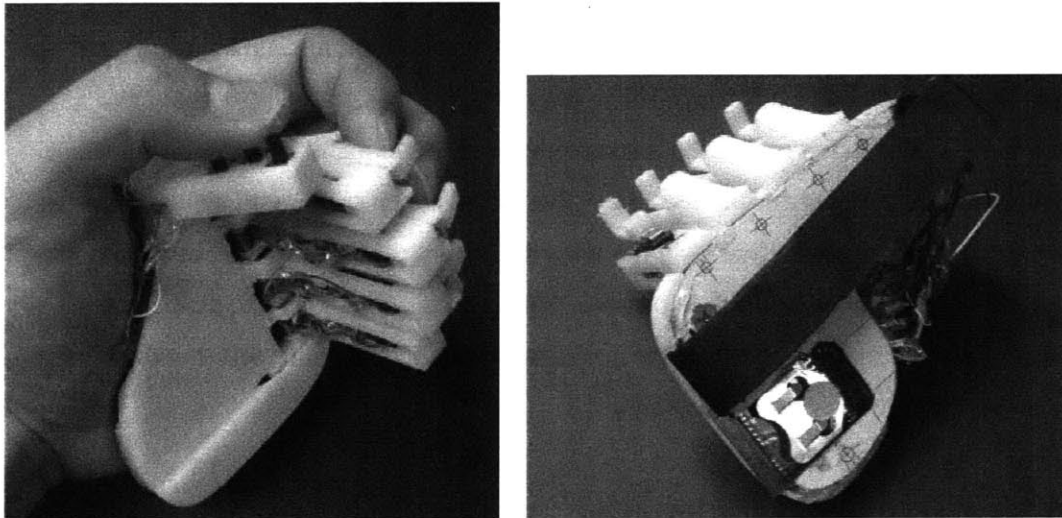


Figure 6.5: Wearable chording keyboard by Alex Mekelburg

6.3 Limitations

The multi-switch has some limitations that affect its operation. The first limitation affects the actual amount of switch data that can be transmitted by the MITes device. Although the multi-switch sensor is physically capable of processing up to 25 switch inputs, the current transmission protocol only allows up to 11 switch inputs to be transmitted (13 if two non-essential bit fields are overridden). It is possible to transmit up

to 25 switch inputs, but this requires overriding the ID field in the transmission packet, which may be undesirable if the ID field is needed to distinguish among several multi-switch devices. The firmware code has an option to override the ID field if the user requires more than 13 switch inputs.

Another limitation affects matrix configurations by limiting the number of distinct switch press combinations. The example matrix of Figure 6.2 can be used to illustrate the distinct switch press combinations. First all, pressing any number of switches in one row or column does not have any limitations. If a row or column has N switches, there are $2^N - 1$ possible combinations. There are also no limitations if multiple switches, one from each row or column, are pressed as a combination. The limitation occurs if two switches in the same column and adjacent rows are pressed along with a switch from a different column but in one of the same two rows. This switch combination turns out to be indistinguishable from pressing two switches in the same column and adjacent rows and two other switches of a different column but the same rows. In our example matrix, pressing both switches of column zero and the switch of column zero and row one is no different than pressing all four switches. The multi-switch sensor will always return an output indicating that all four switches were pressed. In some cases this limitation may not affect an application if the ambiguous combinations do not need to be distinct. A key mapping could make only one of the combinations valid and while defining the other equivalent combinations to be invalid.

6.3.1 Battery Life Estimation

The multi-switch has two different modes of operation that affect its power consumption. The first is the normal active mode whereby the microcontroller is powered up and is processing the outputs. The second is an idle mode which is entered when there is at least 10 seconds of user inactivity. The idle state consumes far less power than the normal active mode (two microamps versus three milliamps) and can help to prolong the life of the battery.

Each switch press also consumes power due to the dissipation of current through the pull-up resistor for each switch press. Multiple switch presses consume more current

than single switch presses. The duration that a switch is held also contributes to the amount of consumed power.

Estimating the battery life is based on the power consumption of the device in the various states it can occupy. When operating normally with no buttons pressed, the multi-switch device draws a continuous three milliamps. Each button press draws 0.3 milliamps. In idle mode the multi-switch draws only two microamps but it returns to normal mode every 30 milliseconds to check for switch presses, which takes about 2 milliseconds. The following table provides battery life for three scenarios. The first is a perpetual idle state to determine the estimate for the maximum battery life possible with the multi-switch. The second is perpetual switch pressing which involves three keys pressed down for two-tenths of a second, three times a second. The last scenario is the case where three buttons are pressed and never let go. Table 6.1 provides the battery life estimates.

Table 6.1: Multi-switch sensor battery life estimates

Scenario	Battery Life* (estimated)
Idle Mode	45 days
Three keys continuously pressed three times a second (held down for 200 ms)	62 hours
Three keys continuously held down	56 hours

* Based on a 220 mAh CR2032 Lithium cell

From the above table, there is a large gap in battery life between the idle mode and other two scenarios. In the general case the multi-switch can probably last two to three weeks with a few hours of continuous usage each day since the remaining time is dominated by idle state power consumption.

6.4 Summary

The multi-switch sensor of the JITQ toolkit interfaces to a set of physical push button switches and transmits their state data wirelessly to a MITes receiver. Switches can be

setup in a direct or matrix configuration depending on the number of switches that are needed. Up to 10 input switches can be interfaced directly or up to 25 with a matrix configuration. Switch presses are processed according to a press-then-release paradigm whereby switches must first be pressed then released in order to transmit the switch states. The multi-switch sensor can be applied to almost any application where switch state monitoring is needed such as keyboards and other tactile-based user interfaces.

Chapter 7

Conclusion

The Just-In-Time questioning toolkit was developed to provide researchers from different fields of study with a set of sensors to aid in the study of human behavior. Many sensors available to researchers are difficult to use or do not provide real-time data that is easily accessible. To address such difficulties, each sensor of the JITQ toolkit was designed with four general criteria: robustness, ease of use, portability, and affordability.

Robustness was a prime consideration when designing the electronics and physical specifications of each sensor. For example, the use of a voltage level shifter on the HRM sensor helps to prolong the life of the microcontroller by minimizing stress on its I/O ports. Zener diodes were employed to prevent analog input voltages from exceeding the specifications of MITes. Physically, each sensor was made robust through the use of pillbox containers and minimal wiring practices. Pillboxes were used for their convenient size and rigid construction. The HRM, UVR, beacon, and current sensors all make use of pillboxes to protect MITes and other electronics from static discharge and collision damage. Wiring was kept to a minimum by using protoboard adapters and solder bridges wherever possible.

The sensors were designed to be easy to use to minimize the amount of training and knowledge needed to operate them. The current sensor utilizes a toggle switch to allow a user to switch between training and normal modes. As an added convenience, the current sensor automatically switches to normal mode after 18 hours of training. The other sensors such as the HRM, UVR, and beacons simply require the battery to be inserted to begin operating. Some tasks such as calibrating the UVR sensors are difficult to do without the right equipment, but once the sensors are calibrated, they operate without further intervention.

Portability was a key feature for the sensors of the toolkit. Sensors that can operate with their own power supply and transmit data wirelessly can be taken almost

anywhere for data collection. The MITes were used as a platform for all the sensors of the JITQ toolkit because of the built-in wireless capability and the coin-sized battery power supply. Each sensor has a MITes transmitter at its core and utilizes the wireless link to transmit data. The compact lithium cell is used by all sensors (except the HRM) and contributes greatly to their portability.

The last of the criteria that influenced the design of the sensors is affordability. Based on the cost estimates, no sensor in the JITQ toolkit costs more than \$100 to make (the most expensive being the HRM at \$92 each). Many of the commercially available sensors will tend to cost more because they have more features than the toolkit's sensors (e.g. the Watt's Up versus the current sensor). The sensors of the JITQ toolkit have the advantage of being designed specifically for JITQ whereas many commercial sensors are not. Using the toolkit's sensors is cost effective because they do not require further modifications, parts, or third-party software to provide the real-time data needed for Just-In-Time questioning.

In summary, the toolkit's sensors fulfilled most of the four criteria, though some more than others. Using the sensors in a Just-In-Time questioning framework can prove useful for studying human behavior. Ultimately, the goal of the toolkit is to allow researchers to acquire new types of data and knowledge that could not be easily (or inexpensively) obtained before.

Appendix A

MITes Standard Extension Modifications

The following section provides directions for extending features on an unmodified MITes device. These features include increasing access to I/O pins and the analog-to-digital converter of the microcontroller. Modifying a MITes device to incorporate these extensions is necessary for some of the sensors developed in the JITQ toolkit and for uses beyond the scope of this document.

A.1 Increasing Access to I/O Pins

An unmodified MITes device only provides two externally accessible I/O pins (as seen in Figure A.1). These pins are connected to bit 3 and bit 6 of Port 0 respectively. Other I/O pins are routed on the PC board of the MITes device to read and control various components such as the on-board accelerometer and the EEPROM IC.

There are a total of 11 I/O pins available on the nRF24E1 microcontroller with 3 on Port 1 and 8 on Port 0. Each one of these pins can potentially be accessed and connected to a pin header for external access. Unfortunately, some I/O pins are restricted in use because they cannot be completely decoupled from their original functionality. Table A.1 itemizes the restrictions on each I/O pin.

Table A.1: I/O Pin Restrictions

I/O Pin	Alias	Restriction
PORT0.0	DIO2	Cannot be used because it controls operation of EEPROM
PORT0.1	DIO3	Input/Output
PORT0.2	DIO4	Input/Output
PORT0.3	DIO5	Input/Output; remove pull-down resistor R9 for general use
PORT0.4	DIO6	Input/Output; power off or remove accelerometer prior to use
PORT0.5	DIO7	Input/Output; same restrictions as DIO6

PORT0.6	DIO8	Input/Output
PORT0.7	DIO9	Input/Output; SOT-23 transistor (T1) should be removed for best results
PORT1.0	DIO0	Input/Output; special care must be taken to ensure this pin is not loaded prior to the MCU's entrance into the main firmware code.
PORT1.1	DIO1	Input/Output; same restriction as DIO0
PORT1.2	DIN0	Input Only; same restriction as DIO0

Making the I/O pins externally accessible requires soldering wires from the I/O pin to a pin header. Pin headers provide a robust means of connecting other devices and boards to the MITes. Not all the wires connecting the I/O pins to the pin header need to be soldered directly to the physical pins of the microcontroller IC. Various pads exist that are connected to the I/O pins and can serve as an alternative soldering point that is less difficult to solder. Figure A.1 points out the locations where wires can be soldered to access each respective I/O pin.

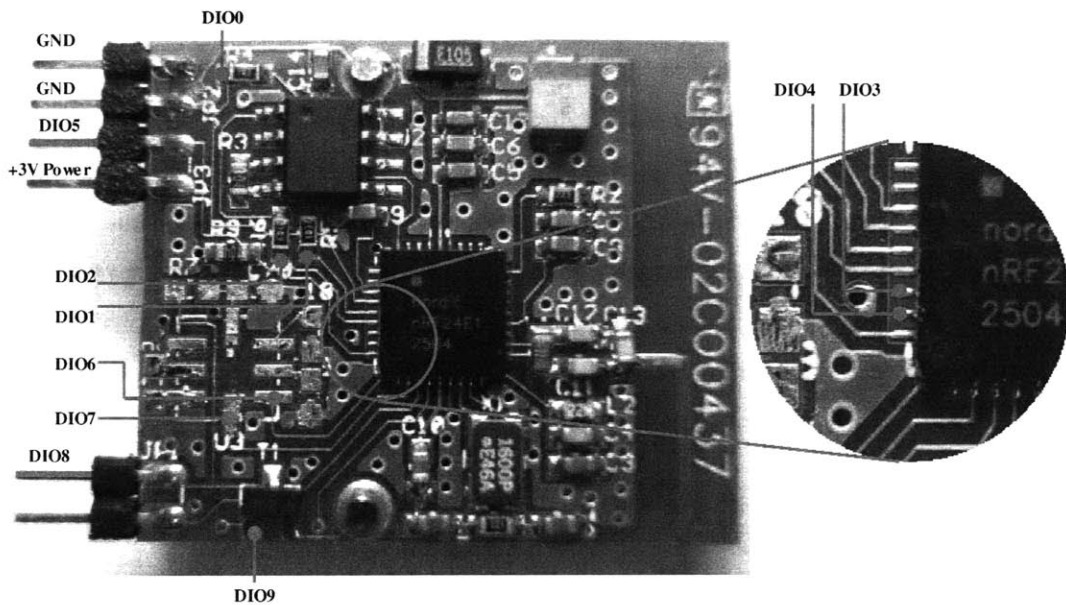


Figure A.1: Solder points to access microcontroller I/O pins

A.1.1 Materials

Qty	Part Description	Place of Acquisition	Part Number/Identifier
1	2mm 6-pin header	Digikey Corp.	S2106-06-ND
1	MITes Transmitter (unmodified)	See Appendix G	N/A
N/A	Hot glue	craft store	N/A

A.1.2 Pinout Diagram

The pinout diagram of Figure A.2 is provided as an example I/O extension. Figure A.1 must be used in conjunction with Figure A.2 to determine which solder pads connect to which header pins.

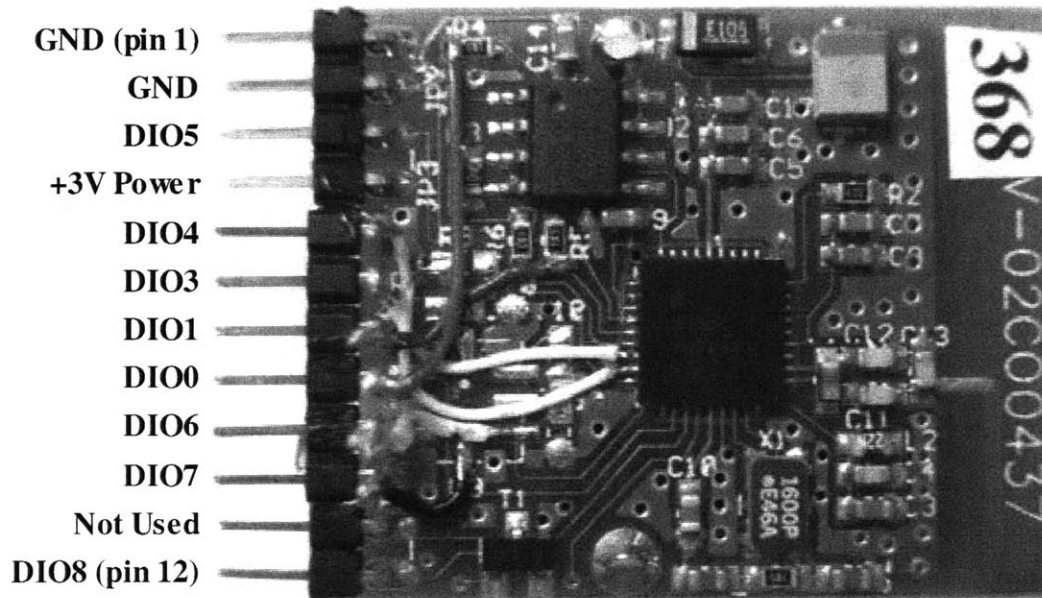


Figure A.2: Multi-switch example pinout diagram

A.1.3 Assembly Procedure

The number of I/O pins required for a specific application will vary and therefore one can choose to omit or rearrange the connections of certain pins as needed. In this section, directions are provided for adding a pin header and connecting I/O pins to that header. This specific modification is in the context of the multi-switch sensor of the JITQ toolkit

and not all available I/O pins will be utilized. If an application requires more (or less) pins, this section serves more as a guide than an exact implementation.

Step 1

Position the 6-pin header on the MITes device between the existing pin headers. The right angle ends of the pin header should be pointing upward. Secure it by applying a bead of hot glue only on the underside of the header and the edge of the MITes board. Hot glue will be applied to the top side of the header once the wires have been soldered. See Figure A.3 and Figure A.4 for visual guidance.

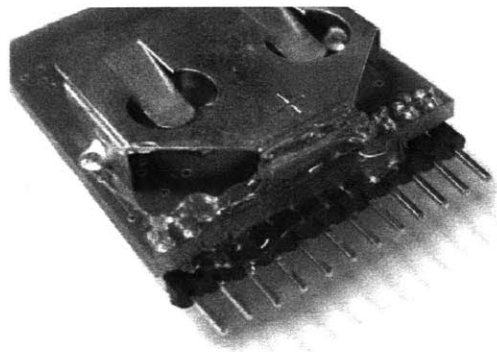


Figure A.3: Header attachment underside view

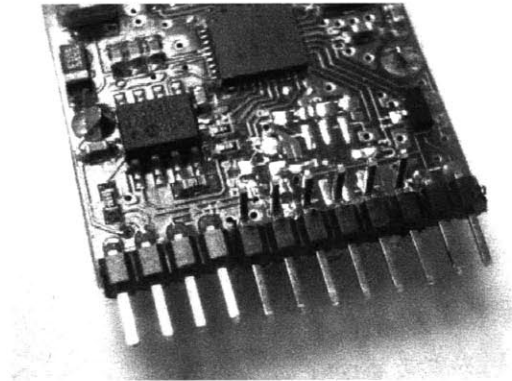


Figure A.4: Header attachment topside view

Step 2

Locate the solder points from Figure A.1 that will be used to access the respective I/O pins. Be sure to correlate port pin aliases and actual port pin numbers using Table A.1. In this case, pins 0 and 1 from Port 1 and pins 1 through 6 from Port 0 will be used. These pins correspond to the pin aliases DIO0, DIO1 and DIO3 through DIO8 respectively.

Step 3

The most difficult wires to solder are the ones to DIO3 and DIO4 because these port pins can only be accessed directly from the microcontroller's pins (as seen in Figure A.1)

which are very small. Small wires should be used to solder to DIO3 and DIO4 and achieving a successful connection can take practice.

To begin, solder a wire to the DIO4 pin. “Wet” the tip of the wire with solder but make sure to leave very little residual solder. Apply liquid flux (with a flux pen) to the area where the wire will be soldered. Place the tip of the wire on top of the DIO4 microcontroller pin and heat it with the soldering iron. The residual solder on the wire should bond to the pin. Tug gently on the wire to verify successful bonding and visually inspect the wire. **Be aware** that tugging too hard on a successful bond can destroy the microcontroller pin and render that pin unusable. Figure A.5 shows a close-up of a successful connection.

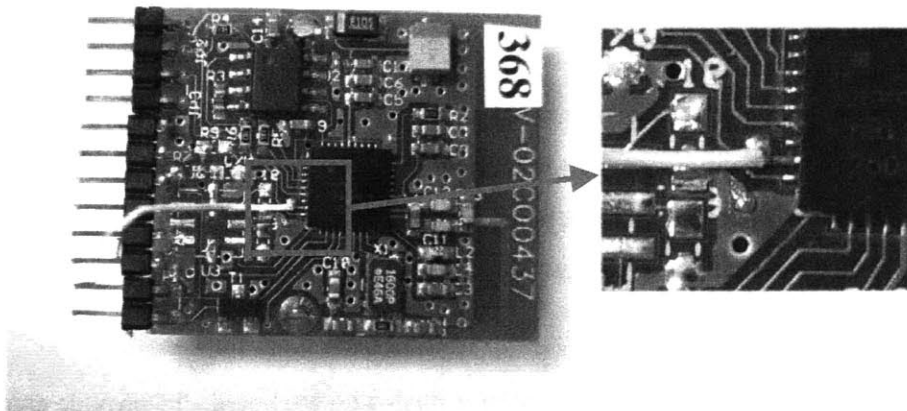


Figure A.5: Close-up of wire connection to DIO4

Step 4

Carefully solder a wire to the DIO3 pin in the same way as the one for the DIO4 pin. Avoid creating a solder bridge to adjacent pins—especially DIO4. A multi-meter should be used to verify absence of solder bridge shorts between pins.

Step 5

Carefully solder the other end of the two wires to the appropriate pin header (refer to Figure A.2 for a mapping of I/O pins to header pins).

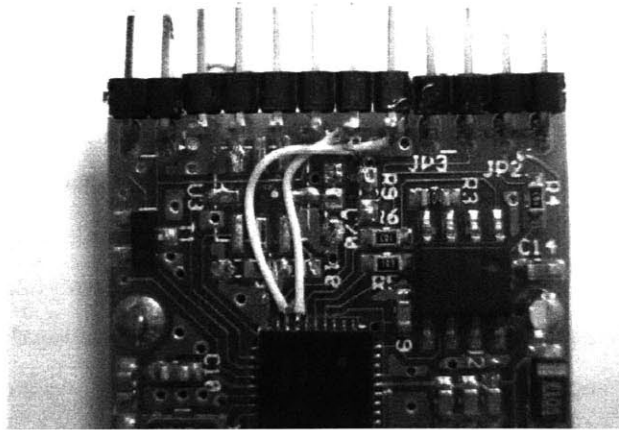


Figure A.6: Connection of DIO3 and DIO4 to the header pins

Step 6

The other wires are not as difficult to solder because the I/O pins can be accessed through larger solder point locations on the MITes board. Solder the rest of the wires to the board and connect them to their respective header pins. The completed wiring should look something like the MITes board shown in Figure A.2.

Step 7

The pin header should be trimmed to make it flush with the board. To provide extra structural support for the pin header, another bead of hot glue should be placed on the top side of the header. Be sure to remove any excess glue that obstructs the pins on the header from mating with the receptacle.

A.2 Utilizing the Analog-to-Digital Converter

A.2.1 Overview

The Analog-to-Digital converter (ADC) is utilized when there is a need to monitor an analog voltage. The microcontroller on the MITes transmitter is equipped with a 10-bit ADC unit with an internal reference voltage of 1.22 volts (i.e. about half the battery voltage). The microcontroller multiplexes 8 different physical pins to the single ADC

unit which allows an application to monitor up to 8 different voltage sources. In the context of the JITQ toolkit, the UV sensor and electrical current sensor make use of the ADC unit to read analog voltages.

A.2.2 Materials

Qty	Part Description	Place of Acquisition	Part Number/Identifier
1	2mm 2-pin header	Digikey Corp.	S2106-02-ND
1	MITes Transmitter (unmodified)	See Appendix G	N/A
N/A	Hot glue	Craft store	N/A

A.2.3 Assembly Procedure

For small applications that monitor one voltage input, using only one of the eight analog input pins on the microcontroller is sufficient. The following directions detail the steps to utilize only one of the analog inputs but additional inputs can be used by attaching wires to the respective microcontroller pins.

Step 1

Attach the 2-pin header by positioning it next to the existing 4-pin header with the right angled end pointing upward. A small bead of hot glue should be placed on the underside of the header to secure it in place. Figure A.7 shows this step.

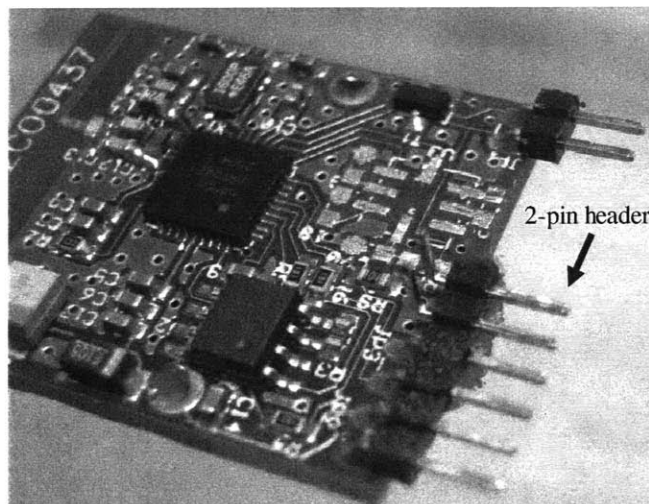


Figure A.7: Attachment of 2-pin header

Step 2

Solder a second small wire to the analog input(s) of choice. In this case, pin 2 (AIN0) of the microcontroller is used.

Step 3

Place a dab of hot glue on the wire near the location where it is attached to the microcontroller. The glue will serve as stress relief when handling the wire. Finally, solder the other end of the wire to one of the two pins on the header.

Step 4

Clip the excess metal from the right angled end of the pin header. Place a final dab of hot glue on the top side of the header to strengthen its adhesion to the board.

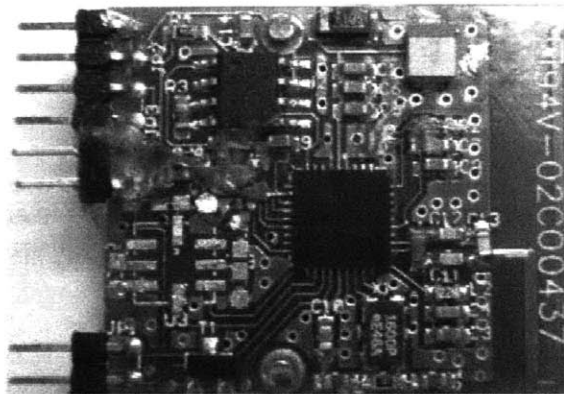


Figure A.8: Finished ADC enabled MITes device

Appendix B

Building the Heart Rate MITes Sensor

The following section provides step-by-step instructions for building the heart rate monitor.

B.1 Materials

Qty	Part Description	Place of Acquisition	Part Number/Identifier
1	Protoboard for MSOP-8	Digikey Corp.	33108CA-ND
1	Protoboard for SOT-23-6	Digikey Corp.	33206CA-ND
1	+3V Voltage Regulator IC	Digikey Corp.	296-12159-1-ND or 296-11871-1-ND
1	10nF Capacitor	Digikey Corp.	PCC103BNCT-ND
1	0.1uF Capacitor	Digikey Corp.	PCC1840CT-ND
1	10uF Capacitor	Digikey Corp.	399-3098-1-ND
1	1.3mm Power Jack	Digikey Corp.	CP-014DPJCT-ND
1	1.3mm Power Plug	Digikey Corp.	CP-002D-ND
1	9V Battery Connector Snap	Digikey Corp.	81-8K-ND
1	7-hole 2mm Receptacle	Digikey Corp.	S2103-07-ND
1	5-3 Volt Level Shifter IC	Maxim IC	MAX3375
1	Indestructo II pill box	www.apothecaryproducts.com	N/A
1	MITes Transmitter (unmodified)	See Appendix G	N/A
1	Polar Receiver Unit	Polar (refer to their contact info on their website, www.polar.com)	2380157
N/A	Hot glue	crafts store	N/A
N/A	Clear Epoxy	hardware store	N/A

B.2 Schematic Diagrams

The POLAR receiver unit has connection pads used to interface with power and communication lines. Figure B.1 identifies these pads.

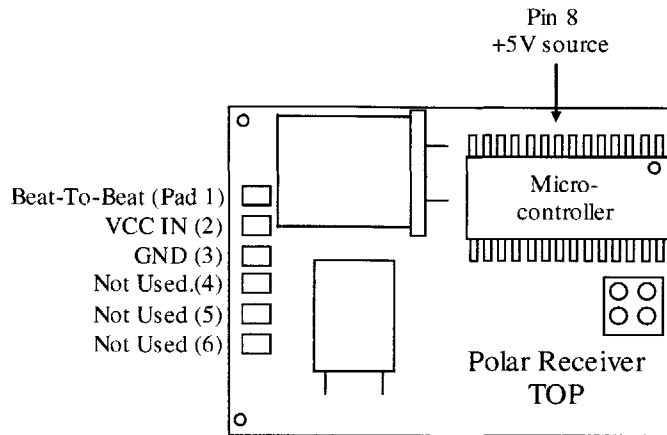


Figure B.1: POLAR receiver connection pad labels

Figure B.2 provides a schematic level view of the Heart Rate MITes sensor. Refer to this schematic while following assembly instructions to ensure correct understanding of the interconnections between components.

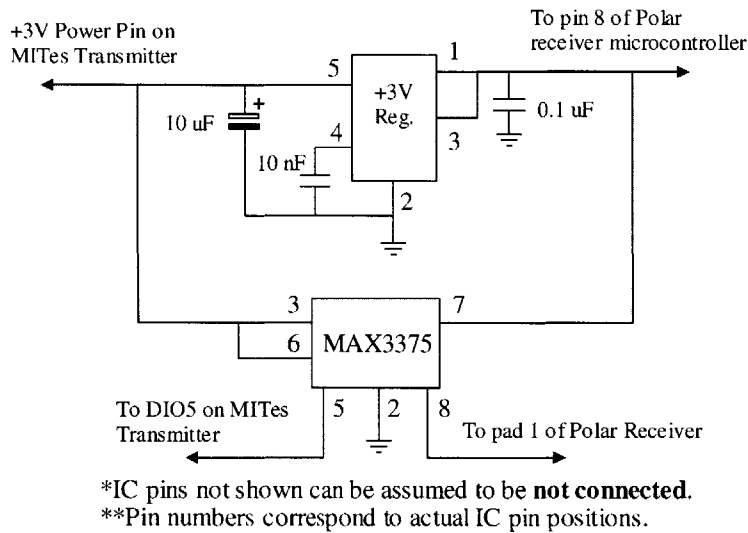


Figure B.2: Schematic of the Heart Rate MITes sensor

B.3 Assembly Procedure

The following section details the step-by-step construction of a Heart Rate MITes sensor to fit in a pillbox.

B.3.1 Building the power plug

Step 1

Solder the wires on the 9V battery connector snap to the 1.3mm power plug such that the positive (red) lead is soldered to the center tab and the negative (black) lead is soldered to the outer tab. The result is a center-positive plug which provides power to the sensor.



Figure B.3: Power plug

B.3.2 Preparing the Case Housing

Step 2

Cut a rectangular hole big enough for the power jack to fit through. The hole should be cut such that the bottom is flush with the inside bottom surface of the box. Use the jack as a sizing reference to mark off the appropriate dimensions for the hole. A drill and sharp hobby knife are recommended for this step. See Figure B.4 as a guide to the location of the hole.

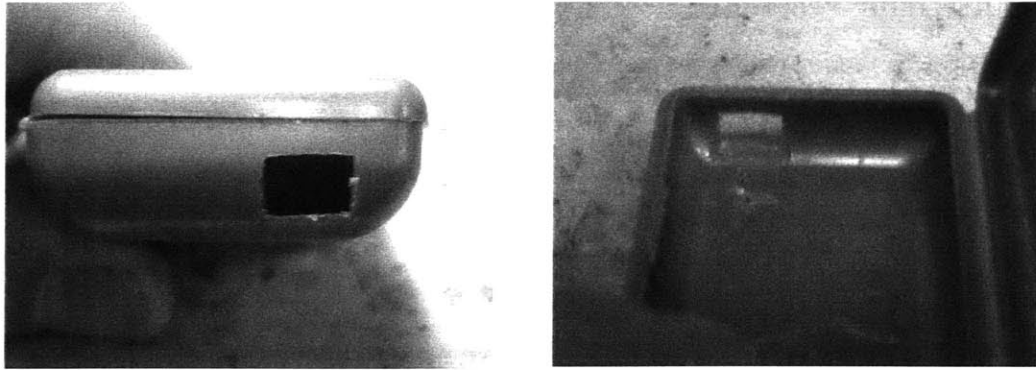


Figure B.4: Different views of power jack hole

Step 3

Test fit and make sure the power jack is flush with the bottom of the box when it passes through the hole. With the jack temporarily in place, test fit the POLAR receiver by placing it such that the bottom surface is facing upwards (the four-pin header will need to be removed prior to fitting). The receiver should rest fairly flat.

Step 4

Place a small piece of clear tape on the rear of the power jack to completely cover the small opening. Doing so will prevent epoxy from seeping into the power jack and freezing the small movable tab inside. If epoxy freezes the internals of the jack, the power plug cannot be inserted and the jack will need to be replaced. See Figure B.5.

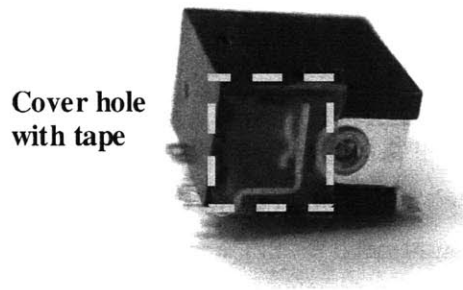


Figure B.5: Tape barrier on the rear of the power jack

Step 5

Attach positive and negative wires to the power jack. The positive is the side with the large metal plate and is connected to the center pin. The negative wire should be attached to both pins on the opposite side. Run the soldered wires along the edges of the box (preferably along the back edge) to avoid any components on the POLAR receiver. See Figure B.6.

Step 6

Use superglue to hold the jack in place and then apply epoxy to permanently affix the jack to the box. Tip: roughen the box surface around the area where the jack will be positioned. This will provide better epoxy adhesion to the box. Also clean the area with alcohol to remove any dirt or oil. Epoxy should be placed along the sides and the back of the jack. Also, place a thin layer of epoxy on the top of the jack. Figure B.7 shows what the power jack should look like when installed.

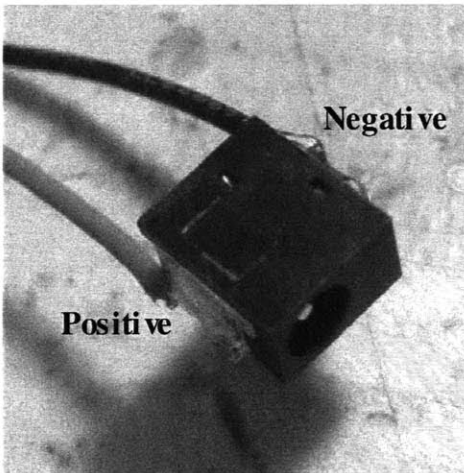


Figure B.6: Power jack with soldered wires

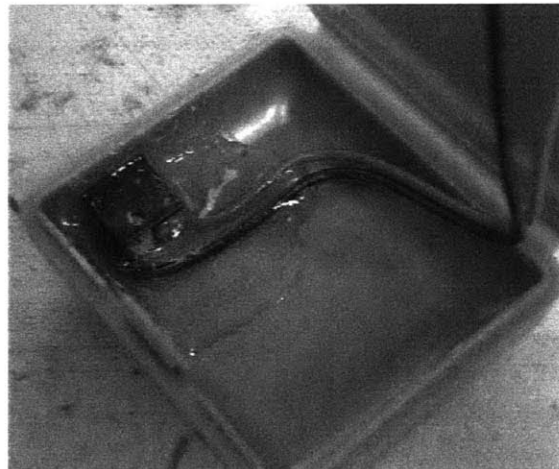


Figure B.7: Finished installation of the power jack

B.3.3 Preparing the Voltage Level Shifter

Step 7

Take the MSOP-8 protoboard adapter board and remove the metal pins from the pads of the board. Be careful not to remove the pads themselves when unsoldering the pins.

Step 8

Mount the MAX3375 IC voltage level shifter IC on the protoboard such that pin 1 is aligned with pad 1 (as seen in Figure B.8). Note that the voltage shifter IC will not fit perfectly on the protoboard adapter because it is not wide enough. A soldering iron with a needle-like tip must be used to solder this IC to the board. Create solder bridges to connect the legs to the pads and then split any cross bridges between adjacent IC legs and pads by using the needle-like tip of the soldering iron.

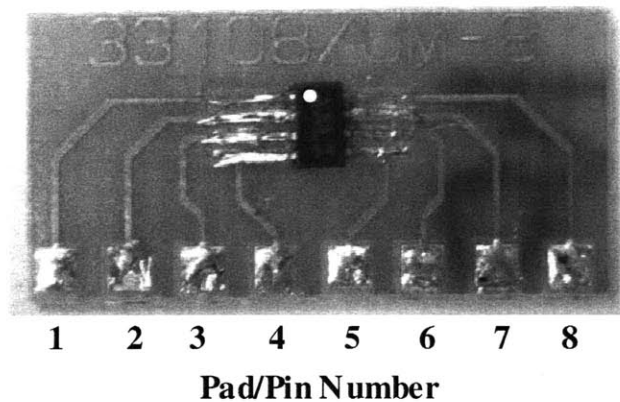


Figure B.8: Voltage shifter IC and protoboard adapter

B.3.4 Preparing the POLAR Receiver

Step 9

Remove the black header and the square 4-pin header from the unit.

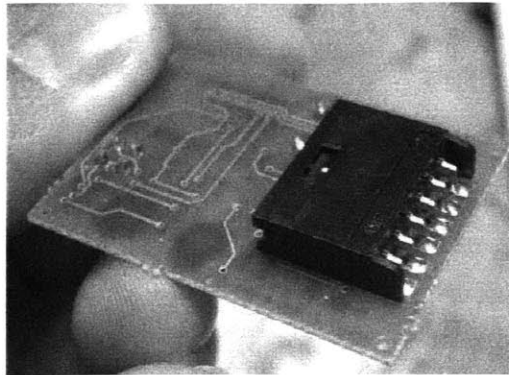


Figure B.9: Black header to remove

Step 10

Make sure the underside of the unit is as flush as possible with the PC board by trimming any protruding through-hole pins (i.e. the crystal oscillator's pins).

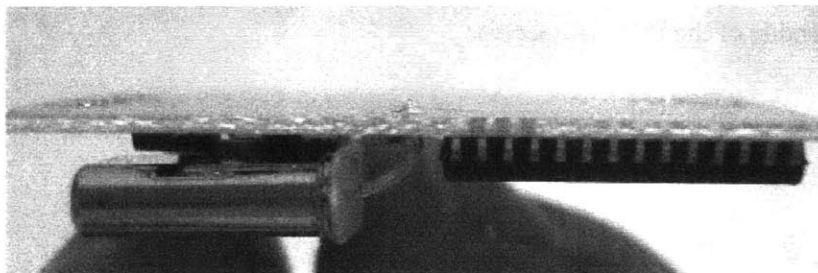


Figure B.10: Flush bottom surface

Step 11

On the underside of the POLAR receiver, position the protoboard adapter board containing the voltage shifter IC such that pin 1 is aligned with pad 1 of the polar receiver. Use superglue or hot glue to secure the board in place on the underside of the POLAR receiver. Solder a bridge to connect pad 1 to pin 1 of the Polar receiver to the voltage shifter IC board respectively. Figure B.11 shows the placement of the voltage shifter IC and the small solder bridge.

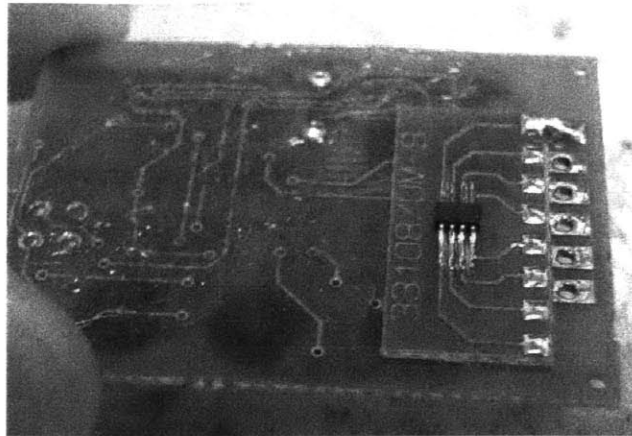


Figure B.11: Voltage shifter IC in position

Step 12

To protect against potential shorts with the MITes device, use hot glue to insulate exposed vias (small plated holes through the PC board) and through-hole pins that appear on the underside of the POLAR receiver.

Step 13

With a small wire, short pin 3 to pin 6 on the voltage shifter IC board.

Step 14

On the topside of the POLAR receiver, solder a wire to pin 8 on the microcontroller. This line is the +5 volt power supply and is used as a reference for the voltage shifter and a power source for the 3 volt regulator. Run the 5 volt wire to the edge of the board and strip enough insulation off the wire such that the metal portion extends through the small hole on the corner of the PCB.

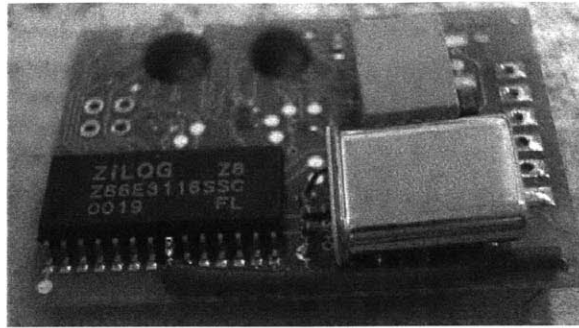


Figure B.12: 5+ Volt wire attachment

Step 15

Flip the board over to the underside and solder a wire from the protruding +5 volt wire in the corner to the VCC pad (pin 7) on the voltage shifter. Solder another wire to the same corner but leave it hanging, it will be connected later.

B.3.5 Preparing the Voltage Regulator

Step 16

Take the SOT-23 protoboard adapter board and remove all the pins from the pads (exactly like the MSOP-8 protoboard adapter).

Step 17

Mount the regulator IC on the board such that pin 1 is aligned with pad 1 of the protoboard adapter.

Step 18

Scratch the traces for pins 1, 2, 4, and 5. Also scratch the trace that runs between pins 4 and 5. Scratching the traces removes the laminate and exposes the metal underneath so that solder can bond to the traces. The capacitor components can now be soldered to the traces.

Step 19

Solder a 0.1 μF capacitor between pins 1 and 2.

Step 20

Solder a 10 nF capacitor between pin 4 and the adjacent pin to its right.

Step 21

Solder the 10 uF capacitor from pin 5 to the adjacent pin to its left. This capacitor should ideally be a ceramic X7R or X5R capacitor. In this case a tantalum is used. With the tantalum, make sure that the positive end (marked side) is soldered to pin 5. Figure B.13 provides a view of the voltage regulator board with the soldered capacitors.

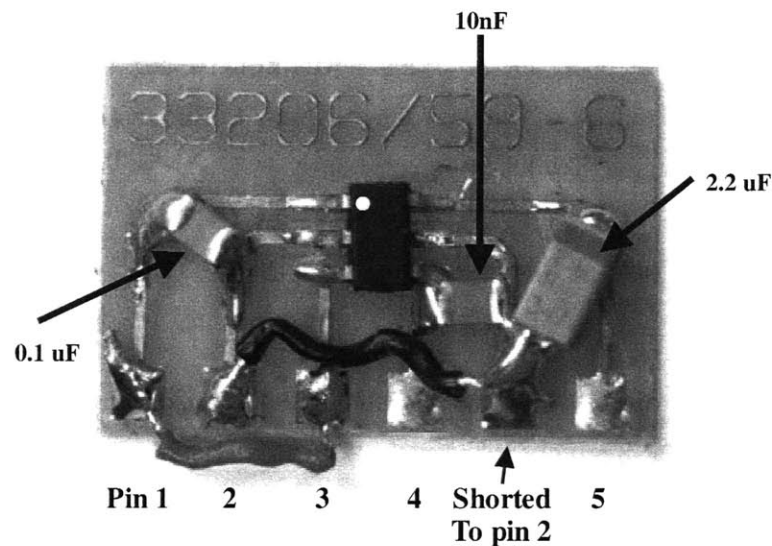


Figure B.13: Voltage regulator board with capacitors

Step 22

Use a small wire to short pins 3 and 1. This step keeps the regulator active and out of the shutdown state. Also, solder a wire to short pin 2 (GND) to the protoboard adapter pad labeled “Shorted to pin 2” shown in Figure B.13.

B.3.6 Preparing the MITes Transmitter

Step 23

Unsolder the metal battery holder to remove it from the PC board.

Step 24

Carefully remove the R9 resistor located between the Accelerometer and the EEPROM. It should have a white label “R9” printed above it. Take care not to remove the pads on which the resistor is soldered.

Step 25

On the underside, solder a bridging wire to connect the two positive terminals (i.e. connect the holes that were soldered to the battery holder). See Figure B.14.

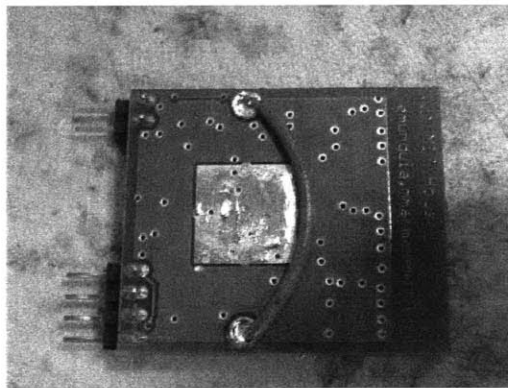


Figure B.14: Positive terminal bridge

Step 26

To help prevent any possibility of shorts, the header pins should be trimmed as flush as possible with the underside of the PC board (similar to what was done for the POLAR receiver’s underside). Hot glue should also be placed on the underside of the header pins to prevent shorts.

B.3.7 Putting It All Together

Step 27

Cut the wires from the power jack so that they are long enough to run along the edge of the box and meet the proper pads on the POLAR receiver (i.e. the VCC (2) and GND (3) pads).

Step 28

Strip the wires and pass them through the holes on the pads and solder them in place. The receiver should be able to sit flat in the box with the wires connected to it. Refer to Figure B.15 as a reference.

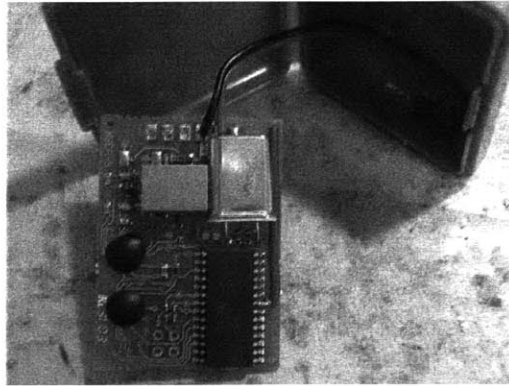


Figure B.15: Attaching power to POLAR receiver

Step 29

Take the wire that was left hanging in Step 15 and cut it short enough such that it can be soldered to pin 1 of the voltage regulator board when positioned at the front of the box. See Figure B.16.

Step 30

Solder a wire from the GND pad on the POLAR Receiver (pad 2) to the GND pin on the voltage regulator (pin 2).

Step 31

Solder a wire from the GND pin (2) on the voltage regulator or POLAR receiver to the GND pin (2) on the voltage shifter. See Figure B.16.

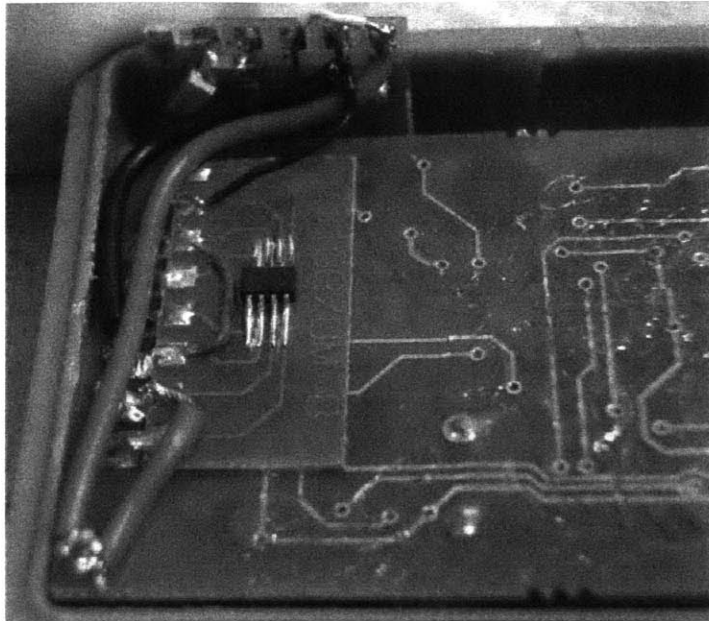


Figure B.16: Installation and connection of voltage regulator

Step 32

Attach a small wire from the 3 volt output of the regulator (pin 5) to the low voltage reference input (pin 3) of the voltage shifter.

Step 33

At this point the system can be tested to make sure the correct voltages are present. Immediately after applying a 9V battery to the power jack, check for any overheating which may be due to incorrect wiring. Disconnect the battery quickly if any overheating occurs. Shorts due to accidental solder bridges or incorrect wiring can cause overheating. If the system is correctly wired, 5 volts should be read at the input of the voltage regulator (pin 1) and 3 volts on its output (pin 5).

Step 34

Cut the 7-hole header receptacle so that two header receptacles of 4 and 2 holes are made (one hole will be destroyed in the process). Insert the header receptacles onto the MITes transmitter's pin headers.

Step 35

Carefully solder a wire from pin 2 on the voltage shifter (or voltage regulator) to the GND pins on the MITes header. Solder a wire from pin 5 of the voltage regulator to the +3V power pin on the MITes device. Finally, solder a wire from pin 5 on the Voltage shifter to DIO5 on the MITes pin header. Refer to Figure A.1 to see which pins correspond to GND, 3V, and DIO5 respectively.

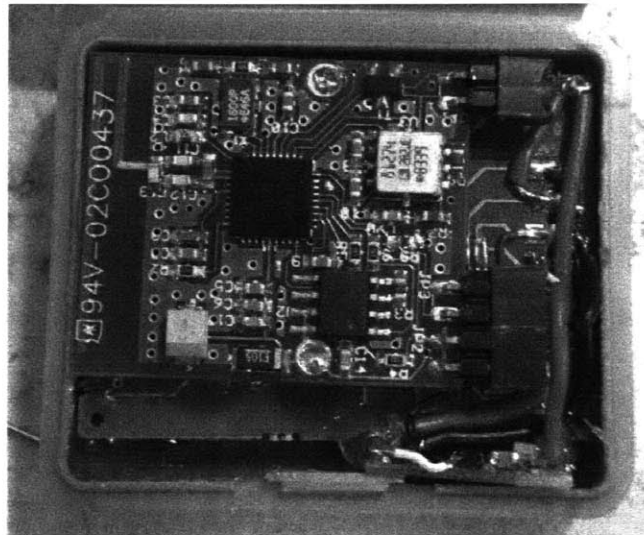


Figure B.17: MITes transmitter with header receptacles

Step 36

Once the wires have been connected, the system should be ready for a preliminary operational test. Program the MITes transmitter with the HRM firmware and test the system with the heartbeat simulator or, even better, the wearable POLAR strap.

Step 37

Once it is verified that the sensor works, position the MITes transmitter in its final resting area and try to close the box lid. The lid should be able to snap and stay shut. If not, try to find the part of the sensor that is preventing the lid from closing and trim until the lid can close.

Step 38

Use hot glue to permanently affix the header receptacles to the Polar receiver. Be careful not to hot glue the MITes transmitter's header pins since the MITes transmitter should be removable.

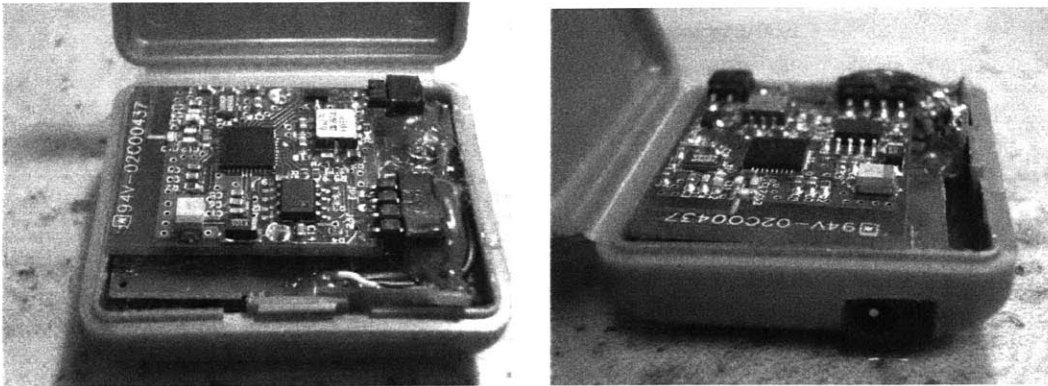


Figure B.18: Completed views of Heart Rate MITes sensor

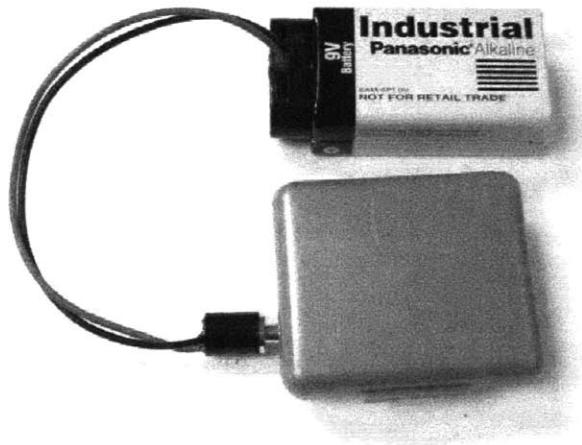


Figure B.19: Heart rate monitor with battery

Appendix C

Building the Ultraviolet MITes sensor

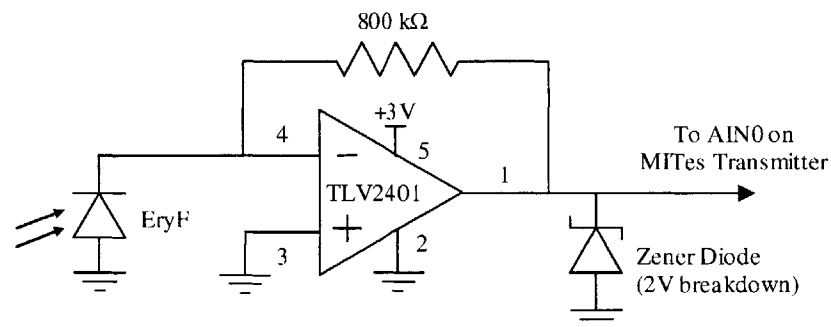
The following section provides details for building the Ultraviolet MITes sensor.

C.1 Materials

Qty	Part Description	Place of Acquisition	Part Number/Identifier
1	EryF Photodiode	Boston Electronics	EryF
1	Zener Diode (2.0V reverse voltage breakdown)	Digikey Corp.	MMSZ4679T1OSCT-ND
1	TLV2401 Micropower Op-Amp	Digikey Corp.	296-10531-1-ND
2	1 Megaohm Resistor (1% or better)	Digikey Corp.	P1.00MCACT-ND
1	SOT-23 protoboard adapter	Digikey Corp.	33206CA-ND
1	Protoboard (grid style)	RadioShack	N/A
1	Indestructo 1 or 2 pillbox	Apothecary Products	N/A
1	MITes Transmitter (Unmodified)	See Appendix G	N/A

C.2 Schematic

The schematic diagram of the UV Sensor is shown below in Figure C.1. The MITes device is not shown but referenced with text.



*Pin numbers correspond to actual IC pin positions.

Figure C.1: Schematic diagram of UV Sensor

C.3 Assembly Procedure

Step 1

Convert an unmodified MITes device into an ADC enabled MITes device by following the steps in section A.2.

Step 2

Drill a hole in the center of the top cover of the box just big enough to snugly fit the round outer casing of photodiode through.

Step 3

Cut a 2x2.5 cm piece of the protoboard. Also, mount the Op-Amp on the protoboard adapter being sure to line up pin 1 with pad 1 (pin 1 is shown in Figure C.2).

Step 4

Arrange the protoboard adapter, photodiode, and 1 MOhm resistor as seen in Figure C.2. Make sure to position the photodiode to leave as little space between the protoboard and the bottom of the photodiode casing. Careful bending of the photodiode's leads will be necessary.

Step 5

Following the schematic shown in Figure C.1, solder bridges on the underside such that pin 1 of the Op-Amp connects to one side of the resistor, pin 2 connects to the anode of the photodiode and GND, pin 3 connects to GND (short it with pin 2), pin 4 connects to the cathode of the photodiode and the other end of the 1 MOhm resistor. Figure C.3 shows the underside of the protoboard with the solder bridges.

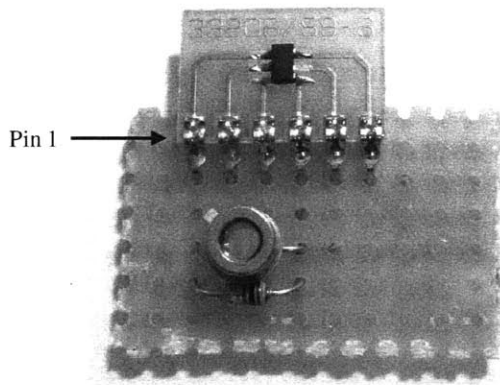


Figure C.2: Protoboard and component arrangement.

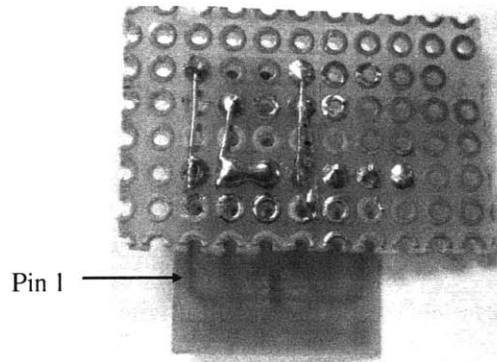


Figure C.3: Protoboard underside

Step 6

Test fit the board by pushing the photodiode through the top cover and make sure the protoboard clears all pillbox edge boundaries. As shown in Figure C.4, leave a gap on the left between the box and the protoboard.

Step 7

On the top of the protoboard adapter, solder the Zener diode with cathode (marked side) towards pin 1 of the Op-Amp IC. Figure C.5 shows this step.

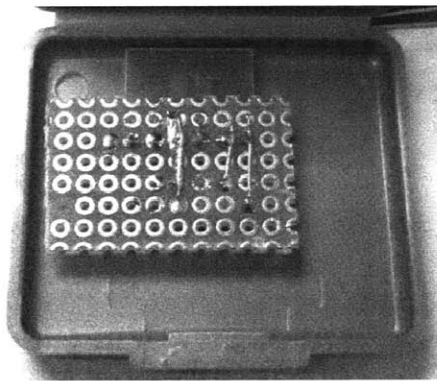


Figure C.4: Test fitting protoboard

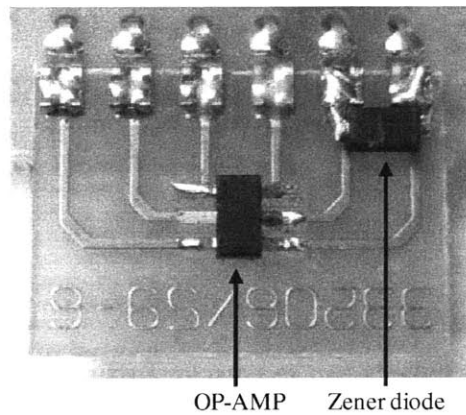


Figure C.5: Zener diode placement

Step 8

To insulate the solder bridges on the underside of the protoboard, use hot glue to cover all exposed metal and solder.

Step 9

Solder power (pin 5), GND (pin 2), and signal (pin 1) wires to the top part of the protoboard and route them to the edge of the board. See Figure C.6.

Step 10

As shown in Figure C.7, reposition the protoboard inside the top cover (make sure the photodiode is inserted into the hole on the top lid). Place the header receptacles on the pins of the MITes device and position it on the protoboard. When the desired positioning is obtained, use hot glue to secure the header receptacles to the protoboard. Do not to allow hot glue to run onto the pin headers on the MITes device since it must be removable from the receptacles.

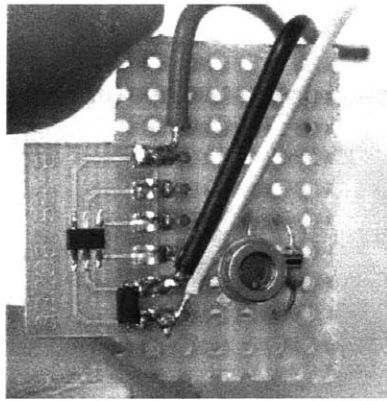


Figure C.6: Soldering wires

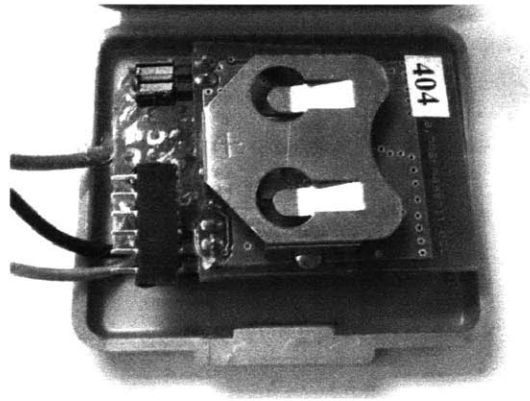


Figure C.7: Positioning MITes device

Step 11

Once the header receptacles are firmly in place, solder the wires to the MITes header receptacle pins. Solder the power wire to the +3V Power pin, the ground pin to the MITes' ground pins, and the signal wire to the header attached to AIN0 (from step 1). Refer to Figure A.1 to locate the power and ground pins.

Step 12

To secure the protoboard to the top cover, first pull the MITes device out of the receptacles and position the protoboard so that the photodiode's top surface is flush with the top cover. The snug fit of the hole on the outer casing of the photodiode should hold the board in place; otherwise manually hold the board in place. Use hot glue on the corners of the protoboard to adhere it in place. Make sure the photodiode remains flush with the top cover until the hot glue hardens. Reinsert the MITes device and the box should easily close.

Step 13

Remove the MITes device from the header receptacles and flash the UV sensor firmware to the device by applying the programming connector to the EEPROM IC. Reinsert the MITes device into the header receptacles. The UV sensor should now be operational.

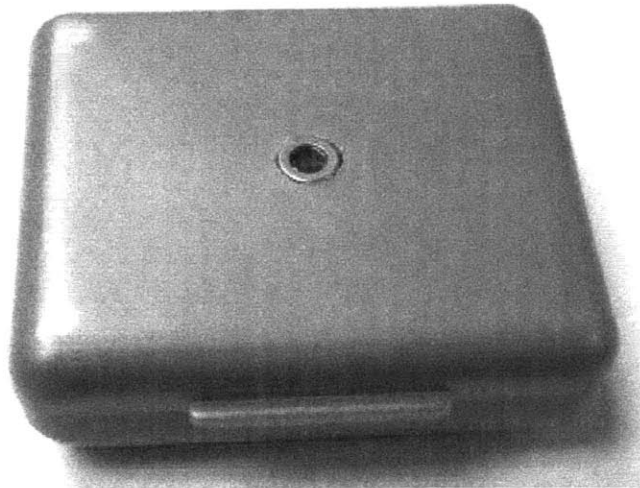


Figure C.8: Finished UV Sensor

Appendix D

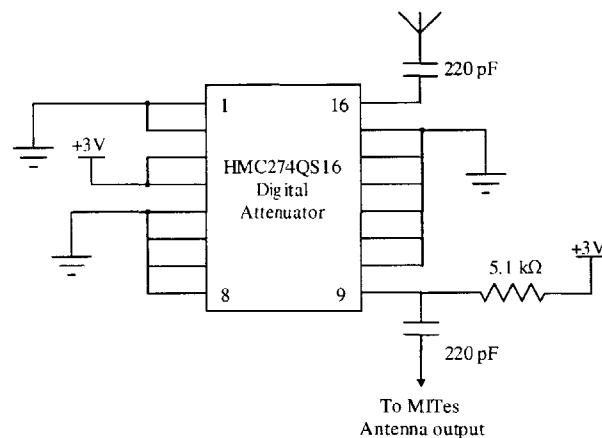
Building the Beacon

This section details the steps involved in modifying a MITes transmitter for use as a proximity and location sensing beacon.

D.1 Materials

Qty	Part Description	Place of Acquisition	Part Number/Identifier
1	Protoboard for MSOP-8	Digikey Corp.	33108CA-ND
1	5.1k Resistor 1/8W	Digikey Corp.	5.1KEBK-ND
2	220 pF Ceramic Chip capacitor	Digikey Corp.	BC1240CT-ND
1	2.45 GHz Chip antenna	Digikey Corp.	ANT-2.45-CHPCT-ND
1	5-hole 2mm Receptacle	Digikey Corp.	S2103-05-ND
1	31 dB Digital Attenuator IC	Hittite Corp	HMC274QS16
1	CR2032 Lithium battery holder	Digikey Corp.	BH908T-C-ND
1	Indestructo 1 or 2 pillbox	Apothecary Products	N/A
N/A	Aluminum Tape	Home Depot (metal ducting section)	N/A
1	MITes Transmitter	See Appendix G	N/A
N/A	Hot glue	crafts store	N/A

D.2 Schematic Diagram



*Pin numbers correspond to actual IC pin positions

Figure D.1: Schematic diagram indicating connections to attenuator IC

D.3 Assembly Procedure

D.3.1 Preparing the MITes transmitter

Step 1

Unsolder the metal battery holder and bridge the two positive terminals with a wire (as was done for the HRM sensor in Figure B.14).

Step 2

Scrape the insulating varnish off the ground plane on each side of the board near antenna end of the MITes device. Also, with a knife remove the microstrip antenna by scraping it off. See Figure D.2.

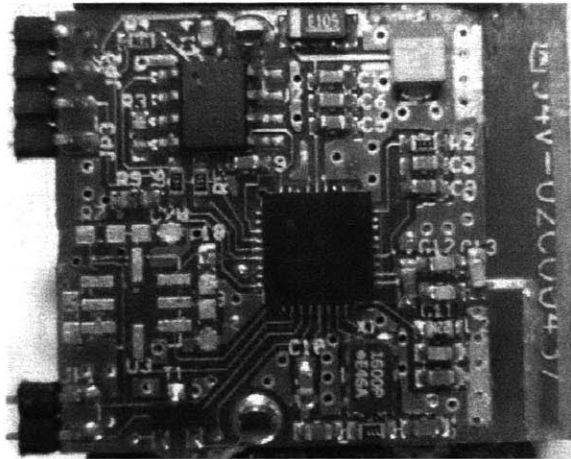


Figure D.2: MITes transmitter preparation

D.3.2 Preparing the attenuator IC(s)

Step 3

Take a protoboard adapter board and remove all the pins that are connected to the solder pads but save them for later use. Cut the trace that runs to pin 5 from the solder pad.

Also remove the trace that runs from pin 8 to the solder pad. This must be done for each attenuator IC that is used. See Figure D.3.

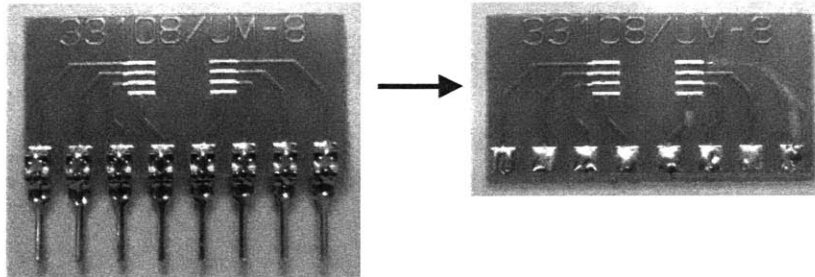


Figure D.3: Preparation of the protoboard adapter board

Step 4

Mount the attenuator IC on the protoboard adapter. Refer to Figure D.4 for orientation and how to match the pins on the IC to the pads on the board. Solder pins 1-2 of the IC together and to pads 1-2. Solder pins 3-4 together and to pads 3-4. Solder pins 5-8 together but do not solder them to any pads. Also, solder pins 10-15 together and to pads 6-7. Pin 9 must connect to pad 5 on the board via a solder bridge and pin 16 left unconnected (for now). Do a check of continuity with a multi-meter to make sure there are no shorts between connections that should not have been soldered together. Refer to the following figures for reference.

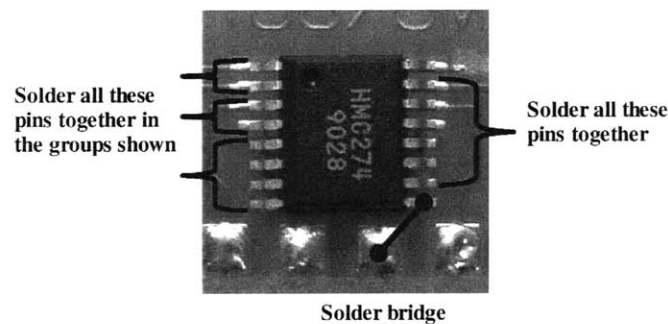


Figure D.4: Detailed view of individual pins

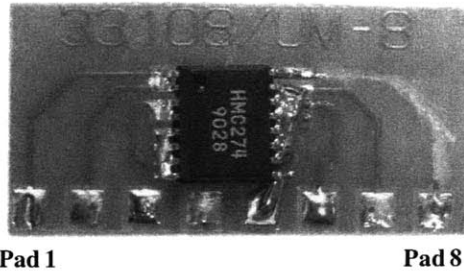


Figure D.5: Finished view of soldered attenuator IC

D.3.3 Mounting the attenuator boards

Step 5

Position the board such that pad 5 lines up with the antenna output of the MITes board. Affix the board in place by applying hot glue to the back side of the attenuator board and the edge of the MITes board but make sure that the adapter board is resting flat against the MITes board. See Figure D.6.

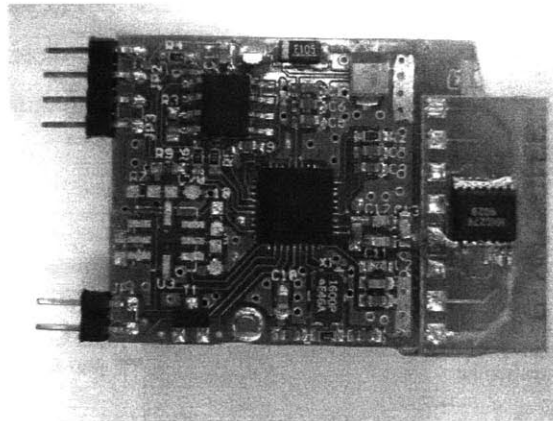


Figure D.6: Attenuator board positioning

Step 6

Connect the scratched ground plane to the attenuator board pads 1-2 and 6-7. Use short wires or the leftover pins from Step 3 to make these connections. Also, solder a 220 pF capacitor between the antenna output and pad 5 (as shown in Figure D.7).

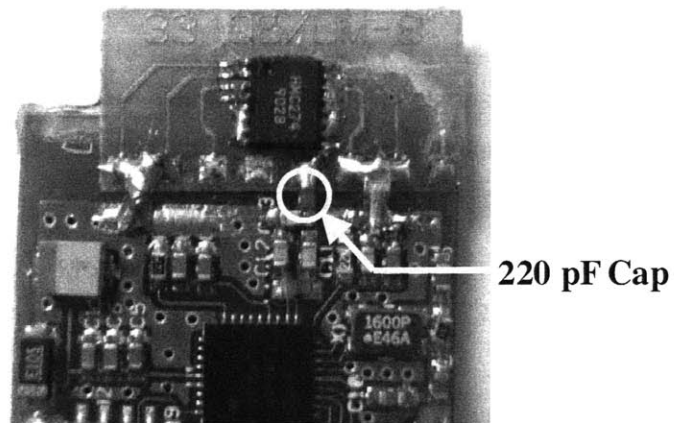


Figure D.7: Connecting ground and 220pF capacitor

Step 7

Connect a 5k resistor between pad 5 and one of the +3V positive terminals of the MITes device. The leads of the resistor should be insulated to prevent shorts. See Figure D.8.

Step 8

Solder a wire between attenuator board pad 3 and the positive terminal of the large capacitor on the side of the MITes board. This step connects a +3V signal to pad 3. Figure D.9 shows this step.

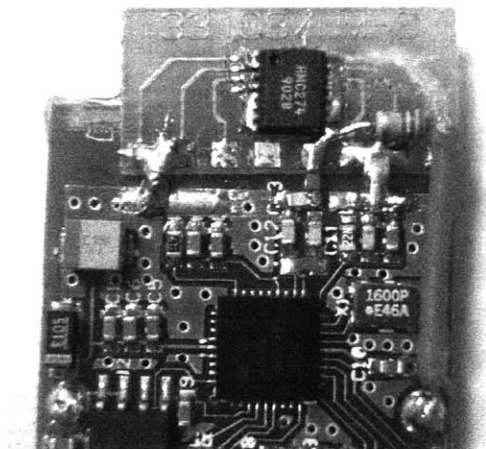


Figure D.8: Attaching the 5k resistor

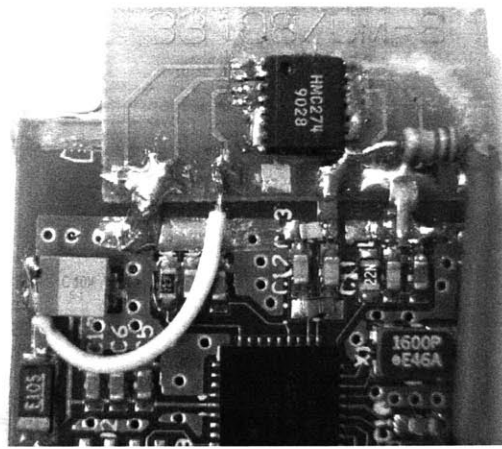


Figure D.9: Connecting +3V signal to pad 3

Step 9

Solder another 220 pF capacitor to pin 16 of the attenuator IC so that it is oriented toward the edge of the board. Make sure not to create a solder bridge between pin 16 and the adjacent pin. Finally solder the antenna to the end of the capacitor such that the arrow points outward, away from the edge of the board.

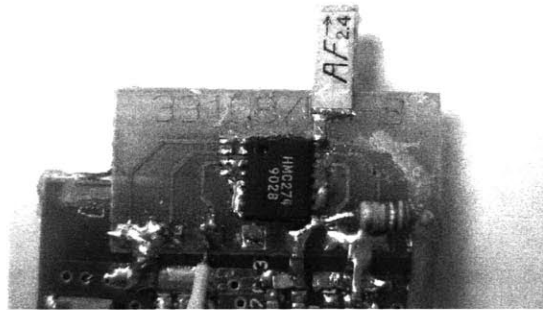


Figure D.10: Attaching 220 pF Cap and Antenna

Step 10

The antenna and capacitor are very fragile at this point. To protect them, apply hot glue around the antenna and capacitor to encase them completely. When the hot glue hardens, it will make the antenna and capacitor structure rigid and more robust. Make sure there is no movement or play by carefully applying pressure to the antenna with a finger tip.

D.3.4 Preparing the shielded pillbox casing**Step 11**

Take an unmodified pillbox and carefully cut off the tab on top cover. Make the cut flush with the edge of the box as seen in Figure D.12.

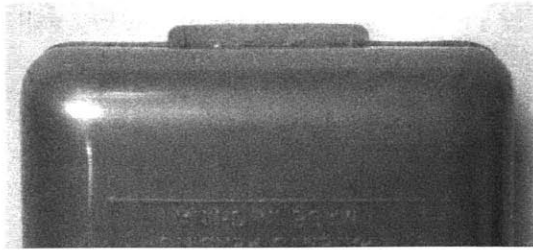


Figure D.11: Box before tab removal

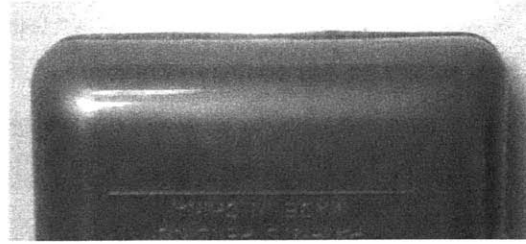


Figure D.12: Box with tab removed

Step 12

Cut a shallow notch on the side edge of the bottom half of the box as wide and deep as the protoboard adapter board. Use the modified MITes board or a spare protoboard adapter board as a sizing guide for the notch. Make another smaller notch on the top lid of the box to make room for the antenna. Note that the antenna notch may require some post trimming when the MITes transmitter is fitted. See Figure D.13 and Figure D.14 for reference.

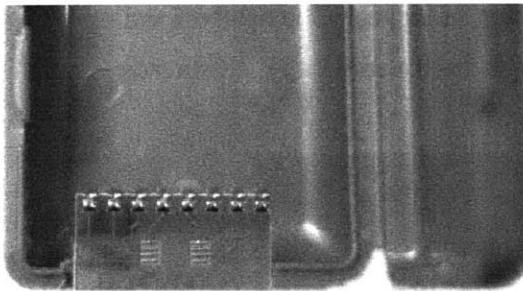


Figure D.13: Notch sizing

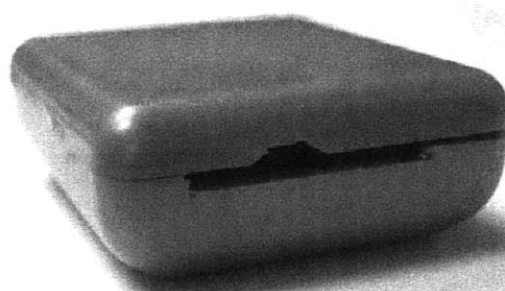


Figure D.14: Finished view of notches

Step 13

Take the aluminum ducting tape and begin wrapping the box. Eight layers of aluminum are required. Make each layer as even as possible by using the fewest number of individual pieces of tape per layer and no gaps. Carefully trim the aluminum tape around the edges and notched areas. Aluminum tape should be placed such that the box can still be opened and closed. To even out wrinkles and keep the corners smooth, the box should

be rolled periodically on a hard surface (such as a table). After eight layers, the box will look similar to one shown in Figure D.15.

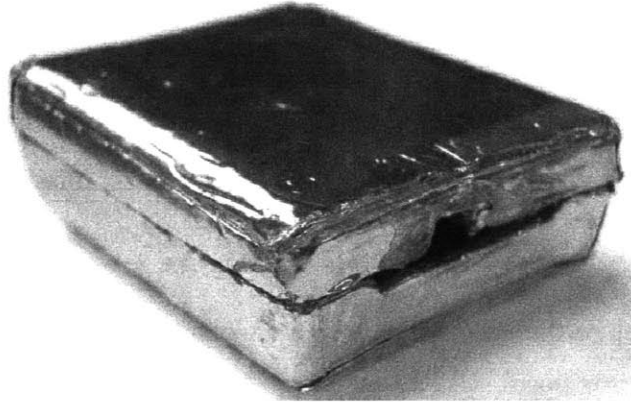


Figure D.15: Box after eight layer aluminum wrapping

Step 14

An extra overlapping lip is needed to block the RF signals that may leak out through the gap between the top and bottom lids. First, acquire and cut a strip of semi-rigid plastic one centimeter wide. Bend the strip around the side (opposite the notches) and front of the box and cut the strip to length. Be sure to crease the corner of the strip (see Figure D.16).

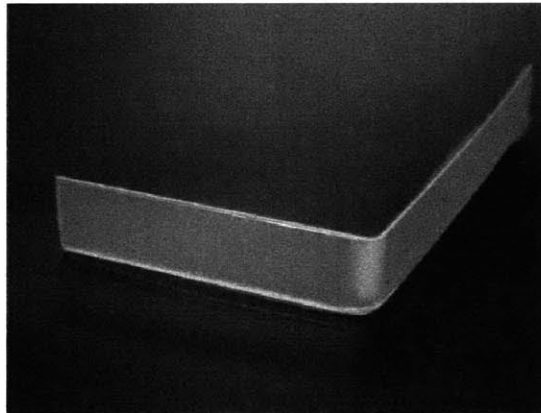


Figure D.16: Plastic strip cut to length and creased

Step 15

Take the plastic strip and position it such that it covers the side and front of the box. Cut a piece of aluminum tape large enough to cover the outer part of the plastic strip with enough left over to attach it to the top lid of the box. Apply another layer of aluminum on the top lid and plastic strip to improve the rigidity of the attachment. Force will be applied to the strip whenever the box is opened thus, it must be quite rigid to resist loss of attachment to the box.

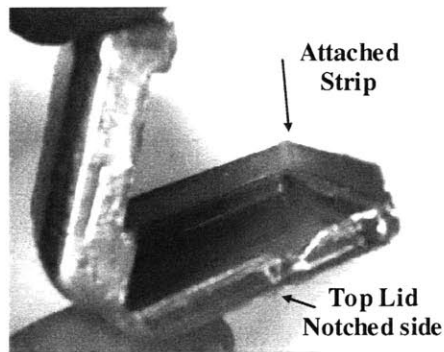


Figure D.17: Side view with strip attached

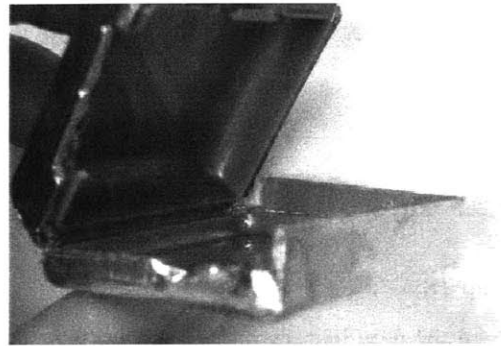


Figure D.18: Front-side view of strip

Step 16

The box is difficult to open due to the plastic strip and the removal of the plastic tab in Step 11. To ameliorate this issue, a pressure point for the thumb is needed to assist in opening and closing of the box. Place a small strip of hot glue along the bottom lid edge near the front of the box. The strip should be about one centimeter long and half a centimeter thick. See Figure D.19 for visual reference.

Step 17

Apply another layer of aluminum tape on the bottom lid of the box and cover the hot glue strip. Figure D.20 is a finished view of the thumb pressure point.

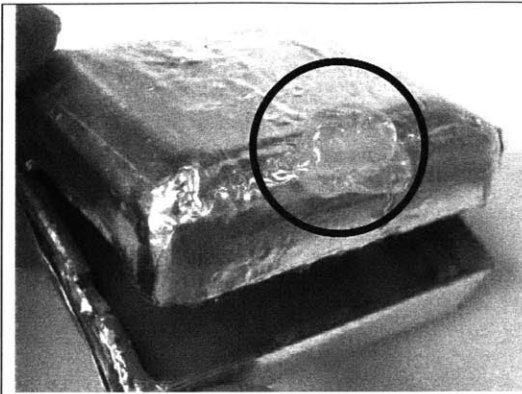


Figure D.19: Location of hot glue for thumb pressure point

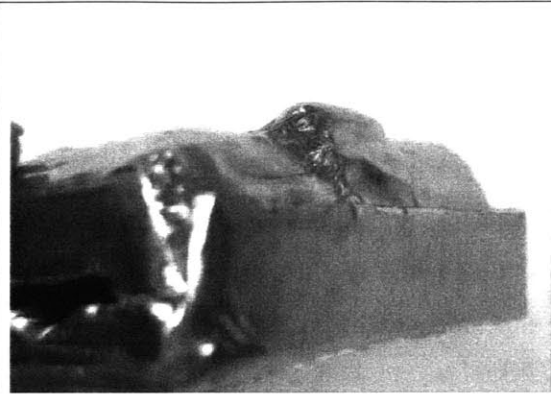


Figure D.20: Finished view of pressure point

D.3.5 Putting it all together

Step 18

Take the new battery holder and outwardly bend the metal leads on the bottom so that they lie as flat as possible with the bottom surface. Cut two wires (positive and negative) about two and one-half inches in length and solder them to the positive and negative leads respectively. Soldering may be difficult because the metal leads are somewhat resistant to bonding with molten solder. Use plenty of flux paste (or liquid) to help the molten solder bond to the metal leads and wire tips.

Step 19

Position the battery holder with wires so that the positive end is oriented towards the front corner of the box (as shown in Figure D.21). Place hot glue on the bottom of the battery holder and glue it to the box in the same position. Try to create as small a gap between the connector and the bottom surface of the box.

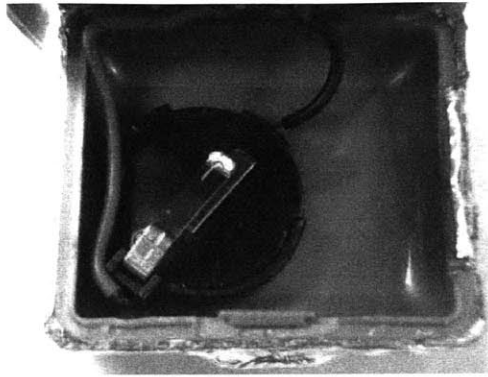


Figure D.21: Positioning battery connector

Step 20

Cut the five-hole header receptacle in half to obtain two 2-hole header receptacles (one hole will be destroyed). Insert the header receptacles onto the MITes' pin headers (one on the two pin header and one on the four-pin header).

Step 21

Position the MITes device inside the box as shown in Figure D.22. Trim and solder the positive wire to one of the positive terminals shared connected by the wire bridge. Solder the negative wire to the square section of the ground plane on the side closest to the antenna.

Step 22

Position the protoboard adapter on the MITes device so that it rests on the notch on the side of the box. Close the box to make sure there is adequate clearance. If the box fails to close, try to pivot the MITes device until clearance is achieved. If the notch for the antenna is not large enough, carefully trim the notch as needed. Take note of the best position of the MITes device.

Step 23

Keeping the MITes device in the best position, use hot glue to affix the header receptacles to the top lid of the box. Do not allow hot glue to run onto the actual pin header on the MITes device. Also, do not let excess hot glue seep onto the rim of the lid

else the box may become difficult to close. The MITes device should be removable from the header receptacles and reinserted at will. Figure D.22 shows a completed view of the beacon with the MITes device in place.



Figure D.22: Completed view of MITes connection

Step 24

To protect against shorts, place a layer of hot glue on the ground plate on the underside of the MITes board (the same plate to which the negative wire is soldered).

Step 25

Program the beacon firmware to MITes device by removing the MITes device from the header receptacles and applying the programming connector to the EEPROM IC. Once the device is programmed, reinsert the MITes device into the header receptacles. The Beacon should now be operational.

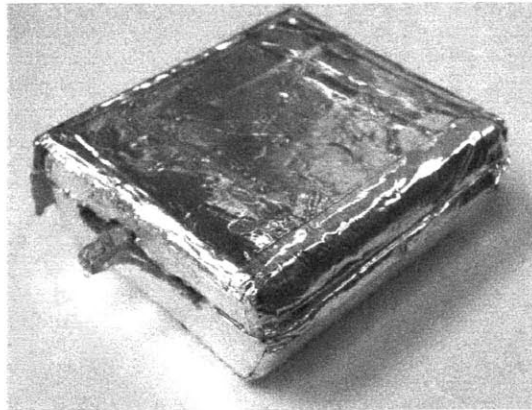


Figure D.23: Finished beacon

Appendix E

Building the Electrical Current Sensor

The following section details the construction of the electrical current sensor.

E.1 Materials

Qty	Part Description	Place of Acquisition	Part Number/Identifier
1	Protoboard for MSOP-8	Digikey Corp.	33108CA-ND
1	TLV2402 Dual Micropower Op-Amps	Digikey Corp.	296-10534-1-ND
3	100 k Ω Resistor	Digikey Corp.	311-100KCCT-ND
1	6.20 k Ω Resistor	Digikey Corp.	311-6.20KCCT-ND
1	4.7 k Ω Resistor	Digikey Corp.	311-4.70KCCT-ND
1	147 Ω Resistor	Digikey Corp.	311-147CCT-ND
1	Schottky Diode (SOT-23)	Digikey Corp.	BAT54FSCT-ND
1	1 uF Tantalum Capacitor	Digikey Corp.	493-2364-1-ND
1	12 position, 2mm single row header receptacle	Digikey Corp.	S2103-12-ND
1	6 position, 2mm single row header	Digikey Corp.	S2106-06-ND
1	Slide Switch SPDT	Digikey Corp.	EG1918-ND
1	CR2032 Lithium battery holder	Digikey Corp.	BH908T-C-ND
1	Current Transformer	www.crmagnetics.com	CR3110-3000
1	MAX4544 Analog Switch (SPDT)	Maxim IC	MAX4544CSA
1	MAX5160 200 k Ω Digital Pot	Maxim IC	MAX5160NEUA
1	Indestructo 1 or 2 pillbox	Apothecary Products	N/A
1	PC board	This is a custom component. Contact Emmanuel Munguia Tapia (emunguia@mit.edu) for information on obtaining the PC board used in this document	
1	MITes Transmitter	See Appendix G	N/A

E.2 Pinout and Schematic Diagrams

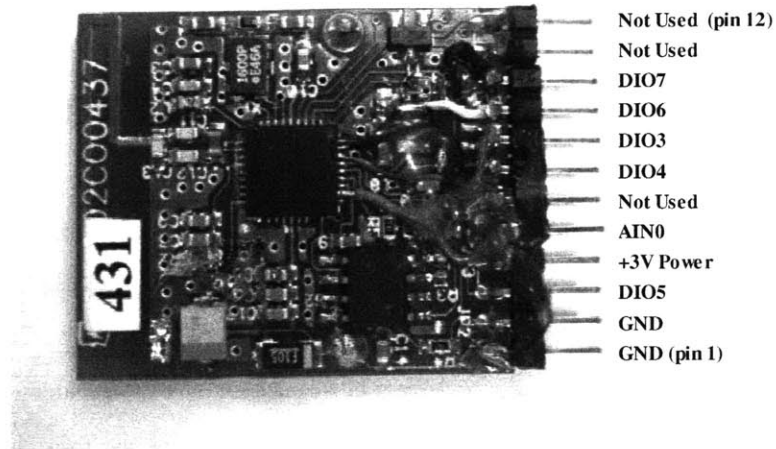
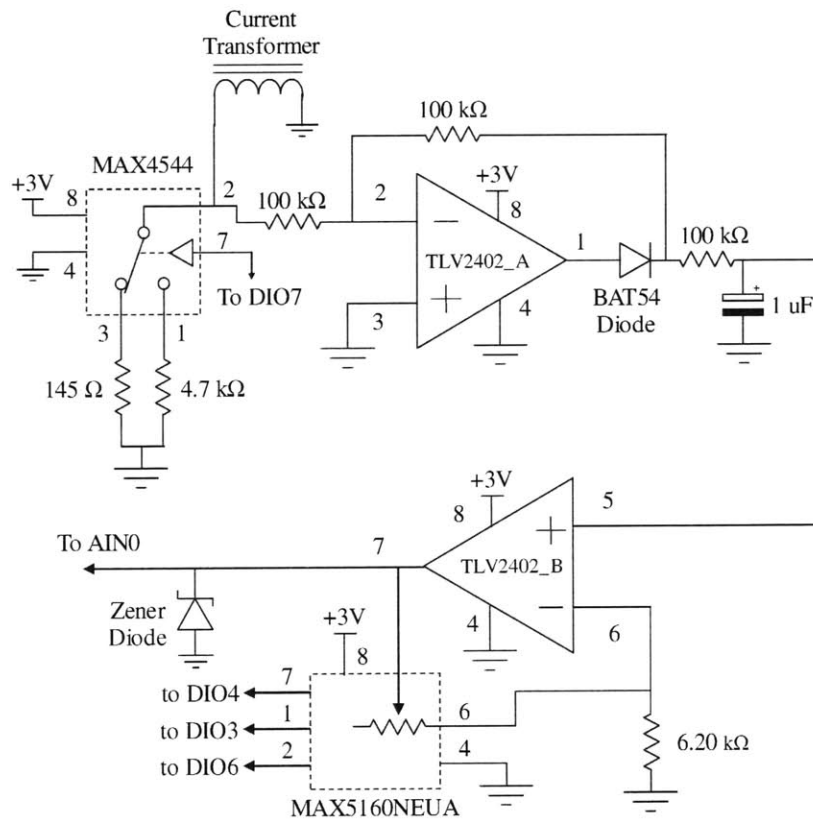


Figure E.1: MITes header pinout



*IC pins not shown can be assumed to be **not connected**.
 **Pin numbers correspond to actual IC pin positions.

Figure E.2: Schematic of Current Sensor

E.3 Assembly Procedure

These specific instructions employ a printed circuit (PC) board that was designed for a slightly different application but is modified here to serve as a base for the current sensor. The exact PC board used here is not required (a custom PC board that implements the schematic diagram in Figure E.2 can be used), but it simplifies the building of prototypes.

E.3.1 Preparing the MITes transmitter board

Step 1

Modify a MITes transmitter board with both I/O and ADC extensions shown in Appendix A. The I/O pins that are used for the current sensor are different from the multi-switch example. Use the pinout diagram of Figure E.1 to determine which solder points (of Figure A.1) to use.

Step 2

Remove the battery clip and bridge the voltage holes (like in Figure B.14).

Step 3

The exposed metal on the bottom surface of the MITes device should be insulated by applying thin layers of hot glue to cover the square ground plate and any other metal that could potentially cause a short. The completed board should resemble the one shown in Figure E.1.

E.3.2 Preparing the PC board

Step 4

Take the PC board and cut it as shown in Figure E.3. The 5x3.4 cm dimensions allow the PC board to fit in the bottom of the pillbox.

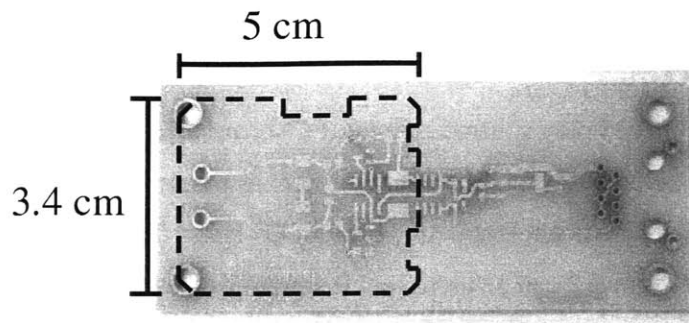


Figure E.3: PC board section of interest

Step 5

The PC board must be prepared before mounting the electronic components. Figure E.4 shows which traces/pads should be removed. There are also points where solder bridges should be made. Note the location of the GND and output pads. The +3V power trace is located under the PC board (shown later in Figure E.7)

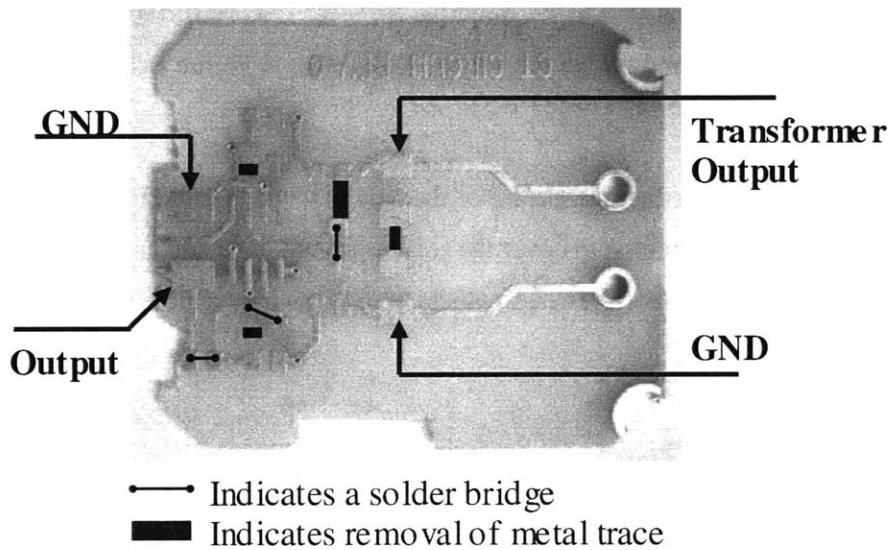


Figure E.4: Description of traces to remove or bridge

Step 6

Mount the Op-Amp, Schottky diode, 100k, 6.20k and 4.7k ohm resistors on the PC board as shown in Figure E.5. Note the orientation of the diode (pin 1 connected to pin 1 of the Op-Amp IC). Also, short pins 3 and 4 of the Op-Amp IC using a solder bridge.

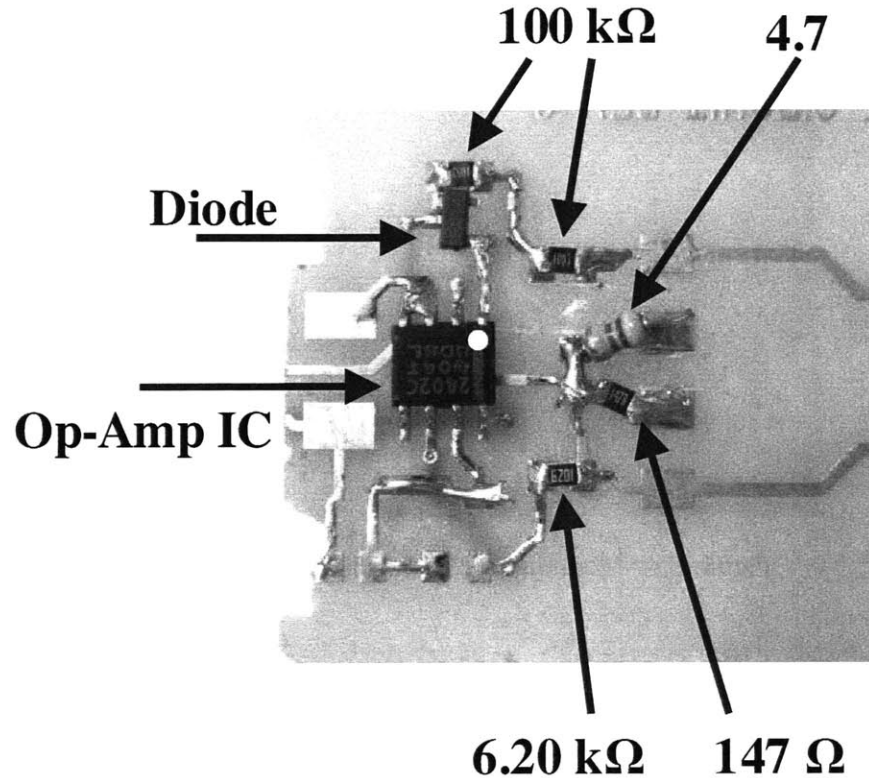


Figure E.5: Mounting the preliminary electronic components

Step 7

Take the MAX4544 IC (analog switch) and very carefully bend upward pins 2 and 4. This bending will allow wires to be soldered to these pins. Position the IC so that pins 1 and 3 are on the pads the 4.7 kΩ and 147 Ω resistors are soldered to respectively. Once positioned, solder the pins to their respective pads.

Step 8

Solder small wires to connect pin 4 of the MAX4544 IC to GND, pin 2 to the output of the transformer, and pin 8 to pin 8 of the Op-Amp IC (for +3V power). Also solder a

wire from pin 7 and run it to the opposite edge of the board (it will connect to the MITes header in step 10). See Figure E.6.

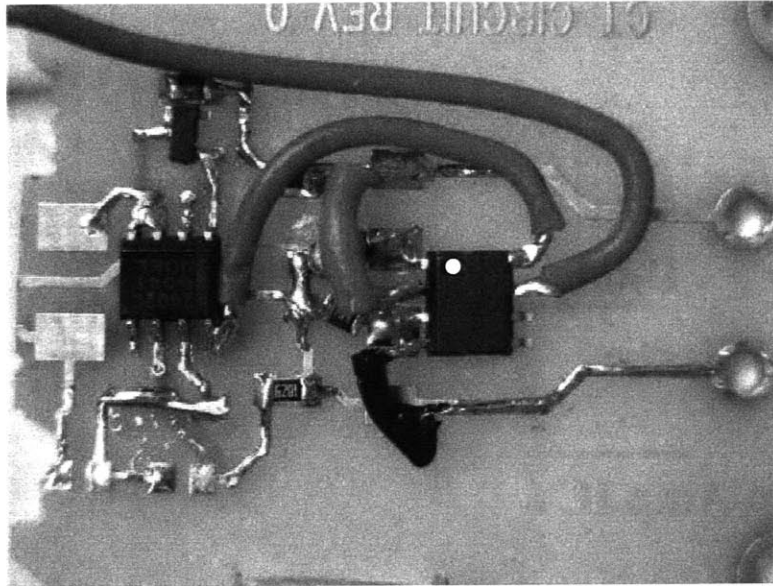


Figure E.6: Mounting MAX4544 IC and attaching wires

Step 9

On the reverse side of the PC board, cut a 2mm gap in the center of the trace that runs from the output of the diode to the input of Op-Amp B (pin 6) as shown in Figure E.7. Solder a 100k resistor in that gap and solder the positive end of a 1.0 uF capacitor to the side of the resistor closest to +3V power trace. Also, solder a wire from the negative side of the capacitor to the GND pad on the other side of the PCB. Figure E.8 shows a finished view of the capacitor and resistor installation.

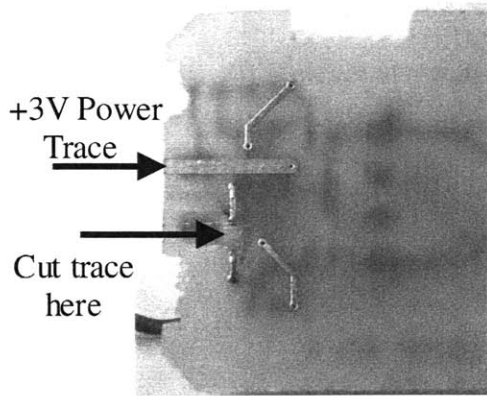


Figure E.7: Cutting 2mm trace gap

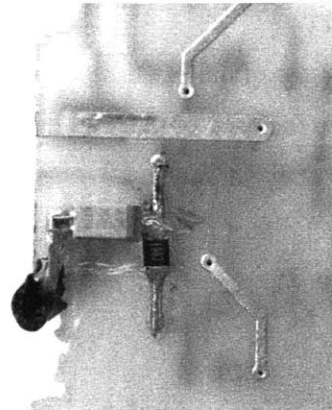


Figure E.8: Finished view

Step 10

Remove the pins from the pads on the protoboard adapter and mount the MAX5160 IC (digital potentiometer) on it. Glue the board in place on the underside of the PC board as shown in Figure E.9. Note that pad 1 corresponds to pin 1 on the IC.

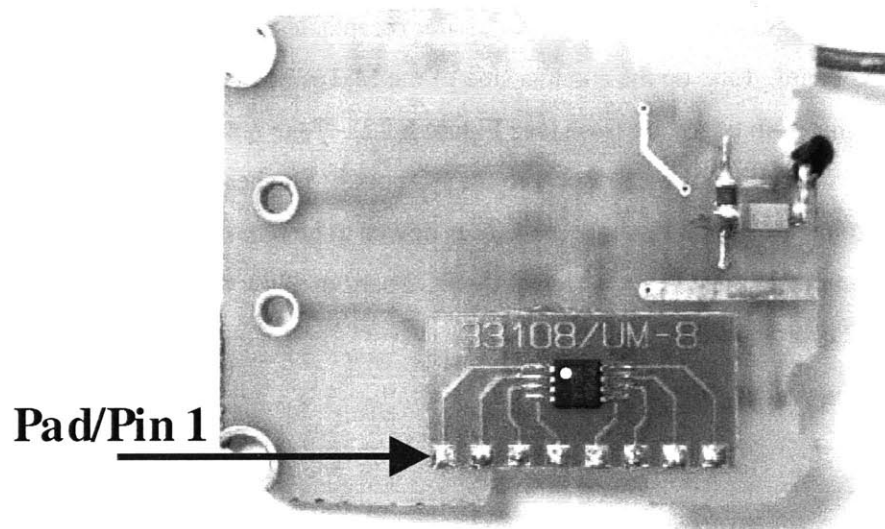


Figure E.9: Mounting MAX5160 IC and protoboard

Step 11

On the top of the PCB solder wires to the pads shown in Figure E.10. Route over the edge to the back of the PCB and solder the wires to pins 5 and 6 of the MAX5160 IC (order does not matter).

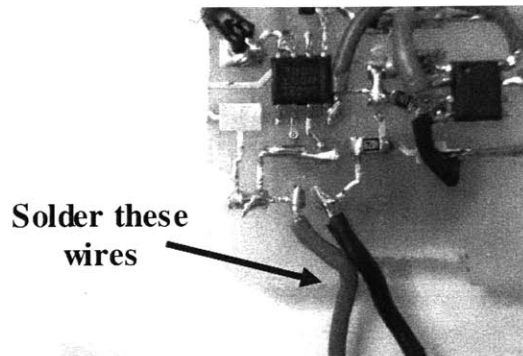


Figure E.10: Attaching digital pot wires

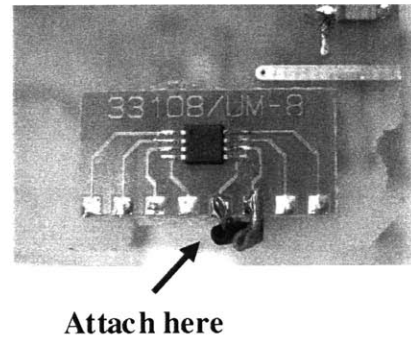


Figure E.11: Connecting wires to protoboard

Step 12

Insert the MITes device into the 12 pin header receptacle and position it on the underside of the PC board. Line up the antenna side of the MITes board with the end of the PC board so that both edges are flush (see Figure E.12). Take note of where the header receptacle is positioned with respect to the PC board. The header receptacle will be secured to the PC board to allow the MITes device to be removable. Also note that the header receptacle must be elevated off the PC board to allow the MITes device to sit flat on the PC board surface.

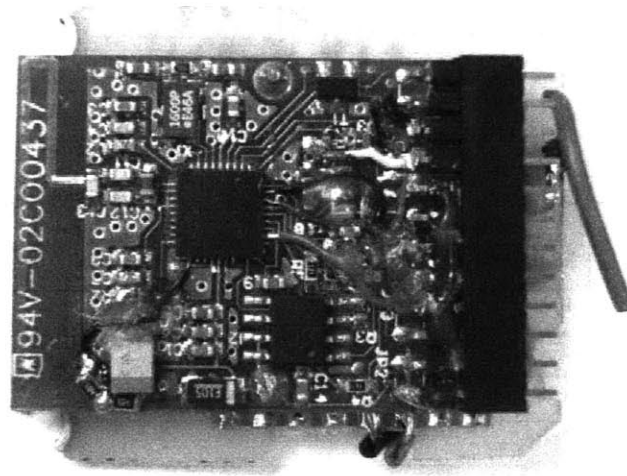


Figure E.12: Positioning MITes device with header receptacle

Step 13

Use hot glue to build a foundation on which to secure the receptacle on the PC board. This step can be done with or without the MITes board still inserted (it may be easier to keep the MITes board inserted as a reference for how much to elevate the header receptacle).

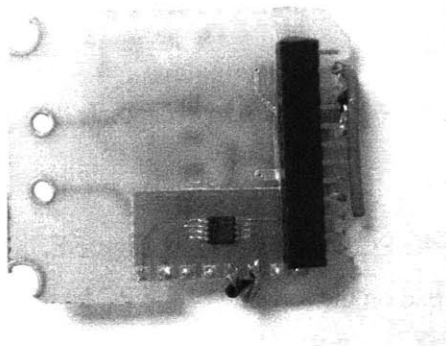


Figure E.13: Header positioning and gluing as seen from above

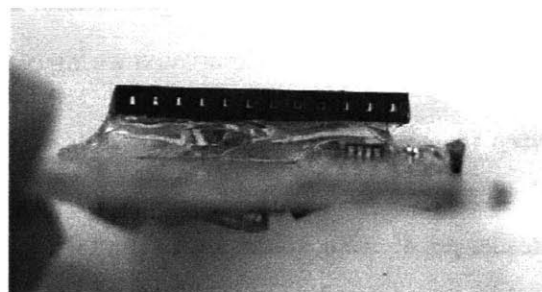


Figure E.14: Header positioning and gluing as seen from the PC board edge

Step 14

The rest of the wiring for the MAX5160 IC can now be done. The following table provides the connections needed between the MAX5160 IC and the header receptacle.

Table E.2: Pin connections for MAX5160 to header receptacle

MAX5160 IC Pin	Header Receptacle Pin
1	8
2	9
4	1 & 2 (Both GND)
7	7
8	4 (+3V Power)

Also connect the wire that was left unconnected in step 5 (from pin 7 of the MAX4544 IC) to header pin 10.

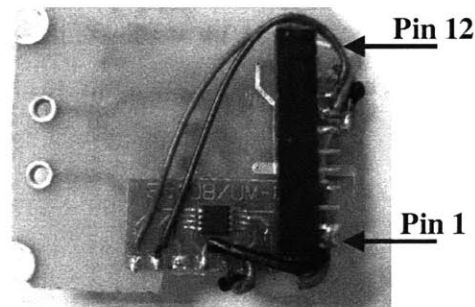


Figure E.15: Completed wiring of MAX5160 IC to header receptacle

Step 15

Solder a wire to connect the +3V Power trace on the PC board (shown in Figure E.7) to header pin 4. Also, solder a wire from the GND pad on the top side of the PC board to header pins 1 and 2.

Step 16

Solder the Zener diode between the output and GND pads on the edge of the board. Make sure the cathode (marked side) is on the output pad and anode is on the GND pad.

See

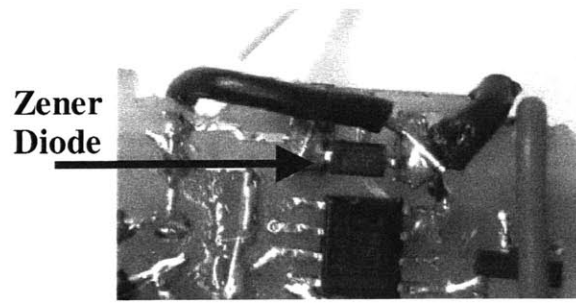


Figure E.16: Mounting Zener diode

Step 17

Solder a wire from the output pad to pin 5 (AIN0) of the header receptacle.

E.3.3 Preparing the pillbox casing

Step 18

Take the pill box and cut a notch on the side for the transformer cable. Also drill two small holes on the bottom of the box to allow the leads on the battery holder to go through. See Figure E.17.

Step 19

Solder two wires to the positive and negative leads of the battery connector. They should be about 2 inches long.

Step 20

Pass the wires through the holes and hot glue the battery connector in place. Hot glue should also be placed on the holes inside the box for insulation. Figure E.18 shows this step.



Figure E.17: Notch and holes on casing

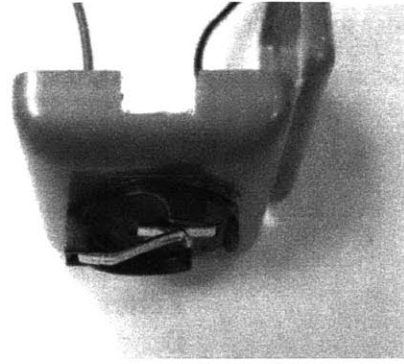


Figure E.18: Battery connector in position with wires

E.3.4 Putting it all together

Step 21

Solder the negative terminal wire from the battery connector to pins 1 and 2 and solder the positive terminal wire to pin 4 of the header receptacle. Be sure to use the notches in the PC board to help route the wires and allow the PC board to fit in the pillbox casing.

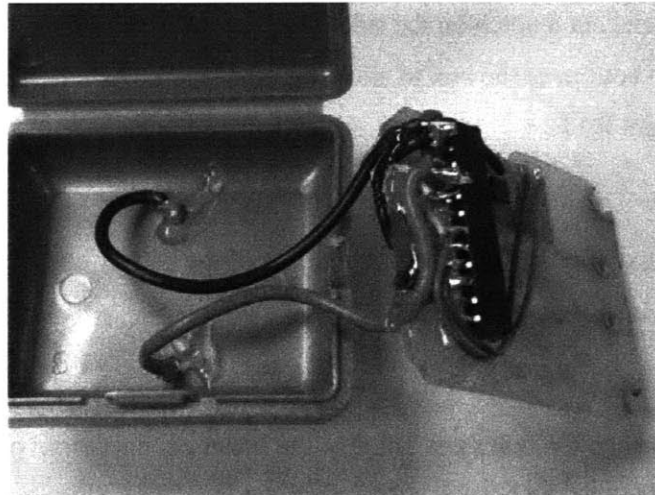


Figure E.19: Attaching battery wires to header

Step 22

Solder the transformer's cables to the holes on the edge of the PC board. Polarity is not an issue since the signal is AC.

Step 23

Take the switch and cut off three of the pins on one side. Place the switch such that the center and one edge pin line up with header receptacle pins 4 and 3 respectively. Solder the pins and clip off the remaining unconnected switch pin. Refer to Figure E.20.

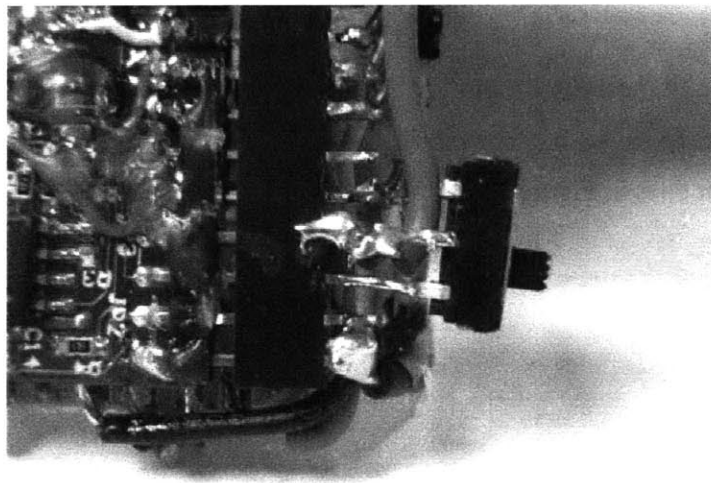


Figure E.20: Connecting the switch

Step 24

Notches must be cut on the box in order to allow the PC board to fit in the pill box with the switch attached. Position the PC board in the box and mark off the location on the box's bottom and top edge where the notches will be cut for the switch. The box will look like the one in Figure E.21. The notches allow the box to close as shown in Figure E.22.

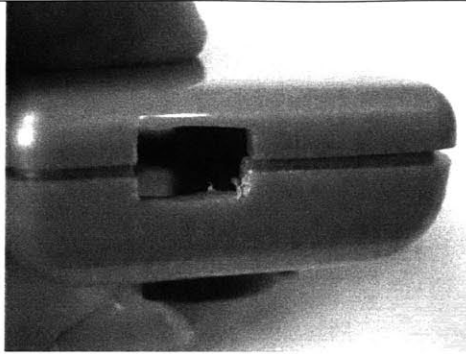


Figure E.21: Notches for the switch

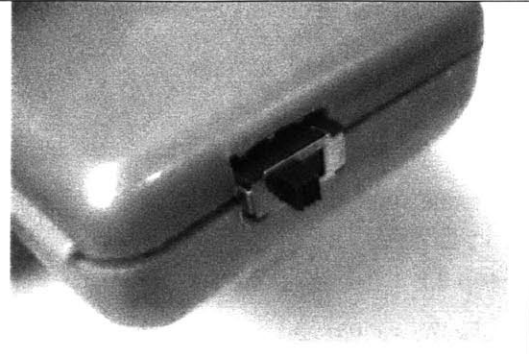


Figure E.22: Closed box view of switch

Step 25

When fitting the PC board in the pill box, it may be necessary to trim its edges. With the MITes device inserted, the box should close without resistance. The completed sensor should look as it does in Figure E.24.

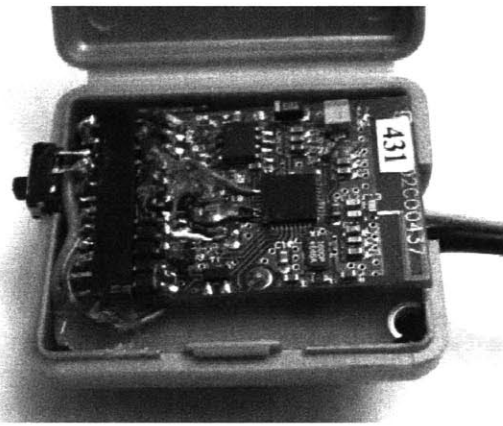


Figure E.23: PC board installed with transformer

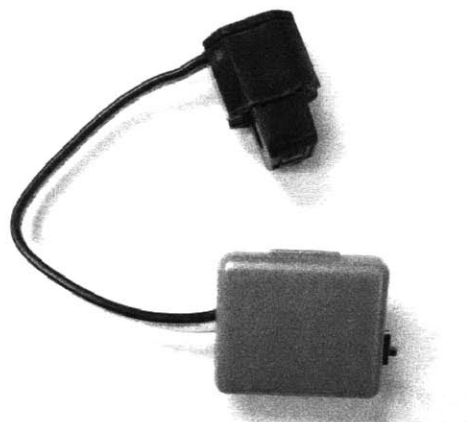


Figure E.24: Finished Current Sensor

Step 26

With the MITes device installed in the box, program the current sensor firmware to its EEPROM IC. Power cycle the sensor and it should be functional.

Appendix F

Additional Current Sensor Tests

In addition to the bread maker machine, eight more appliances were tested using the current sensor and the plots are shown in the figures below. Among these machines are an adjustable setting lamp, multiple speed blender, rice cooker, sliced bread toaster, LCD television set, VCR, and CRT computer monitor. Each of these appliances has a unique current consumption profile that indirectly describes their operation and behavior.

F.1 Adjustable Setting Lamp

The adjustable setting lamp has an analog knob attached to a potentiometer. As the knob is twisted, different amounts of current are allowed to flow through the light bulb giving rise to different intensities. For the lamp test, the knob was slowly twisted from the

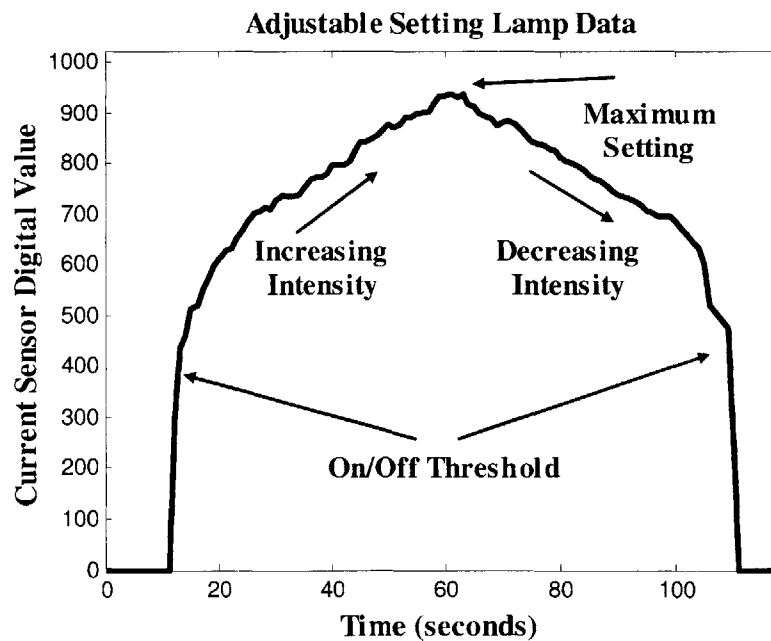


Figure F.1: Current sensor results for adjustable lamp

lowest to the maximum and then back to the lowest intensity value. The current sensor used the 4.7k Ω resistor and a gain of two to rescale the current value range.

F.2 Multiple-Speed Blender

For the test involving the multiple-speed blender, the appliance was stepped through its different speed settings. As can be seen from Figure F.2, there are noticeable steps corresponding to the sub-speeds for both the low and high speed settings. Initial current spikes from the motor when it is switched on are also present in the plot. The current sensor parameters for the blender were the 147 Ω resistor and a gain of nine.

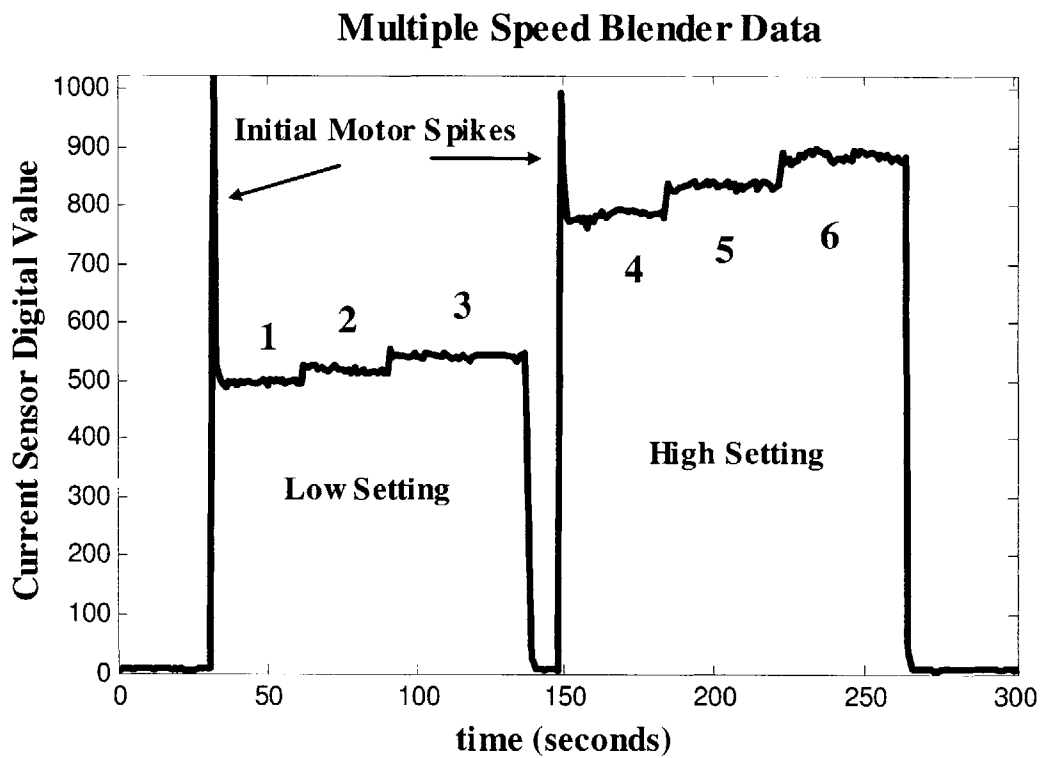


Figure F.2: Current sensor results for blender

F.3 Rice Cooker

The rice cooker appliance has a fairly simple operation sequence. When a cold cooking pot is placed in the appliance, the rice cooker applies some heat to warm up the ingredients. Once the cook button is pressed, the rice cooker begins to draw the necessary current to begin cooking the rice. The cooking period lasts for about 20 minutes. Once the rice cooker detects that the rice is cooked, the appliance shuts down and draws a relatively small amount of current—enough to keep the rice warm. The 147Ω resistor and a gain of 11 were selected for use by the current sensor.

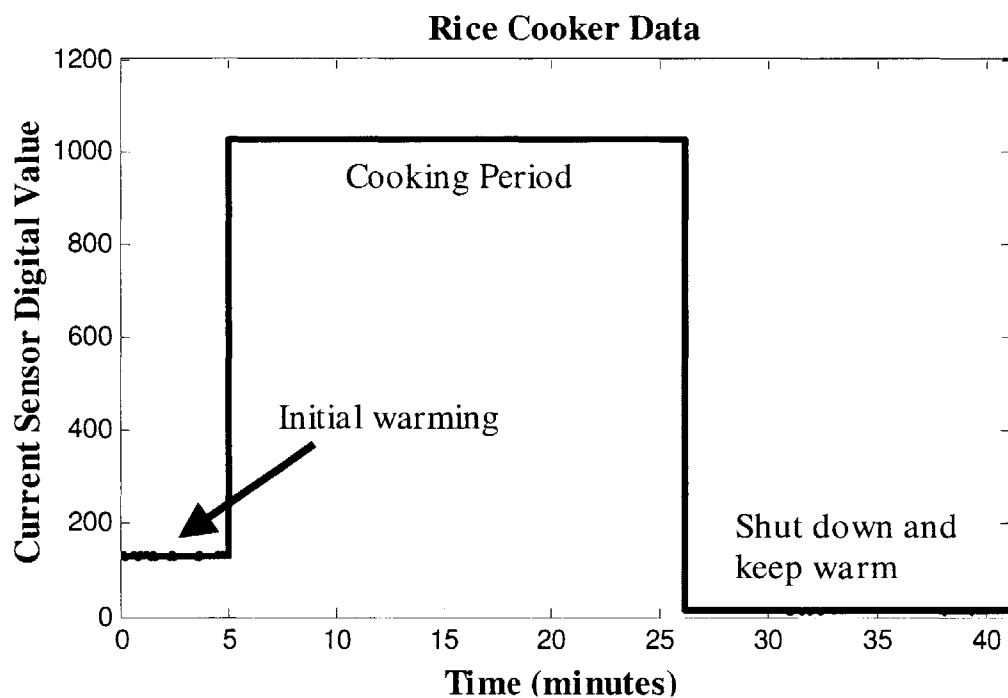


Figure F.3: Current sensor data for rice cooker

F.4 Bread Toaster

The bread toaster test involved using three different toast settings: dark, medium and light. As seen in Figure F.4, the toaster controls the amount bread is toasted by adjusting the amount of time it applies heat. For the low setting, the bread is toasted for about 75 seconds. The medium and dark settings apply heat for about 100 and 130

seconds respectively. For the toaster, the current sensor selected the 147 Ω resistor and a gain of two.

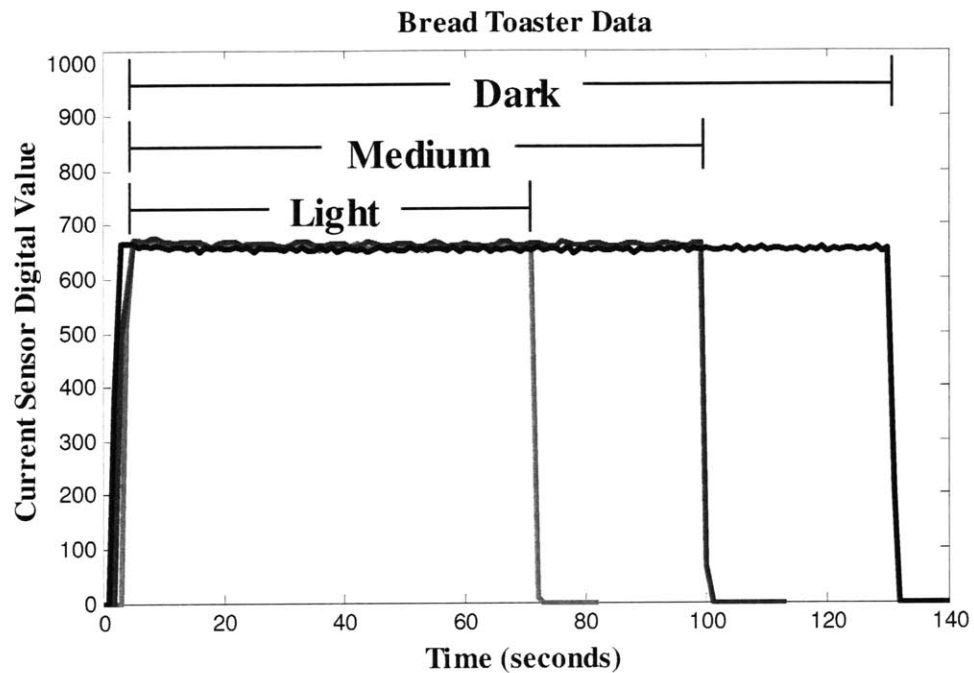


Figure F.4: Current sensor data for toaster

F.5 LCD Television

The LCD television set proved to have only two modes of operation: on and off. As the plot of Figure F.5 shows, the television is initially powered off. The power switch (via the remote control) is then toggled and the television begins to display TV programming. After about one minute, the input to the TV is removed resulting in a blank screen. The current consumption difference between a screen showing TV programming and a blank screen is negligible. Finally, the TV is turned off.

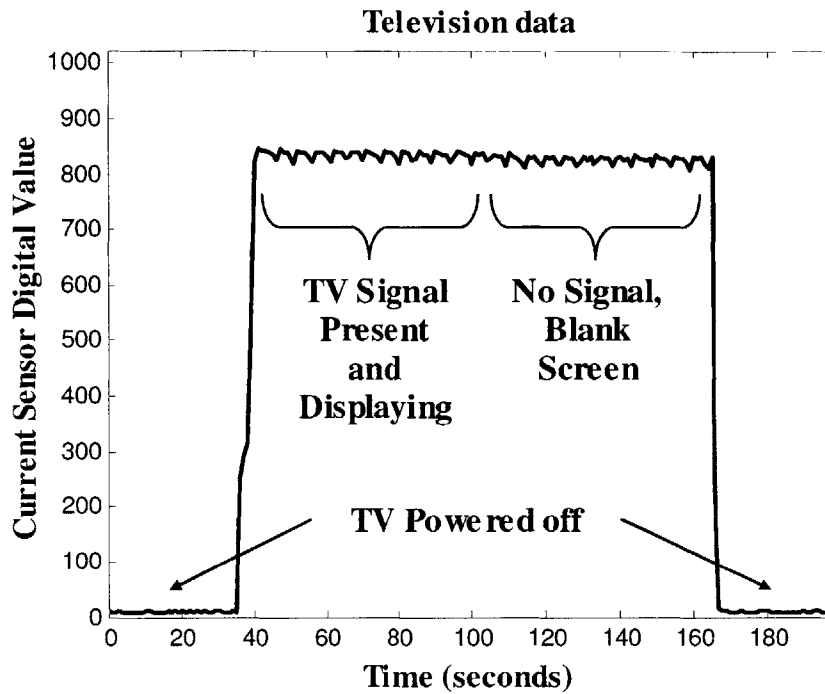


Figure F.5: Current sensor data for Television

F.6 VCR

The VCR has many different states that all use different amounts of current. As seen in Figure F.6, the VCR starts in a standby (a.k.a. “Vampire”) state which consumes the least amount of current. The VCR is then turned on by pressing the power button. Once powered on, the VCR enters an idle state and waits for user commands. The play button is then pressed and the VCR energizes its motors to turn the tape. After about 30 seconds, the VCR is stopped. After idling for about 20 seconds, the rewind button is pressed which causes the motors to spin faster than when playing the tape. The motor speed slows down toward the end as the rewind operation nears completion. Finally the VCR stops, enters idle mode and is then powered off.

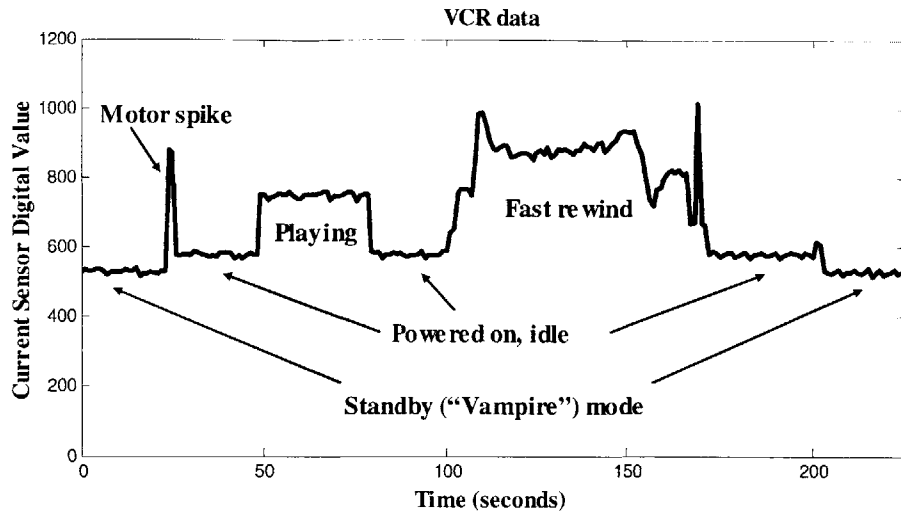


Figure F.6: Current sensor data for VCR

F.7 CRT Monitor

The CRT monitor technically has three states: on, standby, and off. Yet, like the TV, the CRT monitor seems to have only two distinguishable states. The plot in Figure

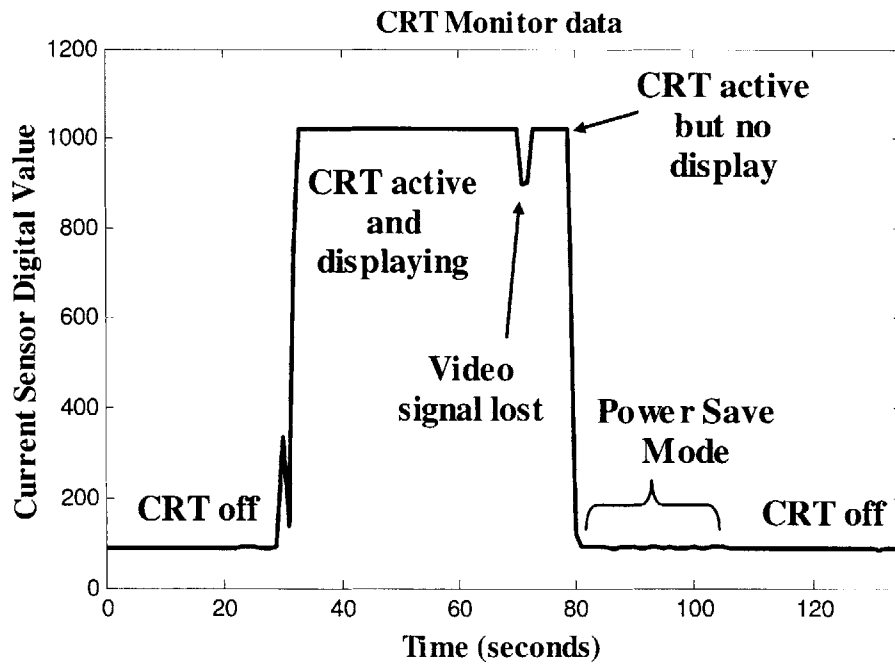


Figure F.7: Current sensor data for CRT Monitor

F.7 starts off with the monitor in the off state. Then the monitor is switched on and begins to display the applied video signal. About 45 seconds later, the video signal is removed. The monitor detects the absence of a signal and goes to standby mode which is indistinguishable from a powered off state. Finally the monitor is powered off, but the current consumption does not noticeably change.

Appendix G

Information for Obtaining the MITes Devices

For more information concerning the MITes devices, please contact Dr. Stephen Intille (intille@mit.edu) and Emmanuel Munguia Tapia (emunguia@mit.edu) at House_n group of the MIT Department of Architecture.

Bibliography

1. Intille, S.S., J. Rondoni, C. Kukla, I. Anaconda, and L. Bao, *A context-aware experience sampling tool*, in *Proceedings of CHI '03 Extended Abstracts on Human Factors in Computing Systems*. 2003, ACM Press: New York, NY. p. 972-973.
2. Intille, S.S., K. Larson, and C. Kukla, *Just-in-time context-sensitive questioning for preventative health care*, in *Proceedings of the AAAI 2002 Workshop on Automation as Caregiver: The Role of Intelligent Technology in Elder Care*. 2002, AAAI Press: Menlo Park, CA.
3. Intille, S.S., *Ubiquitous Computing Technology for Just-in-Time Motivation of Behavior Change (Position Paper)*, in *Proceedings of the UbiHealth Workshop*. 2003.
4. Munguia Tapia, E., Natalia Marmasse, Stephen S. Intille, and Kent Larson, *MITes: Wireless portable sensors for studying behavior*, in *Proceedings of Extended Abstracts Ubicomp 2004: Ubiquitous Computing*. 2004.
5. Jovanov, Emil, Amanda O'Donnell Lords, Dejan Raskovic, Paul Cox, Reza Adhami, and Frank Andrasik, *Stress Monitoring Using a Distributed Wireless Intelligent Sensor System*, in *IEEE Engineering in Medicine and Biology Magazine*. May/June 2003. p. 49-55.
6. Beaudin, Jennifer S., Emmanuel Munguia Tapia, and S.S. Intille, *Lessons learned using ubiquitous sensors for data collection in real homes*, in *Extended Abstracts of the 2004 Conference on Human Factors in Computing Systems*. 2004, ACM Press: New York, NY. p. 1359-1362.
7. Thieden, E., M. S. Agren, and H. C. Wulf, *The wrist is a reliable body site for personal dosimetry of ultraviolet radiation*. *Photodermatology, photoimmunology & photomedicine*, 2000. **16**(2): p. 57-61.
8. Thieden, Elisabeth, Peter A. Philipsen, Jane Sandby-Moller, Jakob Heydenreich, and Hans Christian Wulf, *Proportion of Lifetime UV Dose Received by Children*,

- Teenagers and Adults Based on Time-Stamped Personal Dosimetry*. Journal of Investigative Dermatology, Dec. 2004. **123**: p. 1147-1150.
9. McKinlay, A. F. and B. L. Diffey, *A reference action spectrum for ultraviolet induced erythema in human skin*. CIE Journal, 1987. **6**: p. 17-22.
 10. Priyantha, N.B., A. Chakraborty, and H. Balakrishnan, *The Cricket location-support system*, in *Proceedings of the Sixth Annual ACM International Conference on Mobile Computing and Networking (MOBICOM)*. 2000, ACM Press. p. 32-43.
 11. *White Paper: nRF24Ex in a wireless keyboard design*. 2003, Nordic VLSI ASA.